

https://dspace.org/

Shear stresses and discharges in compound channels

Holden, Andrew

2015-01-27
http://hdl.handle.net/10539/16799

Downloaded from a DSpace repository. https://dspace.org/

SHEAR STRESSES AND DISCHARGES IN COMPOUND CHANNELS

Andrew Holden

A project report submitted to the faculty of Engineering, University of the Witwatersrand, Johannesburg, in partial fulfilment of the requirements for the degree of Master of Science in Engineering.

Johannesburg, 1986

DECLARATION

I declare that this project report is my own, unaided work. It is being submitted for the Degree of Master of Science in Engineering in the University of the Witwatersrand, *Johannesburg*. It *has not* been submitted before for any degree or examination in any other University.

A. P. Hobbs

(Signature of candidate)

19 day of December 1986

ABSTRACT

In a compound channel consisting of a deep main channel and shallow flood plains, turbulence at the interfaces of the main channel and flood plains complicates discharge computations and the analysis of boundary shear stress profiles.

Flume studies were carried out using a compound channel in which the flow depth and slope of main channel bank were varied and boundary shear stresses were measured. It was found that a sloping bank generally reduces the intensity of turbulence, except for steep banks at very low flow depths. The measured shear stresses were used to develop a model for shear stress profiles on the flood plain, using a dimensionless form of the apparent shear stress on the interface as the independent variable representing turbulence intensity. Using published flume data with a range of roughnesses and geometries, existing methods of predicting the apparent shear stress and of computing discharges were evaluated, and some new methods developed.

This work is dedicated to the pursuit of excellence in Engineering research.

Acknowledgements

I would like to express my appreciation to Dr. Chris James, my supervisor, who has guided me through my research project by giving me much excellent advice, at the same time allowing me ample leeway to exercise my own initiative. I wish to thank Mr. John Davis and Mr. Chris Coleman, technicians in the Civil Engineering laboratory at the University of the Witwatersrand, for their patience and help in constructing the laboratory apparatus for my experiments.

I am very grateful to my father, Mr. F L Holden, for his continual interest and concern at every stage of this project. I am also very much indebted to my friends, especially Craig Koetsier, for their support and encouragement throughout the duration of the project.

Part of the work described in this report contributes to the research programme of the Research Organisation of the Chamber of Mines of South Africa. The loan of instrumentation and funding for apparatus from the Chamber of Mines is gratefully acknowledged, as well as financial assistance from the CSIR Foundation for Research Development, without which my Master's studies would not have been possible.

TABLE OF CONTENTS

CHAPTER 1: INTRODUCTION 1
1.1 Problem statement 1
1.2 Turbulence phenomenon 4
1.3 Velocity and shear stress profiles 8
1.4 Aims 11

PART 1: SHEAR STRESS PROFILES 15

CHAPTER 2: FLUME EXPERIMENTS 16
2.1 Background 16
2.2 Compound section 18
2.3 Preston tube 21
2.4 Instrumentation 23
2.5 Experimental procedure 28

CHAPTER 3: RESULTS 32
3.1 Shear stress profiles 32
3.1.1 Main channel 36
3.1.2 Flood plain 38
3.2 Effect of bank slope 39
3.3 Peak shear stress on flood plain 41
3.4 Summary 41

CHAPTER 4: DATA ANALYSIS 43
4.1 Rajaratnam and Ahmadi's model 43
4.2 Relative apparent shear stress proposition 46
4.3 Shape equations 47
4.4 Peak shear stress on flood plain 50
4.5 Length of interaction zone 52
4.6 Shear stress profile model 53

PART 2: DISCHARGE COMPUTATION AND RELATIVE APPARENT SHEAR STRESS PREDICTION 59

CHAPTER 5: DISCHARGE COMPUTATION 60
5.1 Survey of discharge computation methods 60
5.1.1 Composite channel approach 61
5.1.2 Correction factors 63
5.1.3 Interface approach 63
5.2 Development of improved methods 68
5.2.1 Popular method 71
5.2.2 Lambda-method 73
5.2.3 Area method 75
5.2.4 k-method 78
5.2.5 Modified k-method 80
5.2.6 Assessment of methods 84

CHAPTER 6: RELATIVE APPARENT SHEAR STRESS PREDICTION 86
6.1 *Previous research* 86
6.2 Assessment of equations 88
6.3 *Development of a new equation* 96

CONCLUSIONS 104

APPENDICES 110

APPENDIX A: OBSERVED SHEAR STRESS PROFILES 111

APPENDIX B: RAJARATNAM AND AHMADI'S RELATIONSHIP FOR APPARENT SHEAR STRESS 124

APPENDIX C: COMPUTER PROGRAMS 127
C1 Programs for data manipulation 128
C2 Shear stress profile model 138
C3 Discharge computation 141
C4 Relative apparent shear stress prediction 149

APPENDIX D: PUBLISHED FLUME DATA 157

REFERENCES 160

LIST OF FIGURES

1.1 Cross sections of compound channels..... 3
1.2 Components of a compound channel..... 3
1.3 Vortices in a compound channel..... 5
1.4 Lateral profiles of shear stress and velocity in a symmetrical compound channel..... 10
1.5 Vertical velocity profiles..... 10
1.6 Three-dimensional cut-away of a compound channel..... 12

2.1 Compound channel with sloping main channel bank..... 17
2.2 Cross section of a compound channel built in a laboratory flume..... 17
2.3 Detail of section with sloping main channel bank..... 17
2.4 Overall layout of flume and measuring apparatus..... 20
2.5 Detail of upstream end of flood plain..... 20
2.6 Preston tube..... 22
2.7 Fuji pressure transducer for measuring differential pressures..... 25
2.8 Diagrammatic representation of the instrumentation..... 25
2.9 Receiver..... 26
2.10 Traversing mechanism on which Preston tube is mounted..... 26
2.11 Horizontal scale on traversing mechanism..... 27
2.12 Mounting apparatus for Preston tube..... 27
2.13 Preston tube in a cup of water between experiments..... 31
2.14 Evidence of many hours of hard work..... 31

3.1 Measured shear stress profiles for series A experiments, presented in a dimensionless form..... 33
3.2 Measured shear stress profiles for series B experiments, presented in a dimensionless form..... 34
3.3 Measured shear stress [illegible] for series C experiments,

presented in a dimensionless form..... 35
3.4 General form of dimensionless shear stress profiles..... 38
3.5 Comparing flood plain shear stress profiles for different slopes of main channel bank..... 40
3.6 Peak shear stress ratio..... 42

4.1 Universal dimensionless shear stress profile..... 44
4.2 Relationship for junction shear stress..... 44
4.3 Curves drawn through the points in fig. 4.1..... 44
4.4 Family of curves representing shape equations for shear stress profile model..... 49
4.5 Curve for parameter "a", equations 4.9..... 49
4.6 Relationships for peak shear stress ratio on flood plain... 51
4.7 Relationship for length of the interaction zone in the food plain..... 53
4.8 Family of curves generated using the shear stress profile model..... 55
4.9 Forms of shape equations..... 56
4.10 Observed data superimposed on curves generated by shear stress profile model..... 57

5.1 Diagonal interfaces for calculating an effective hydraulic radius (Posey, 1967)..... 61
5.2 Sub-division of channel using vertical interfaces..... 63
5.3 Inclined division line used in Yen and Overton's approach (Yen and Overton, 1973)..... 66
5.4 Vertical, horizontal and inclined division lines evaluated by Wormleaton, Allen and Hadjipanos (1982)..... 66
5.5 Definition sketch for symbols used in chapters 5 and 6..... 69
5.6 Error in discharge computation, as tested on the data of Wormleaton, Allen and Hadjipanos (1982)..... 72
5.7 Values of k derived from the data of Wormleaton, Allen and Hadjipanos (1982)..... 73
5.8 Area adjustment..... 76
5.9 Intersecting diagonals at low flow depths..... 76
5.10 Probable shapes of zero shear stress interfaces..... 76

5.11 Relationship for the k-factor in the modified k-method..... 81
5.12 Iterative procedure used in QCOMP for calculating k..... 84

6.1 Definition sketch for the equation of Prinos and Townsend (1984), equation 6.3..... 89
6.2 Assessment of the Wormleaton equation in conjunction with the popular method..... 93
6.3 Assessment of the Wormleaton equation in conjunction with the k-method..... 94
6.4 Assessment of the Prinos equation in conjunction with the k-method..... 94
6.5 Assessment of the Wormleaton equation in conjunction with the modified k-method..... 95
6.6 Assessment of the Prinos equation in conjunction with the modified k-method..... 95
6.7 Iterative proce[illegible]ed in TPRED for calculating τ_x..... 96
6.8 Geometrical par[illegible]s for equations 6.8 and 6.12..... 98
6.9 Symbols used [illegible]ight and co-workers..... 103
6.10 Assessing equations 6.8 and 6.12, using the flume data of Wormleaton, Allen and Hadjipanos (1983) and Knight and Demetriou (1983)..... 103

B1 Curve for equation B5..... 126
B2 Relationship for b_p, equation B3..... 126

C1 Definition sketch..... 128

LIST OF TABLES

2.1 Patel's calibration equations for the Preston tube..... 22

2.2 Experimental results..... 29

3.1 Values of τ_{cj}/τ_{pj} for fig. 3.1..... 36

5.1 Pertinent parameters in published flume data..... 69

LIST OF SYMBOLS

A_c	cross sectional area of main channel region, assuming vertical interface(s) separating the main channel from the flood plain(s)
A_c'	modified cross sectional area of main channel
A_p	cross sectional area of flood plain region, assuming vertical interface(s) separating the main channel from the flood plain(s)
A_p'	modified cross sectional area of flood plain
ΔA	area adjustment for the area method of discharge computation
b_p	length scale for flood plain
d	flow depth on flood plain
D	flow depth in main channel
d/D	depth ratio
D/d	inverse depth ratio
h	height of flood plain bed above main channel bed (D - d)
i	counter used in summations or iterative calculations
k	modification factor for main channel wetted perimeter
k_c	modification factor for main channel wetted perimeter
k_p	modification factor for flood plain wetted perimeter
l	length of diagonal interface between main channel and flood plain
l_p	length of interaction zone in flood plain region
n	Manning's roughness coefficient
n_c	Manning's roughness coefficient for main channel
n_e	equivalent Manning's roughness coefficient for compound section
n_i	Manning's roughness coefficient for the i'th section of a compound channel
n_p	Manning's roughness coefficient for flood plain
P	wetted perimeter of the entire cross section of a compound channel
P_c	physical wetted perimeter of main channel
P_c'	modified physical wetted perimeter of main channel
P_i	wetted perimeter of the i'th section of a compound channel
P_p	physical wetted perimeter of flood plain
P_p'	modified wetted perimeter of flood plain

Q	discharge of compound channel
Q_c	discharge of main channel region
Q_p	discharge of one flood plain region
R	hydraulic radius of compound channel
R_c	hydraulic radius of main channel
R_i	hydraulic radius of the i'th section of a compound channel
R_p	hydraulic radius of flood plain
S	longitudinal bed slope
SF_c	shear force on the physical wetted perimeter of the main channel
SF_p	shear force on the physical wetted perimeter of a flood plain
v	average velocity
v_c	average velocity in main channel region
v_p	average velocity in flood plain region
v_c/v_p	velocity ratio
Δv	velocity difference between main channel and flood plain $(v_c - v_p)$
W_c	width of main channel
W_p	width of flood plain
y_c	height above bed of main channel
y_p	height above bed of flood plain
z_c	lateral distance across main channel; $z_c = 0$ at the junction of the main channel and flood plain
z_p	lateral distance across flood plain; $z_p = 0$ at the junction of the main channel and flood plain
α	slope of main channel bank
γ	unit weight of water $\gamma = \rho g$ where ρ is the density of water, and g is the acceleration due to gravity
θ	angle of inclination to the horizontal of an inclined interface dividing the main channel and flood plain regions
λ	apparent shear stress ratio used in the λ-method for discharge calculation; λ is defined as the ratio of the apparent shear stress on a diagonal or horizontal interface, to the average shear stress in the main channel
ν	kinematic viscosity of water
τ_a	apparent shear stress on vertical interface between main channel

and flood plain

τ_{ai} apparent shear stress on a diagonal or horizontal interface between the main channel and flood plain regions

τ_c local boundary shear stress in the main channel at a position defined by z_c

$\bar{\tau}_c$ average shear stress acting on the physical wetted perimeter of the main channel

τ_{cj} shear stress on the main channel bed at the junction of the main channel and flood plain

τ_p local boundary shear stress on the bed of the flood plain, at a position defined by z_p

$\bar{\tau}_p$ average shear stress acting on the physical wetted perimeter of the flood plain

τ_{pj} shear stress on the flood plain bed at the junction of the main channel and flood plain

τ_{pm} maximum shear stress on bed of flood plain

$\tau_{p\infty}$ plateau shear stress on the bed of a wide flood plain, sufficiently far from the turbulent interface not to be influenced by the momentum transfer mechanism

τ_r relative apparent shear stress ($\tau_a/\gamma dS = \tau_a/\tau_{p\infty}$)

NOMENCLATURE

Apparent shear stress: Average shear stress on the interface between the main channel and flood plain.

Asymmetrical compound channel: A compound channel consisting of a deep main channel and a shallow flood plain on one side of it.

Bankfull: An elevation corresponding to the height of the flood plain bed above the main channel bed.

Compound channel: An open channel having a deep main channel and one or two shallow flood plains.

Depth ratio: Ratio of flow depth on flood plain (d) to flow depth in main channel (D).

Diagonal interface: A longitudinal plane separating the main channel and flood plain flows, intersecting the water surface at the centre line of the main channel.

Geometry: A general term referring to the proportions and shape of a compound channel cross section.

Horizontal interface: A horizontal plane on the same level as the bed of the flood plain, separating the main channel flow from the flood plain flow.

Inclined interface: An interface that is inclined into the main channel.

Interaction zone: Region on either side of the main channel - flood plain junction, in which the flow velocities and boundary shears are influenced by the turbulence at the junction. Also referred to as the *turbulent interaction zone*, *momentum diffusion zone* or *mixing region*. (Refer to section 1.3.)

Interface or *vertical interface*: A vertical longitudinal plane at the junction of the main channel and flood plain separating the main channel flow from the flood plain flow. Sometimes the term is loosely used to refer to a horizontal, diagonal or inclined interface; when this is the case it is evident from the context.

Junction: The vertical division between the main channel and flood plain, at the top of the main channel bank.

Main channel bank: The side wall of the main channel. It may be vertical (a rectangular section) or inclined (*trapezoidal section*).

Momentum transfer mechanism: The process by which there is a net lateral transfer of longitudinal momentum from the main channel to the flood plain.

Shear stress profile or *lateral shear stress profile*: Distribution of boundary shear stresses laterally across the width of the section.

Symmetrical compound channel: A compound channel having two shallow flood plains on either side of a deep main channel.

Turbulence intensity: The intensity of turbulence generated by the turbulent eddies at the interface.

Turbulence phenomenon: For the purpose of this report this is defined as the occurrence of turbulent eddies in the vicinity of the main channel - flood plain junction, resulting in an exchange of momentum between the main channel and flood plain regions, a net loss of energy from the compound channel, a reduction in discharge carrying capacity of the compound channel, and distorted shear stress and velocity profiles.

Velocity profile or *lateral velocity profile*: Distribution of depth-meaned velocities laterally across the width of the section.

Vertical velocity profile: Distribution of point velocities in a longitudinal vertical plane at any position in the cross section.

CHAPTER 1: INTRODUCTION

1.1 PROBLEM STATEMENT

A compound channel is one having a deep main channel and either one or two shallow flood plains (fig. 1.1). It may be symmetrical (a flood plain on either side of the main channel) or asymmetrical (a flood plain on one side only). The following examples are sited by Wormleaton, Allen and Hadjipanos (1982):

- Natural rivers are often flanked by flood plains which are only inundated at times of flooding.
- Many flood improvement schemes consist of a main channel with flood plains or berms.
- Sometimes canals are built with side berms.
- A tidal river may consist of a main estuarial canal in which the flow is confined for part of the tidal cycle, flanked by extensive sand banks which act as side storage zones for the remaining part of the cycle.

Channels with a simple cross section such as rectangular or trapezoidal channels, can easily be analysed for shear stresses, velocities and discharges. However the analysis of compound channels is complicated by the presence of turbulence at the interface between the main channel and flood plain. The average velocity on the flood plain is usually considerably lower than that in the main channel, because the flow depth is less on the flood plain, and also because a flood plain bed is usually rougher than the main channel bed, especially in natural rivers where the flood plain is often covered with vegetation. This difference in velocity implies that the main channel is a body of water moving faster than the body of water on the flood plain. These two bodies of water interact at the interface between the main channel and flood plain (fig. 1.2), resulting in turbulence in this region. The turbulence takes the form of a bank of vortices with vertical axes along the interface (Myers and Elsawy,

1975). The velocity difference results in longitudinal shear stresses on the interface plane, which can be of appreciable magnitude. In the literature the average shear stress on this interface is referred to as the *apparent shear stress*.

The main channel flow has a higher momentum than the flood plain flow, because of its higher velocity (James, 1984). The vortices at the interface act as a momentum exchange mechanism in which momentum is being exchanged between the main channel and flood plain. The net effect is a lateral transfer of momentum from the main channel to the flood plain (Wormleaton, Allen and Hadjipanos, 1982). This will be referred to as the *turbulence phenomenon*.

A very important parameter in the study of this subject is the *depth ratio*, d/D, which is the ratio of the flow depth on the flood plain to that in the main channel (fig. 1.2). The turbulence phenomenon is most significant at low depth ratios, ie. low flow depths, which is when the velocity difference is the greatest.

The turbulence phenomenon results in a distortion of the velocity profiles and boundary shear stress profiles. The shear stresses on the flood plain are increased while those in the main channel are decreased. The energy lost in the turbulent eddies results in a net reduction of the discharge carrying capacity of a compound channel. This report is concerned with both these issues: the study of boundary shear stress patterns and the discharge characteristics of compound channels, with a view to developing predictive relationships.



(a) symmetrical section



(b) asymmetrical section

Fig. 1.1: Cross sections of compound channels.

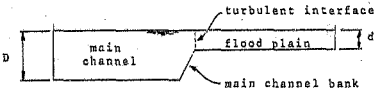


Fig. 1.2: Components of a compound channel.

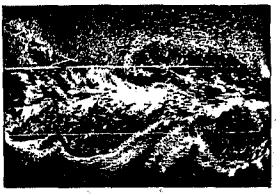
1.2 TURBULENCE PHENOMENON

Let us take a detailed look at the turbulence phenomenon in compound channels. The results of previous researchers need to be examined in order to gain a good qualitative understanding of this phenomenon, and to be familiar with the present state of development of this subject.

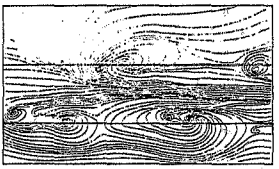
Attention started being focused on turbulence in compound channels in the 1960's. Zheleznyakov (1965,1971) was one of the first to investigate the momentum transfer mechanism. Using a laboratory flume he demonstrated that the discharge of a compound channel decreases as stage rises above the bankfull level. He showed that as the flow depth increases the importance of the phenomenon decreases. He also conducted field experiments that confirmed the significance of the phenomenon in the calculation of overall discharge. Barishnikov and Ivanov (1971) reached similar conclusions to Zheleznyakov, and measured reductions in the section discharge capacity caused by the momentum transfer effect.

Sellin (1964) conducted flume experiments on a symmetrical compound section, photographing the vortices at the interface between the main channel and flood plain. He used a camera mounted on rails above the flume and running parallel with the axis of the channel, driven at a speed equal to the average velocity of the vortex cores. Aluminium powder was scattered on the surface of the water in order to make the vortices more readily visible. Fig. 1.3(a) shows one of the photographs, in which the twin white lines mark the junctions of the main channel and flood plains. Fig. 1.3(b) is a streamline pattern that was constructed from the photograph. The photograph and streamline pattern assist in visualising the turbulent eddies. Sellin's main conclusion was that a momentum transfer mechanism operates between the main channel and flood plain, evidenced by vortices at the interface.

Sellin found that at the bank-full stage a discontinuity exists on a rating curve for a compound channel. He studied the transition region and concluded that a sharp increase in flow resistance occurs when the flood plain is inundated. He found that for low flow depths on the flood



(a) Photograph of vortices, plan view.



(b) Surface streamline patterns developed from the photograph.

Fig. 1.3: Vortices in a symmetrical compound channel (Sellin, 1964).

plain, the discharge of the compound section can be appreciably less than the sum of the discharges obtained by introducing a smooth vertical wall at the interface.

Sellin used the results of his flume studies to evaluate the conventional method for dividing a flood plain from the main channel and calculating the discharge. He found that this yields erroneous results, significantly over-estimating the discharge. He stated that the magnitude of this error indicates that the momentum transfer mechanism cannot be ignored.

Wright and Carstens (1970) studied the apparent shear stress on the interface plane between a main channel and a flood plain. They observed that this shear stress acts as a drag force on the main channel flow and a propulsive force on the flood plain flow.

Myers (1978) measured considerable apparent shear stresses on the interface, demonstrating the danger of ignoring this effect in compound channel analysis. He found that at low flow depths, the apparent shear stress increases sharply as flow depth decreases. This establishes two important facts about the turbulence phenomenon: (1) it is significant at low flow depths, and (2) a relationship exists such that as the depth ratio d/D decreases, the turbulence intensity increases.

Myers observed that the values of apparent shear force on the interface were significantly greater than the shear force that would be exerted on a solid boundary or flood wall at the interface. He concluded that this is the reason why the discharges are over-estimated using the conventional computation techniques, which assume an imaginary flood wall at the interface to divide the main channel and flood plain. This assumption does not adequately account for the high flow resistance posed by the interface on the main channel flow, and results in serious over-estimation of the carrying-capacity for a given flow depth. He maintained that only at considerable flood plain depths could such a subdivision be justified. He stated that research is necessary to provide a more rational basis for uniform flow computations in compound channels.

Myers and Elsawy (1975) conducted flume studies in which they examined lateral shear stress profiles (ie. the distribution of boundary shear stress across the width of the compound channel). They observed irregularities in the pattern of shear stresses in the main channel, and attributed it to the presence of the momentum transfer mechanism.

Radojkovic (1976) showed that the turbulence mechanism could be visualised as follows: because the average velocity in the main channel is greater than on the flood plain, the faster-moving body of water exerts a propelling force on the water in the flood plain region. The slower-moving body of water on the flood plain is exerting a retarding

drag on the water in the main channel. This results in high longitudinal shear stresses on the interface, and also causes the lateral shear stress profiles on the beds of the main channel and flood plain to be distorted.

Zheleznyakov (1971) suggested that the turbulence phenomenon results in an increase in the energy loss of the channel; for a compound channel, energy is not only being lost through boundary resistance, but through the turbulence at the interface. This additional energy loss results in a reduction of discharge capacity.

Radojkovic (1976) described the turbulence phenomenon more specifically in terms of energy. The mechanism is a transfer of energy from the main channel, which is a region of high velocity and hence high energy, to the flood plain, a region of low velocity and energy. In this process some of the energy taken from the main channel is dissipated through the turbulent eddies in the vicinity of the interface. The remaining energy is transferred to the flood plain. The energy lost from the main channel results in a reduction in the carrying-capacity of the main channel; the energy transferred to the flood plain slightly increases its carrying capacity; the net effect is a reduction in the carrying capacity of the compound channel, due to the energy loss in the turbulent eddies. The energy lost from the main channel is evidenced by decreases in the velocities and boundary shear stresses, while the energy imparted to the flood plain is evidenced by increases in the velocities and boundary shears in the vicinity of the junction.

Prinos, Townsend and Tavoularis (1985) measured turbulence intensities throughout the cross section, as root mean square turbulent velocities in the longitudinal, vertical and lateral directions. They found that turbulence is highest at the junction of the main channel and flood plain, and decreases as one moves laterally away from the junction plane into the main channel or flood plain. They found that the turbulence intensity increases as flow depth decreases, and is greater when the flood plain is roughened.

Researchers in this field generally recognise the following factors as those that influence the turbulence intensity:

- *Flow depth*, represented by the depth ratio. Researchers have used various forms of the depth ratio, such as d/D, D/d and d/(D-d). In this report d/D is used as far as possible, because it is easy to visualise; d/D increases as flow depth increases, it is equal to zero at bankfull, and approaches 1.0 asymptotically for very large flow depths. d/D will be referred to as the depth ratio, and D/d as the inverse depth ratio.

- *Bed roughness*. The rougher the flood plain bed is relative to the main channel, the lower is the average flood plain velocity relative to that in the main channel, and the higher is the turbulence intensity at a given flow depth.

- *Geometry*. This includes width of flood plain, *symmetrical* or *asymmetrical* section, and the slope of the main channel bank. All these factors influence the *turbulence intensity* because they define the boundaries within which the momentum exchange occurs.

Parameters representing these three factors will be dealt with in detail *in chapter 6*.

1.3 VELOCITY AND SHEAR STRESS PROFILES

The turbulence at the junction of the main channel and flood plain is evidenced in distorted velocity and shear stress profiles. Rajaratnam and Ahmadi (1981) conducted flume studies using a rectangular, asymmetrical section. They measured profiles of velocities and boundary shears, which have provided a clearer understanding of this subject.

The general shape of their lateral velocity profiles is shown in fig. 1.4. The velocity has an undisturbed plateau value on the flood plain, and an undisturbed peak value in the main channel. At the extreme ends the velocity dips due to the influence of the side walls. In the vicinity of the junction the velocity profile is distorted; this is a region of

transition from the high main channel velocity to the low flood plain velocity.

The lateral shear stress profile (shear stress on the beds of the main channel and flood plain) is also distorted in this region, as can be seen in fig. 1.4. The shear stress on the flood plain is high at the junction, and tapers off towards a plateau. In the central region of the main channel the shear stress is at its undisturbed peak value, and decreases towards the junction with the flood plain. The distortion of the shear stress profiles in the vicinity of the junction can be described as a drawing down of the shear stress profile in the main channel, and an increase in the shear stresses on the flood plain. The shear stresses decrease at the extreme edges of the compound section due to the edge effects of the side walls.

The shaded region in fig. 1.4 indicates the region in which there is turbulence. It is referred to in the literature as the *mixing region*, *interaction zone*, *turbulent interaction zone* or *momentum diffusion zone*. This is the region that is affected by the lateral transfer of momentum, and it is characterised by distorted velocity and shear stress profiles, turbulence, eddies and mixing. It extends from the point in the main channel where the velocity and shear stress profiles start dipping, to where they reach their plateau values in the flood plain region. Rajaratnam and Ahmadi maintained that outside of this region the flow is not disturbed by the turbulence phenomenon. This is confirmed by Pasche and Rouve (1985) who stated that in a real channel, provided it is sufficiently wide, the flow on either side of the interaction zone is not influenced by the turbulence.

Fig. 1.5 shows typical vertical velocity profiles measured by Rajaratnam and Ahmadi. In the central region of the main channel (fig. 1.5(a)) the velocity distribution is logarithmic; near the junction it is decreased in magnitude and has a dip near the water surface. This is caused by the braking effect that the flood plain flow has on the main channel flow, slowing it down. The vertical velocity profiles on the flood plain are increased in magnitude (fig. 1.5(b)) because the main channel flow is

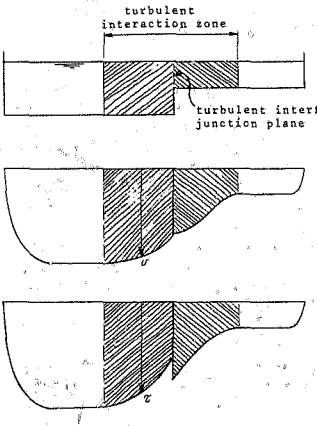
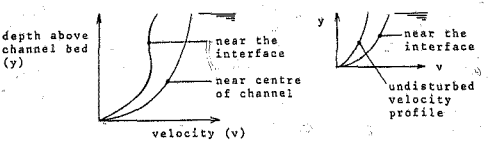


Fig. 1.4: Lateral profiles of shear stress and velocity in an asymmetrical compound channel.



(a) main channel (b) flood plain

Fig. 1.5: Vertical velocity profiles.

exerting a propulsion on the flood plain flow in the interaction zone. However, the logarithmic shape is maintained.

Knight, Demetriou and Hamed (1983) published a diagram that aids visualisation of the turbulence phenomenon and its effects (fig. 1.6). The bank of vortices at the interface is represented by spirals, and the momentum exchange by arrows. Contra-rotating secondary flow cells near the bed of the main channel induce perturbations in the bed shear stress about a mean curve, which is shown dotted in the figure. The shapes of the vertical velocity profiles indicate the complex nature of the velocity field. These profiles (u) may be integrated to give the depth-mean velocities ($\bar{u}$), shown as lateral velocity profiles. These in turn may be integrated over the widths of the main channel and flood plain to give section mean velocities, $\bar{\bar{u}}$. Discharge for each subsection can be calculated from the section mean velocities. This fact is utilised later in this report when discharge computation techniques are evaluated.

Knight and Lai (1985) observed lateral shear stress profiles that are very similar to those described in this section, indicating that these shapes are general.

1.4 AIMS

Knight and Demetriou (1983) stated that with increasing use being made of mathematical models to describe the hydraulic and sediment processes in compound channels, it has become particularly important to be able to model the turbulence phenomenon properly. Indeed, the increasingly intensive research over the past two decades is evidence of the importance that engineers are attributing to this subject.

It is very difficult to obtain field data with which to study overbank flow, because the stage of a river flooding its banks changes too quickly for all the necessary shear stress measurements to be taken (Myers and Elsawy, 1975). For this reason laboratory studies have to be resorted

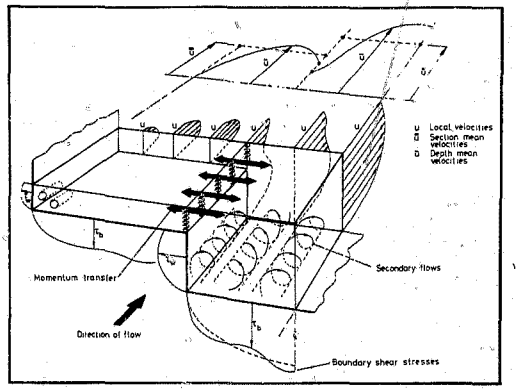


Fig. 1.6: Three-dimensional cut-away of a compound channel, showing velocity and shear stress profiles, and a diagrammatic representation of the momentum exchange mechanism. (Knight, Demetriou and Hamed, 1983.)

to, and all the research in this field to date is based on the results of flume measurements. In the present study empirical relationships are developed using flume measurements collected by the author as well as published flume data.

This study has a dual purpose: to investigate boundary shear stresses in a compound channel with a view to developing a model describing the shear stress profiles on the flood plain, and to formulate an improved discharge computation technique for compound channels.

It is important to be able to predict the shear stress profiles on a flood plain for different flow conditions in order to model sediment transport

processes (Bairol and Ervine, 1984). An example of this is James's model for sediment transport and deposition in compound channels (James, 1984). This utilises the findings of Rajaratnam and Ahmadi (1984), who stated that the vertical velocity profiles on a flood plain can be described using the usual logarithmic velocity distribution law, provided the correct local value of the shear velocity ($\sqrt{(\tau/\rho)}$) is used. A means of predicting the shear stress profiles on the flood plain is required in order to find these local values.

The importance of developing improved discharge computation methods has been established in 1.2. Engineers often need to compute the discharge of a compound channel, for example when plotting flood lines or producing rating curves. The average flow velocities in the main channel and flood plain regions are sometimes required when modelling sediment and hydraulic processes in compound channels, and a discharge computation technique is required to provide these velocities. An example is James's model, which uses the average velocities to calculate shear velocities and the distribution of transverse diffusivity. There is no existing method or equation that is sufficiently accurate or reliable for these purposes, and this project addresses this issue.

This report is divided into two main sections: part 1 deals with shear stress profiles, and part 2 with discharge computation and apparent shear stress on the interface. In part 1, results of the author's flume experiments are presented. Using the boundary shear stresses measured in these experiments a model is developed for predicting the shear stress profile on a flood plain. A dimensionless form of the apparent shear stress on the interface has been adopted as the independent parameter representing the turbulence intensity. A general relationship is therefore required to predict the value of the apparent shear stress in any given field situation. In part 2 this matter is addressed, along with discharge computation methods. Two existing equations for the apparent shear stress require a discharge computation method to calculate a Δv term, which is the difference in average velocity between the main channel and flood plain. Hence these two items, discharge computation and shear stress prediction, are considered together. A new equation for the apparent shear stress is also developed. The author's flume data could not

be used for developing discharge computation methods, because accurate measurement of discharge was not possible. Accordingly published flume data were used, incorporating a fairly wide range of bed roughnesses and flood plain widths.

This study applies mainly to low flow depths (d/D less than about 0,5). For greater flow depths the turbulence intensity is very low and the turbulence phenomenon considerably less important. The author's flume experiments were carried out in a section with smooth boundaries, so it has to be assumed that the results apply to rough channels. This also places an upper limit to the turbulence intensity (represented by the apparent shear stress); higher levels of intensity are possible if the flood plain is roughened.

PART 1: SHEAR STRESS PROFILES

CHAPTER 2: FLUME EXPERIMENTS

2.1 BACKGROUND

Part 1 of this report describes the author's flume experiments and presents the results, leading up to the development of an empirical model for predicting the shear stress profiles on a flood plain. Comparison is made with an existing model.

The only existing means of predicting the shear stresses in the interaction zone on the flood plain is a set of equations presented by Rajaratnam and Ahmadi (1981). These equations were developed empirically from flume experiments similar to those conducted by the author. Rajaratnam and Ahmedi obtained uniform flow in an asymmetrical, rectangular compound channel with a smooth concrete finish. They used a pitot-static tube to measure lateral profiles of boundary shear stress for various flow depths, from which empirical equations were derived to describe the shear stress profiles on a flood plain. This model has a number of shortcomings:

1. All the parameters are expressed as a function of depth ratio, which is treated as the only independent variable; roughness and geometric factors are not accounted for.
2. The equations apply to smooth channels only.
3. The model only considers a rectangular section.

The third item is important for practical applications, since a section with a sloping main channel bank often occurs in the field (fig. 2.1). For natural rivers the main channel can generally be more accurately represented by a trapezoidal section than a rectangular one.

Pasche and Rouve (1985) identified the importance of the slope of the main channel bank in the momentum exchange process. The only specific observations that they could make were that a sloping bank can reduce the

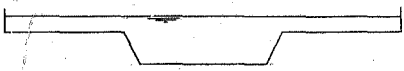


Fig. 2.1: Compound channel with sloping main channel bank.

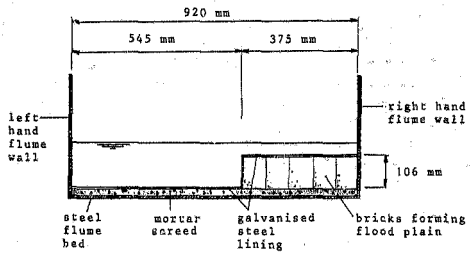


Fig. 2.2: Cross section of compound channel built in a laboratory flume, looking downstream.

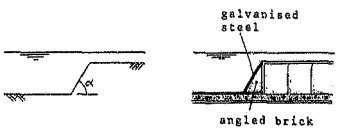


Fig. 2.3: Detail of section with sloping main channel bank.

turbulence intensity, and that it is most significant when the main channel and flood plain have the same roughness, but does not seem to be important when the flood plain is very rough relative to the main channel. They concluded that "for a complete understanding of this phenomenon, additional investigations with varying bank slopes should be conducted in compound channels with smooth boundaries."

Because of the importance of the bank slope and the scarcity of existing flume data for anything other than rectangular sections, the author conducted flume experiments in which the slope of the main channel bank was varied. An asymmetric channel with smooth boundaries was constructed in a laboratory flume, in which lateral bed shear stress profiles were measured for various flow depths and bank slopes, so that the effect of the slope of the main channel bank could be studied and incorporated into a model for the shear stresses on the flood plain.

When developing such a model it is advantageous to have other data with which to compare results. This provides a standard of reference for observed data, as well as a starting point for developing a new model. To enable meaningful comparisons to be made with Rajaratnam and Ahmadi's results, the author used a compound section with similar dimensions to those used by Rajaratnam and Ahmadi.

To the author's knowledge this is the first time that the effect of the slope of the main channel bank has been studied.

2.2 COMPOUND SECTION

A 920mm wide flume with a horizontal floor was available for these experiments. In order to obtain uniform flow the bed should have a longitudinal slope. By studying similar experiments conducted by other researchers a slope of 1 in 1000 (0,001) was selected, and a bed with this slope was formed by casting a mortar screed on the floor of the flume. Precision surveying equipment was used to obtain the desired slope.

Contraction joints were provided at one metre intervals down the flume so as to control cracking of the screed.

The flood plain was formed using bricks, and the section lined with galvanised steel to provide a uniform, smooth boundary. A length of 16m in the flume was built up as a compound section, of which about 11m was lined with galvanised steel. Fig. 2.2 shows a cross section of the flume, giving the dimensions and showing the materials of construction. The angle of inclination to the horizontal of the main channel bank is designated α (fig. 2.3). Three values of α were used: 30°, 60° and 90°. For the 30° and 60° angles, the bank was formed using specially shaped strips of galvanised steel and cut bricks.

Fig. 2.4 shows the layout of the flume and measuring apparatus, viewed from the downstream end. Fig. 2.5 is a view of the upstream end of the brick flood plain. On the left hand side of the flood plain at the junction with the main channel, angled bricks form a main channel bank with a 60° slope. Angled bricks rest against the upstream face of the flood plain to create a reasonably smooth transition. On the left of these bricks the corner is filled in with plasticine to aid in smoothing the transition so as to reduce the turbulence at the entrance to the compound section.

It was particularly important to do a set of experiments with a rectangular geometry ($\alpha = 90^\circ$) so as to have a reference to compare with Rajaratnam and Ahmadi's results. An asymmetrical section (one flood plain) was chosen so as to utilise the full width of the flume and provide as wide a main channel and flood plain as possible. A wide main channel was important so that the left hand wall would not influence the turbulence at the interface. This placed a limit on the maximum flow depth on the flood plain for it to be hydraulically wide. A wide flood plain is important because there must be sufficient width for the shear stress profile to decay to its undisturbed plateau value.

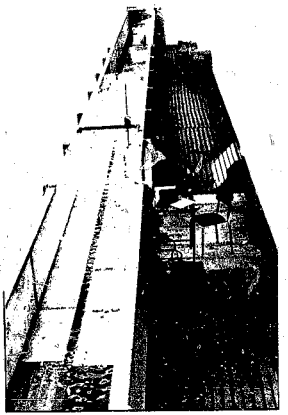


Fig. 2.4: Overall layout of flume and measuring apparatus, looking from the downstream end.

The main channel and flood plain can be clearly distinguished. Half way down, the flume is spanned by a traversing mechanism on which the measuring apparatus is mounted. Alongside the flume the instrumentation can be seen.

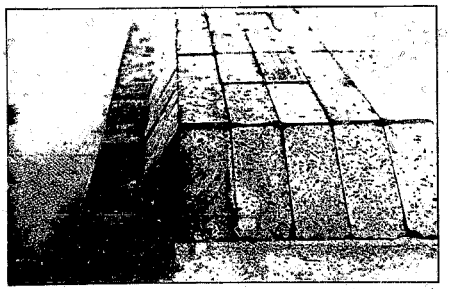


Fig. 2.5: Detail of upstream end of flood plain, looking in the downstream direction.

2.3 PRESTON TUBE

A Preston tube was used to measure the boundary shear stresses (fig. 2.6). Also known as a pitot-static tube, it consists of two concentric tubes, the inner having an opening at the tip, and the outer one opening through some side holes. At the top of the Preston tube these two concentric tubes have separate tappings. The instrument is suspended in the water with the horizontal bottom arm flat against the bed or side wall, and the end hole facing into the flow. The end hole (inner tube) registers the total energy head because the fluid velocity is zero just inside this opening, and the side holes (outer tube) measure the piezometric head. The difference in pressure between the two tubes is the velocity head. Calibration curves are available to convert this into a boundary shear stress reading.

The reason for selecting the Preston tube was because it is small, facilitating the measurement of local shear stresses. Most researchers doing similar experiments on compound channels have used this instrument for their boundary shear stress measurements, which indicates that it is satisfactory for this purpose. Myers and Elsawy (1975) tried a number of sizes of tube and found that the smallest size, which was 1,8mm in diameter, was the most satisfactory, because it minimised disturbance to the flow and gave more local values of shear stress. The author used a 2mm diameter tube for his experiments. For shear stress measurements to be accurate the tube diameter must not be greater than one fifth of the boundary layer thickness. Hence using a 2mm diameter tube limited the flow depth to a minimum of 10mm on the flood plain.

Preston (1954) published the first calibration curves for using the pitot-static tube to measure the shear stress on a smooth boundary (hence the name "Preston tube"). Subsequent experiments suggested that Preston's calibration was in error, and Patel (1965) developed a revised calibration curve by experimenting with tubes of various diameters. His curve shows virtually no scatter, which indicates that it can be used with confidence. The three equations in table 2.1 were fitted to the curve.

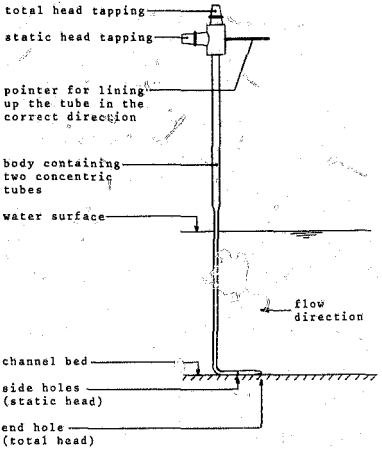


Fig. 2.6: Preston tube

TABLE 2.1: PATEL'S CALIBRATION EQUATIONS FOR THE PRESTON TUBE.

Range of y	Range of x	Equation
0 - 1,5	0 - 2,9	$y = 0{,}50x + 0{,}037$
1,5 - 3,5	2,9 - 5,6	$y = 0{,}8287 - 0{,}1381x + 0{,}1437x^2 - 0{,}0060x^3$
3,5 - 5,3	5,6 - 7,6	$x = y + 2\log(1{,}95y + 4{,}10)$

x and y are dimensionless

x and y are defined as follows:

$$x = \log(\Delta p d^2/4\rho\nu^2) \qquad (2.1)$$

$$y = \log(\tau d^2/4\rho\nu^2) \qquad (2.2)$$

where log is to base 10

Δp = pressure difference between the total and static tubes

d = outside diameter of Preston tube

ρ = density of water

ν = kinematic viscosity of water

τ = boundary shear stress

This calibration applies to flow over smooth boundaries. If the reader is interested in rough boundaries he should consult Hwang and Laursen (1963) and Ghosh and Jena (1971).

2.4 INSTRUMENTATION

Two elements for measuring the boundary shear stresses have been discussed: the Preston tube (which registers a pressure difference) and Patel's calibration to translate this pressure difference into shear stresses. An instrument for measuring the pressure difference remains to be considered.

Initially an electronic digital micromanometer was used for this purpose. Two tubes linked the Preston tube to the micromanometer. These tubes did not have any water in them, but the pressure difference at the Preston tube tappings was conveyed to the micromanometer via the medium of air in the tubes. This arrangement was found to be unsatisfactory; the micromanometer readings were erratic and sometimes erroneous, because of air leaks at the joints, the very low pressure differences that were being measured, and the readings being dependent on the temperature and initial absolute pressure of the air in the tubes.

A Fuji pressure transducer was finally adopted, shown in fig. 2.7. This instrument operates with the connecting tubes filled with water, and the transducer at a lower elevation than the Preston tube, as indicated in fig. 2.8. The tubes have to be carefully bled to remove all air, as even the smallest air bubbles result in meandering or erroneous pressure readings. It was found that bleeding could be successfully achieved by the following means:

- Transparent tubes were used so that air bubbles were visible.
- A siphon effect was created in the tubes to remove all the air.
- Air was removed from the Preston tube by forcing water through it.
- Connections between the tubes and the Preston tube were made underwater.

The components of the system (represented graphically in fig. 2.8) are the pressure transducer, receiver and a 24 volt power supply. The receiver, shown in fig. 2.9, consists of a pointer gauge and a plotter. It has a quick response to pressure changes, which meant that when the experiments were in progress the needle oscillated somewhat, and a mean reading had to be taken at each point. Generally the reading oscillated with an amplitude of the order of 1% of the mean reading, with occasional surges of greater magnitude. A few simple resistor-capacitor circuits were tried unsuccessfully to dampen out the oscillations. These oscillations were caused by currents resulting from irregularities in the channel walls and bed, and slight unsteadiness in the flow. Despite a constant head tank being used to supply the water, small unsteadiness in a flume of this nature is unavoidable because of pumping surges.

The Preston tube was mounted on a traversing mechanism spanning the width of the flume (fig. 2.10). The vertical arm of this mechanism could be moved laterally across the width of the flume, and vertically up and down. A horizontal scale for lateral movement (fig. 2.11) and a vertical scale with a fine adjustment screw enabled the Preston tube to be positioned anywhere in the compound section. A "Meccano" mounting for the Preston tube was designed and constructed by the author (fig. 2.12). With this apparatus the orientation of the Preston tube could be adjusted in three planes: longitudinal, lateral and rotational. Consequently readings

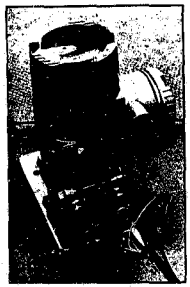


Fig. 2.7: Fuji pressure transducer for measuring differential pressures.

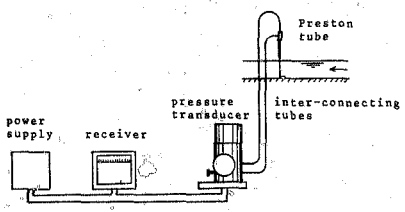


Fig. 2.8: Diagrammatic representation of the instrumentation.

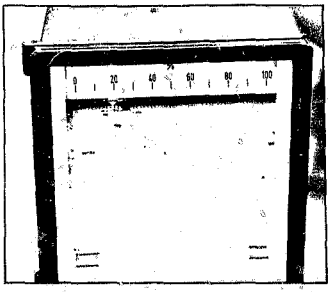


Fig. 2.9: Receiver

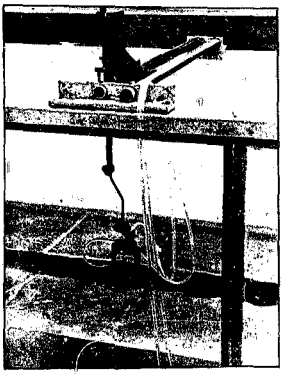


Fig. 2.10: Traversing mechanism on which Preston tube is mounted. Transparent interconnecting tubes are draped over the side of the flume.

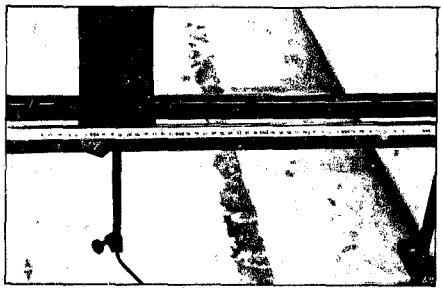


Fig. 2.11: Horizontal scale on traversing mechanism.

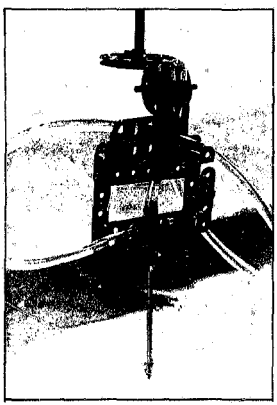


Fig. 2.12: Mounting apparatus for Preston tube.

could be taken on the side walls and the Preston tube could be finely adjusted until it was perfectly straight relative to the flow direction.

2.5 EXPERIMENTAL PROCEDURE

Shear stress measurements were taken approximately half way down the flume to ensure fully developed flow and to minimise the effect of draw-down curves. Glass sides to the flume facilitated viewing the flow and the measuring apparatus.

Table 2.2 summarises the experiments. A total of 22 successful runs were made, in three sets: series A with a rectangular main channel, series B with a 60° main channel bank, and series C with a 30° bank. In each series the depth ratio d/D was varied between about 0,10 and 0,43. The minimum flow depth on the flood plain was 12mm, which is 2mm more than the absolute minimum dictated by the diameter of the Preston tube. The need for a hydraulically wide flood plain limited the maximum flow depth to 80mm. As many depth ratios as possible were used so as to collect a comprehensive set of results.

A steady flow was provided by a constant head tank, the water being circulated by pumps. Discharges were measured with a venturi meter in the supply pipe. An upstream valve in the supply pipe was used to control the discharge, and a downstream weir to counteract the drawdown curve and obtain the *desired flow depth*. It was found that if the discharge was too low, the turbulence at the interface would be too small for the results to be meaningful. If the discharge was too high, the water surface would be very ripply and uneven, and the pressure transducer readings would oscillate a lot, making it difficult to take average readings. Thus the choice of discharge and flow depth for each experiment was a compromise between these two states.

Many trial runs were made before starting on the programme of experiments. The purposes of these runs were to learn how to use the instrumentation,

TABLE 2.2: EXPERIMENTAL RESULTS

series	designation	d (mm)	D (mm)	d/D	discharge (l/s)
A	A12	12	118	0,102	28,0
$\alpha = 90^0$	A13	13	119	0,109	27,0
	A20	20	126	0,159	32,0
	A30	31	137	0,226	38,5
	A40	39	145	0,269	45,0
	A60	60	166	0,361	45,5
	A80	81	187	0,433	47,5
B	B12	13	119	0,109	32,0
$\alpha = 60^0$	B14	14	120	0,117	32,0
	B18	18	124	0,145	35,5
	B19	19	125	0,152	35,0
	B30	30	136	0,221	40,0
	B40	42	148	0,284	45,5
	B60	61	167	0,365	46,0
	B80	76	182	0,418	49,0
C	C12	12	118	0,102	32,0
$\alpha = 30^0$	C15	15	121	0,124	34,0
	C20	20	126	0,159	34,5
	C30	30	136	0,221	36,5
	C40	42	148	0,284	40,0
	C60	60	166	0,361	45,0
	C80	80	186	0,430	49,5

to develop successful methods of bleeding the tubing, and to learn by trial how and where to take readings, and what discharges and flow depths to use. The instrumentation was rigorously tested for reliability, resolution and repeatability (ie. two readings taken at the same place should be the same).

In each experiment a lateral shear stress profile was measured, Preston tube readings being taken along the entire wetted perimeter at intervals of 10 to 20mm. The temperature of the water was taken before and after each experiment so as to be able to use the correct value of kinematic viscosity (ν) when applying Patel's calibration curve. It was found that by leaving the end of the Preston tube in a cup full of water when the flume was drained, the tubes did not need to be bled for each experiment (fig. 2.13). As the experiments proceeded the measured data was plotted out to ensure that the scatter was within reasonable limits, and that the shapes of the curves were not erroneous.

Because of the oscillation of the receiver's needle, a mean reading was taken visually at each point. It was found that the best way to take the readings was to space them closely (at 10 to 20mm intervals) and not to spend a long time in taking each reading. This was chosen in preference to measuring fewer points and taking more time over each to establish a better mean, because an electronic averaging device would have been necessary to take sufficiently accurate mean readings.

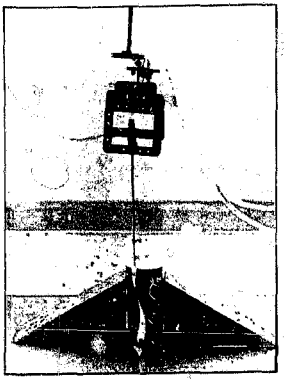


Fig. 2.13: Preston tube in a cup of water between experiments.



Fig. 2.14: Evidence of many hours of hard work.

CHAPTER 3: RESULTS

3.1 SHEAR STRESS PROFILES

Appendix 1 contains the shear stress profiles that were measured in the flume experiments described in the previous chapter. Smooth curves were drawn through the measured points, and these curves are presented in figs. 3.1 to 3.3 in a dimensionless form. The symbols in the definition sketch on these figures are defined as follows:

z_f = lateral distance across width of flood plain.
$z_p = 0$ at the junction.
z_c = lateral distance across width of main channel.
$z_c = 0$ at the junction.
τ_p = shear stress on the bed of the flood plain at a position defined by z_p
τ_c = shear stress on the boundary of the main channel at a position defined by z_c
τ_{pj} = shear stress on the flood plain at the junction
$\tau_{p\infty}$ = shear stress on the flood plain at infinity, ie. the plateau value for a wide flood plain
τ_{cj} = shear stress on the bed of the main channel at the junction

Presenting the profiles in this dimensionless form makes comparisons easy, and a qualitative idea can be gained of the behaviour of the shear stress profiles as the flow depth is varied. It is interesting to note that the general shapes of the curves for the rectangular geometry (fig. 3.1) is the same as the curves observed by Rajaratnam and Ahmadi (1981) and Knight and Lai (1985).

In fig. 3.1 it is not possible to compare the main channel and flood plain profiles because the former are shown relative to τ_{cj} and the latter are relative to τ_{pj}, and τ_{cj} is not equal to τ_{cj}. This problem is not en-

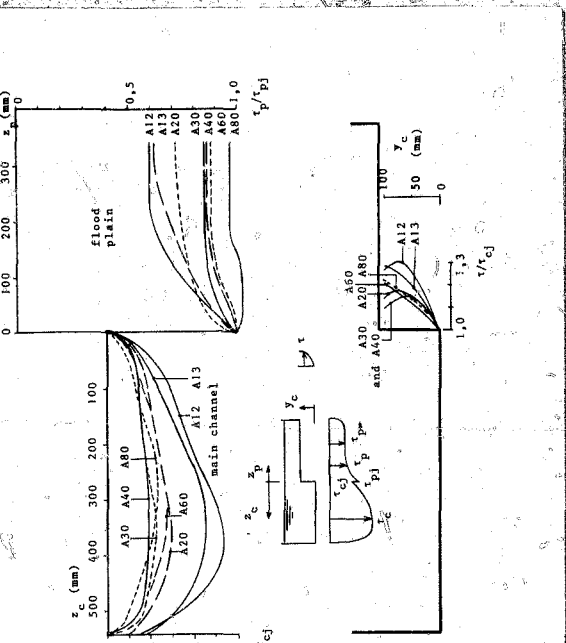


Fig. 3.1: Measured shear stress profiles for series A experiments, presented in a dimensionless form.

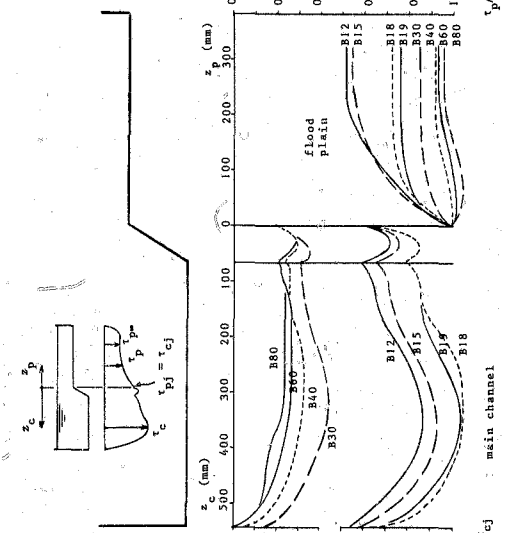


Fig 3.2: Measured shear stress profiles for series B experiments, presented in a dimensionless form.

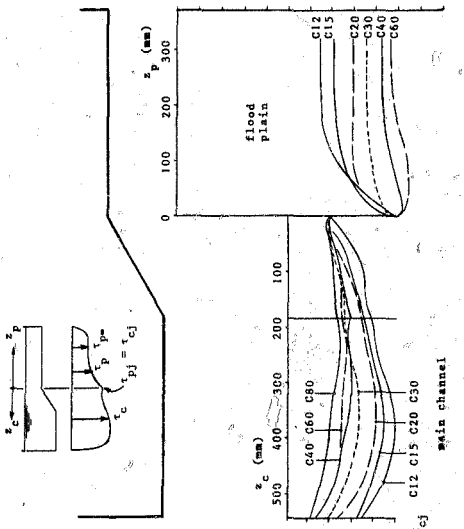


Fig. 3.3: Measured shear stress profiles for series C experiments, presented in a dimensionless form.

TABLE 3.1: VALUES OF τ_{cj}/τ_{pj} FOR FIG. 3.1.

experiment	τ_{cj}/τ_{pj}
A12	0,87
A13	0,92
A20	0,99
A30	0,94
A4C	0,89
A60	0,82
A80	0,87

countered with figs. 3.2 and 3.3 because in both these figures $\tau_{cj} \approx \tau_{pj}$. To clarify this issue in fig. 3.1, the relative magnitudes of τ_{cj} and τ_{pj} are given in table 3.1.

3.1.1 MAIN CHANNEL

For all three sets of experiments, the shear stress on the bed of the main channel has a peak value near mid channel. The profiles are distorted, being drawn down near the junction, because the flow in this region is slowed down by the interaction with the slower-flowing flood plain flow. For the rectangular geometry, the distortion of the profiles on the main channel bed generally decreases with increasing flow depth, because the turbulence intensity is decreasing. The 60° geometry behaves differently. For low depth ratios, distortion *increases* as the flow depth increases; then a reversal occurs, and the distortion starts *decreasing* with increasing flow depth, as for the rectangular geometry. The profiles for the 30° geometry behave in the same manner as for the rectangular geometry, ie. distortion of the profiles decreases with increasing flow depth. The behaviour of the shear stress profiles in the main channel

is complex, and needs further research for understanding and quantifying the patterns.

There is a "skewness" in the shapes of the main channel profiles: as z_c increases away from the junction, the shear stress initially increases sharply; then it flattens out somewhat before again increasing until it reaches the peak. Knight and Lai (1985) identified a similar pattern in their observed shear stress profiles and termed it the "skewing effect". Knight, Demetriou and Hamed (1983) attributed it to secondary flow cells that spiral along the bed of the channel (fig. 1.6).

The shapes of the profiles on the main channel bank for the 90° geometry are the same as those observed by Rajaratnam and Ahmadi. The trend is greater distortion for smaller flow depth. For experiments A60 and A80 the shear stress does not rise to a peak and then trail off, but it follows a continually rising curve. Rajaratnam and Ahmedi's curves exhibited the same behaviour at high flow depths. The shear stresses on the 60° bank all display a definite, well-defined peak. Those on the 30° bank have a completely different shape: they are not hump-shaped, but rise steadily as z_c increases. For low flow depths there is a dip in the profile near the junction.

The main channel shear stress profiles were not studied any further in this project because of time constraints. The main channel profiles are more complex than the flood plain profiles, and would require a detailed study using various geometries, widths and heights of the main channel, both with one flood plain (asymmetrical) and two flood plains (symmetrical). The shear stress profile on the flood plain has particular importance in that it can be used as a basis for describing the distribution of flow velocity; the vertical velocity profile at any location on the flood plain can be related to the local shear stress using a logarithmic equation. This is not valid in the main channel. (Rajaratnam and Ahmadi, 1981: p54.) The remainder of this study therefore concentrates on the flood plain shear stresses.

3.1.2 FLOOD PLAIN

By studying the shear stress profiles on the flood plain for the three sets of experiments, it can be seen that they form a family of curves as shown in fig. 3.4. Here it can be clearly seen that the plateau shear stress ($\tau_{p=}$) consistently increases relative to τ_{pj} as flow depth increases, ie. the higher the flow depth, the smaller is the distortion of the profiles.

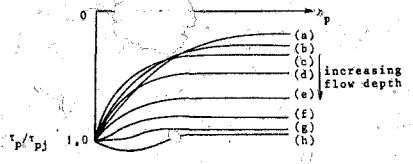


Fig. 3.4: General form of dimensionless shear stress profiles.

A reversal occurs in the shapes of the profiles at a low flow depth (about 20mm for the rectangular geometry). For flow depths smaller than this value, the initial part of the curve falls away more steeply as the flow depth increases (curves (a), (b) and (c) in fig. 3.4). For flow depths greater than this value, the curve flattens out as flow depth increases (curves (d), (e) and (f)). This continues until τ_{pj} is no longer a sharp point, but a peak plateau which extends into the flood plain (curve (g)). Then as flow depth increases further this peak moves away from the interface and into the flood plain region (curve (h)). τ_{pj} is no longer the peak shear stress on the flood plain, but a maximum τ_{pm} occurs close to the interface. Thus as flow depth increases, the position of maximum shear stress moves away from the junction and over the plain. For clarity

the maximum shear stress on the flood plain will be referred to as τ_{pm}, which coincides with τ_{pj} for low flow depths (very intense turbulence).

3.2 EFFECT OF BANK SLOPE

The effect that the slope of the main channel bank has on the shear stress profiles can be seen in fig. 3.5. The flood plain shear stress profiles are presented here in a new dimensionless form in which the shapes can be easily visualised. τ_p/τ_{pm} is the local shear stress relative to the plateau shear stress. z_p/l_p is a dimensionless lateral distance across the flood plain; l_p is the length of the interaction zone in the flood plain region, and values were obtained visually from the measured profiles. z_p/l_p is zero at the junction and is equal to 1,0 at the end of the interaction zone, where τ_p becomes τ_{pm}. The general trend noticeable from these curves is that as the flow depth increases, ie. turbulence becomes less intense, the curves progress from an exponential decay to a flat-topped curve.

The sloping main channel bank shifts the shear stress profile fairly significantly for d = 12mm. For d = 20mm and 30mm there is very little difference. For d = 40mm and 60mm the absolute differences are small, but larger in terms of percentages. In general τ_p/τ_{pm} is not altered by more than about 13%. Generally the shear stresses for the 60° geometry are lower than for a vertical bank, and those for the 30° geometry are even lower. The exception is the profile for the 12mm flow depth, where the shear stresses for the 60° bank are higher than for the vertical bank. As will be shown in 3.3, a sloping bank results in a lower turbulence intensity and therefore reduced shear stresses, except for a steep bank at a very low flow depth.

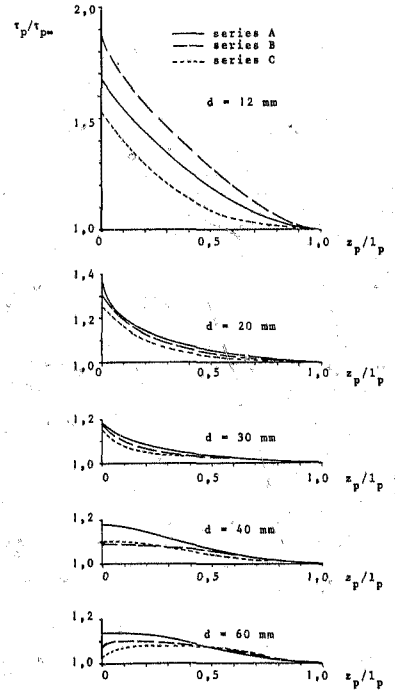


Fig. 3.5: Comparing flood plain shear stress profiles for different slopes of main channel bank.

3.3 PEAK SHEAR STRESS ON FLOOD PLAIN

Fig. 3.6 gives the peak shear stress ratio, $\tau_{pm}/\tau_{p\infty}$, as a function of the depth ratio. The peak shear stress ratio gives the distortion of the shear stress on the flood plain, and hence can be considered as a measure of turbulence intensity. As d/D increases, $\tau_{pm}/\tau_{p\infty}$ decreases, because the turbulence intensity increases with increasing flow depth. This graph was plotted while experiments were in progress to monitor the effect of the main channel bank slope on the turbulence intensity, and to ensure that the points were falling on smooth curves, which was a check against erroneous measurement of τ_{pm} and $\tau_{p\infty}$. This graph is significant in that a relationship for $\tau_{pm}/\tau_{p\infty}$ is important when developing a model for predicting shear stress profiles.

In fig. 3.6 it can be seen that for most conditions a sloping bank reduces $\tau_{pm}/\tau_{p\infty}$, and the more gentle the bank, the lower is $\tau_{pm}/\tau_{p\infty}$ for a given depth ratio. The conclusion that can be drawn from this is that a sloping bank reduces the turbulence intensity, because it results in a more gentle transition from the fast-flowing main channel to the shallow, slower-flowing flood plain.

At d/D approximately equal to 0,13 there is a crossing over of curves; for d/D less than this value $\tau_{pm}/\tau_{p\infty}$ for the 60° geometry is larger than for the rectangular geometry. This indicates that for very low flow depths, turbulence at the interface is more intense for a 60° geometry than for a rectangular geometry, and the 60° bank induces a more efficient momentum transfer than the 90° bank at low flow depths.

3.4 SUMMARY

This chapter has been mainly concerned with a qualitative appreciation of the results: the general shapes of the shear stress profiles, the effect that the steepness of the main channel bank has on the flood plain

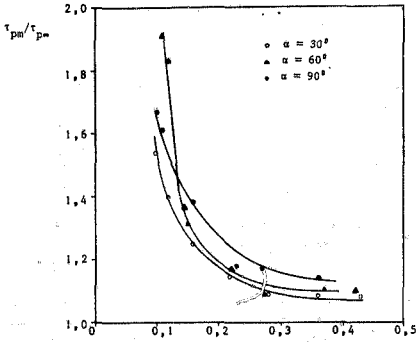


Fig. 3.6: Peak shear stress ratio.

shear stress profiles, the peak shear stress ratio $\tau_{pm}/\tau_{p\infty}$ being a measure of the turbulence intensity, and the observation that a sloping main channel bank results in a lower turbulence intensity than a vertical bank (except for a steep bank at very low flow depths, in which case the turbulence intensity is higher than for a vertical bank at the same low depth). The profiles of $\tau_p/\tau_{p\infty}$ are altered by up to about 13% by introducing a sloping bank.

In the next chapter the flood plain shear stress profiles will be analysed to develop predictive relationships.

CHAPTER 4: DATA ANALYSIS

The objective of this chapter is to develop a model for predicting the shear stress profile on a flood plain of a compound channel.

4.1 RAJARATNAM AND AHMADI'S MODEL

Rajaratnam and Ahmadi's model is described here since it will be referred to a number of times.

Rajaratnam and Ahmadi (1981) ensured that their flood plain was wide enough for the shear stress τ_p to reach its plateau value of $\tau_{pm} = \gamma dS$ where γ is the unit weight of water and S is the bed slope (for uniform flow). They plotted all their flood plain data as shown in fig. 4.1 in which the dimensionless parameter on the vertical axis represents the local shear stress, and z_p/b_p on the horizontal axis is a dimensionless lateral distance across the flood plain. b_p is defined such that $z_p = b_p$ when $(\tau_p - \tau_{pm})/(\tau_{pj} - \tau_{pm}) = 0,50$. The equation of the curve in fig. 4.1 is:

$$(\tau_p - \tau_{pm})/(\tau_{pj} - \tau_{pm}) = e^{-0,693x^2} \qquad (4.1)$$

where $x = z_p/b_p$.

It is important to note that this equation was not obtained by fitting a curve to the data points that are shown on the graph. It was an attempt to describe the shear stress profile using a curve of the same form as one describing lateral velocity profiles in the flood plain region (*Rajaratnam and Ahmadi, 1981; p50*).

From their measured shear stress profiles an average value of b_p was found to be:

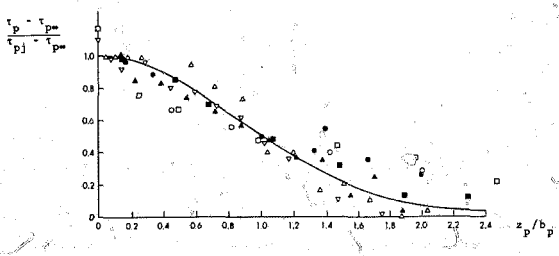


Fig. 4.1: Universal dimensionless shear stress profile.
(Rajaratnam and Ahmadi, 1981)

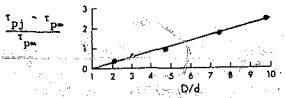


Fig. 4.2: Relationship for junction shear stress.
(Rajaratnam and Ahmadi, 1981)

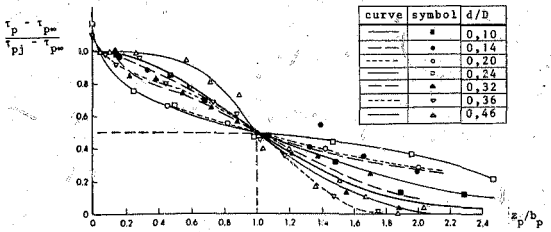


Fig. 4.3: Curves drawn through the points in fig. 4.1.

$$b_p = 0{,}64h \tag{4.2}$$

where h = height of step
$= D - d$

τ_{pj} is calculated from the equation of the straight line in fig. 4.2:

$$(\tau_{pj} - \tau_{p\infty})/\tau_{p\infty} = 0{,}2\,(D/d - 1) \tag{4.3}$$

All Rajaratnam and Ahmadi's shear stress profiles rose to a peak at the junction (ie. $\tau_{pj} = \tau_{p\infty}$) because they did not use high enough flow depths for the turbulence intensity to be sufficiently low for a hump to develop in the curve.

Before developing a model for shear stress profiles, a close examination of Rajaratnam and Ahmadi's universal curve (fig. 4.1) will throw some light on the subject. By drawing individual curves through the points plotted on this graph, it becomes evident that what seems to be scatter is actually a systematic deviation dependent on the depth ratio, as is demonstrated in fig. 4.3. When the author's data were plotted in the same form, a similar family of curves resulted. It can be concluded that equation 4.1 is an over-simplification, and a family of curves must be sought for.

Equations 4.1 to 4.3 express the shear stress distribution as a function of the depth ratio only. For the author's model to be a significant improvement on these equations, other parameters affecting the turbulent intensity must also be taken into account, including the slope of the main channel bank.

4.2 RELATIVE APPARENT SHEAR STRESS PROPOSITION

When developing a model for any parameter that is influenced by the turbulence phenomenon, one of the main considerations is what to use as the independent variables to represent the turbulent intensity. The approach that all researchers have used until now has been to use the depth ratio, roughness factors and geometric parameters. It would be very much more convenient if one independent parameter could be chosen to represent the turbulent intensity, embracing the effects of all these variables.

When surveying the literature it is evident that the apparent shear stress on the interface between the main channel and the flood plain, τ_a, is generally considered to be an indicator of the level of turbulence intensity. Knight, Demetriou and Hamed refer to it in their various articles.[1] Myers (1978) measured apparent shear stresses on the interface and interpreted them as a measure of the turbulence intensity. He maintained that the apparent shear stress can be thought of as representing the intensity of vorticity in the mixing region.

The author has chosen a dimensionless form of the apparent shear stress to account for the turbulent intensity, namely τ_a/τ_{pm} or $\tau_a/\rho gDS$, which will be referred to in this report as the *relative apparent shear stress* and abbreviated to τ_r (τ-ratio). This is a universally applicable independent parameter representative of the turbulence intensity. The use of a parameter such as τ_r means that the model to be developed in this section can be applied to any given roughness, geometry and flow depth, provided that the relative apparent shear stress is known.

Values of τ_a were found for each experiment by integrating the distorted portion of each observed shear stress profile (suggested by Rajaratnam and Ahmadi (1981), p55):

---

[1] Knight and Demetriou (1983), Knight, Demetriou and Hamed (1983), Knight, Demetriou and Hamed (1984), Knight and Hamed (1984).

$$\tau_a d = \int_{z_p=0}^{z_p=l_p} (\tau_p - \tau_{p\infty}) dz_p \qquad (4.4)$$

Values of $\tau_{p\infty}$ were found by assessing the observed profiles.

There are three elements to be considered in this model for shear stress profiles:

1. Shape equations describing the shapes of the profiles: a family of curves in a similar form to fig. 4.1.
2. Peak shear stress on the *flood plain: a means of* predicting τ_{pm}.
3. Length of interaction zone: a predictor for l_p.

4.3 SHAPE EQUATIONS

Curves were fitted to the observed shear stress profiles on the flood plain using a curve-fitting package for the HP9816 micro computer (Hewlett-Packard statistical software library for Series 200 computers, regression analysis disk 98820-13318). The equations are of the form:

$$(\tau_p - \tau_{p\infty})/(\tau_{pm} - \tau_{p\infty}) = f(x) \qquad (4.5)$$

which can be expressed as

$$\tau_p/\tau_{p\infty} = 1 + (\tau_{pm}/\tau_{p\infty} - 1)\, f(x) \qquad (4.6)$$

where $f(x) = ae^{-bx^k} - ce^{-dx}$ (4.7)

$$x = z_p/l_p \qquad (4.8)$$

Values for the constants a, b, c, d and k were found for each profile, and were plotted as functions of the relative apparent shear stress τ_r on a semi-log scale. It was found that by dividing the relative apparent

shear stress into three ranges, relationships could be defined for the constants such that a family of curves could be defined. The relationships are given below.

τ_r = 0,02 - 0,10:

$a = 1{,}006 + 4{,}435e^{-11{,}34(\tau_r - 0{,}02)^{0{,}156}}$ (for τ_r = 0,022 - 0,07)

$a = 1{,}103\ [\log(0{,}101/\tau_r)]^{0{,}00194}$ (for τ_r = 0,07 - 0,10)

$b = 0{,}56 \log \tau_r + 4{,}32$

$c = -0{,}912\ (\log \tau_r + 1)$

$d = 36{,}7 \log \tau_r + 67{,}9$

$k = -4{,}10 \log \tau_r - 1{,}46$ ...equations (4.9)

τ_r = 0,10 - 0,25:

$a = 1{,}0$

$b = 0{,}56 \log \tau_r + 4{,}32$

$c = 0$

$d = 0$

$k = -4{,}10 \log \tau_r - 1{,}46$ ...equations (4.10)

τ_r = 0,25 - 6:

$a = 1{,}0$

$b = 4{,}05 - 0{,}253\ \tau_r$

$c = 0$

$d = 0$

$k = 1{,}0$ ...equations (4.11)

It is important that the first equation for "a" in set (4.9) must not be used for τ_r less than 0,022, because this would result in a large error. The relationship for "a" for τ_r from 0,02 to 0,10 is shown in fig. 4.5.

The family of curves is shown in the form of equation 4.5 in fig. 4.4, which can be used directly for manual plotting of a shear stress profile. Each curve represents a value of τ_r, ie. each curve corresponds to a particular level of turbulence intensity. Note that the curves should ideally have an ordinate of zero when $z_p/l_p = 1{,}0$, but in fig. 4.4 they have a small positive value. This arises because of the choice of best-fitting shape parameters. However, τ_p is generally within 5% of

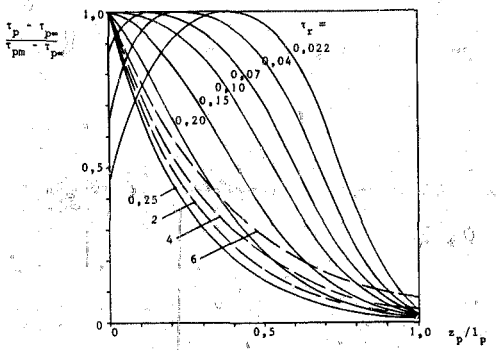


Fig. 4.4: Family of curves representing shape equations for shear stress profile model.

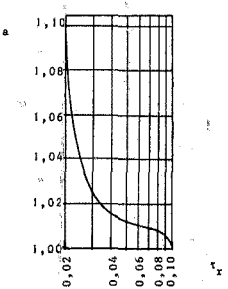


Fig. 4.5: Curve for parameter "a", equations 4.9.

$\tau_{p\infty}$ at $z_p = l_p$, which is acceptable when one considers that the shear stress drops asymptotically to its plateau value of $\tau_{p\infty}$.

This set of curves demonstrates the convenience of using a single parameter to represent the turbulence intensity, namely τ_r. If the two parameters d/D and α were used *instead of* τ_r, *then a separate family* of curves would be required for each value of α, with each family of curves having d/D as its independent variable. If other parameters that influence the turbulence phenomenon were also considered, then the solution would become impossibly complicated.

To use these equations values of l_p and τ_{pm} are needed. The equations are dimensionless and describe only the shape of a profile, and actual magnitudes are obtained by inputting values for τ_{pm} and $\tau_{p\infty}$ hence the term "shape equations". The alternative would have been to imbed the effects of τ_{pm} into the equations in empirical constants, expressing $\tau_p/\tau_{p\infty}$ as a function of τ_r and z_p/l_p only. However, the form chosen is more versatile in that the user can input whatever values of τ_{pm} he chooses.

4.4 PEAK SHEAR STRESS ON FLOOD PLAIN

Fig. 4.6 shows the peak shear stress ratio $\tau_{pm}/\tau_{p\infty}$ plotted *versus* τ_r on a semi-log scale, which prevents crowding of points at low values of τ_r. The following curve was fitted to the data (the solid line in fig. 4.6):

$$\tau_{pm}/\tau_{p\infty} = 1{,}09 + 0{,}0116\ (\log \tau_r + 2)^{4{,}09} \qquad (4.12)$$

This graph does not display excessive scatter, which promotes confidence in the proposition that τ_r can be used as the independent parameter representing turbulence intensity.

Comparison with Rajaratnam and Ahmadi's data is made possible by combining two of their equations:

$$\tau_{pm}/\tau_{p\infty} - 1 = 0{,}24\ (D/d - 1) \qquad (4.13)$$

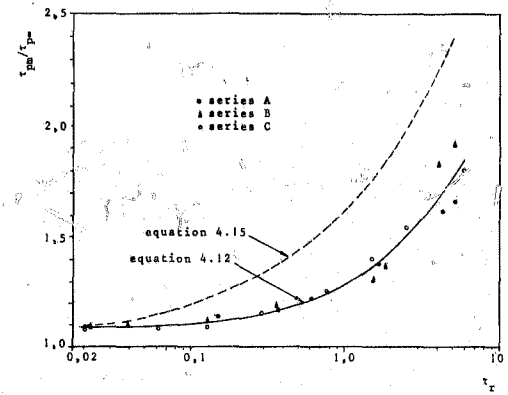


Fig. 4.6: Relationships for peak shear stress on flood plain.

$$\tau_a/\tau_{p=} = 0{,}15\ (D/d - 1)^2 \qquad (4.14)$$

to yield:

$$\tau_{pm}/\tau_{p=} = 1 + 0{,}620\ \sqrt{\tau_r}. \qquad (4.15)$$

Equation 4.15 is plotted as a dashed line on fig. 4.6. Two observations are readily apparent:

1. The shapes of the two curves are the similar, namely concave upwards, which supports the general form of equation 4.12.
2. The magnitudes of $\tau_{pm}/\tau_{p=}$ predicted by Rajaratnam and Ahmadi's relationship are significantly larger than those predicted by equation 4.12 (by 1,00 to 1,36 times).

The second factor is critical since it is important to know that a relationship is reliable if it is to be used for predictive purposes. The

discrepancy between the two curves is probably because of the position where the junction shear stresses were measured. *In the author's experiments* τ_{pj} was measured at the top of a rounded corner; if the edge of Rajaratnam and Ahmedi's flood plain was a sharp corner, then different values would have been measured. It must be borne in mind that the validity of equation 4.14 is questionable, the reasons for which are discussed in Appendix 2, where the derivation of this equation is given. In view of the uncertainties in Rajaratnam and Ahmadi's relationship, the use of equation 4.12 is recommended. However, further research is necessary to clarify this issue.

What is probably of most significance is that $\tau_{pm}/\tau_{p=}$ can definitely be expressed as a unique function of τ_r, irrespective of the slope of the main channel bank.

4.5 LENGTH OF INTERACTION ZONE

The length of the interaction zone on the flood plain, l_p, is the *lateral* distance across the flood plain from the junction to a point where the shear stress is no longer influenced by the turbulent interaction mechanism. In order to define a relationship for this quantity a value of l_p was selected for each experiment by visually assessing the measured shear stress profiles, and identifying the point at which τ_p is approximately equal to $\tau_{p=}$. Values of l_p/d were plotted versus τ_r as in fig. 4.7. τ_r was used as the independent variable in keeping with the relative apparent shear stress proposition. l_p/d was adopted because this is the most appropriate way of representing l_p, since the mixing in the interaction zone is caused by large eddies which presumably have a size *proportional* to d (*Rajaratnam* and Ahmadi, 1981: p52). The following equation was fitted to the data in fig. 4.7:

$$l_p/d = 3,17 + 0,569\ (\log \tau_r + 2)^{3,43} \qquad (4.16)$$

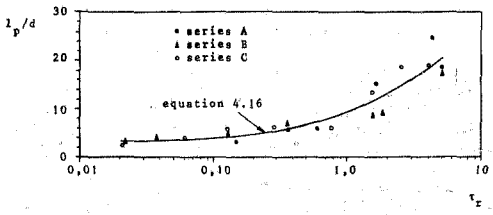


Fig. 4.7: Relationship for the length of the interaction zone on the flood plain, l_p.

There is a fair amount of scatter in fig. which is associated with the subjective assessment of l_p.

4.6 SHEAR STRESS PROFILE MODEL

The model for predicting shear stress profiles on a flood plain consists of the shape equations, 4.9 to 4.11, represented graphically as a family of curves in fig. 4.4; a relationship for the peak shear stress, equation 4.12, shown in fig. 4.6; and a predictor for the length of the interaction zone, equation 4.16, shown in fig. 4.7.

The model was used to generate the set of dimensionless curves shown in fig. 4.8, the only input parameter being τ_r for each curve. Note the interesting progression in curve shape as τ_r varies from 6,0 to 0,022: from an exponential decay to a flat-topped curve to a peaked curve. This graph can be used to plot out a profile instead of using the equations. Fig. 4.9 is a representation of the shape equations, showing the general forms of the profiles for the three ranges of τ_r.

In fig. 4.10 the author's observed data have been superimposed on curves generated by the prediction model. Virtually all the curves display a good fit, which indicates that the model can be used with confidence.

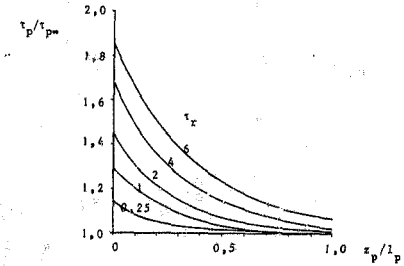
In the light of current thought concerning the turbulence phenomenon, the relative apparent shear stress can be considered to be a good indicator of turbulence intensity. The use of τ_r as the independent parameter representing the turbulence intensity in a compound channel has been successfully demonstrated in developing a shear stress profile model from the author's data, as shown by the good correlations in the relationships for τ_{pm} and l_p (figs. 4.6 and 4.7), and by the good fit between the curves generated by the model and the observed data from which the shape equations were derived (fig. 4.10).

This model has two main limitations:

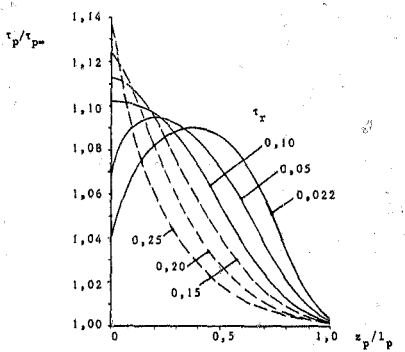
1. The range of τ_r considered (0,022 to 6). As will be seen in part 2, τ_r can reach values as high as 30 for very high levels of turbulence.
2. The data on which the model is based comes from a compound channel with smooth boundaries.

The first consideration imposes a limit on the range of applicability of the model. Concerning the second limitation, it is known that if the flood plain is rough relative to the main channel, the apparent shear stress is greatly increased. The question that this poses is whether the model is applicable to such situations, which often occur in practice. Pasche and Rouve (1985) observed that the momentum exchange when the flood plain is very much rougher than the main channel, appears to be of the same nature as that observed in compound channels of uniform roughness. Taking this statement to its logical conclusion, this implies that the same techniques can be applied when the flood plain is rough as when it is smooth, and the shear stress profile model can safely be applied to rough flood plains. However, further research is required to confirm this.

A program for the shear stress model on the MP85 micro computer is listed and detailed in Appendix C.



(a) τ_r = 0,25 - 6,0



(b) τ_r = 0,022 - 0,25

Fig. 4.8: Family of curves generated using the shear stress profile model.

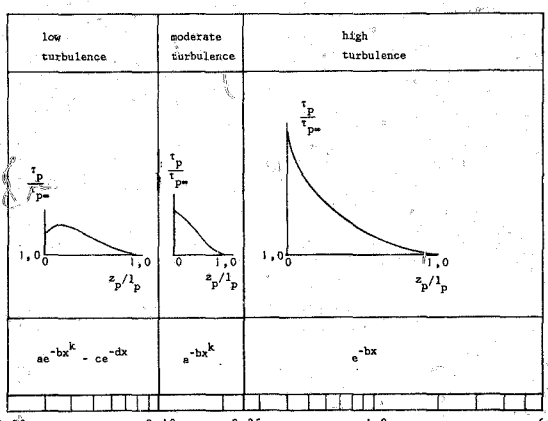


Fig. 4.9: Forms of shape equations.

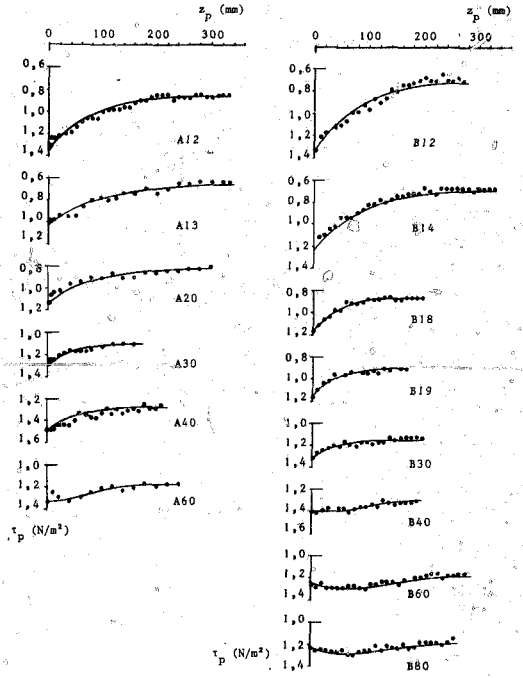


Fig. 4.10: Observed data superimposed on curves generated by shear stress profile model.

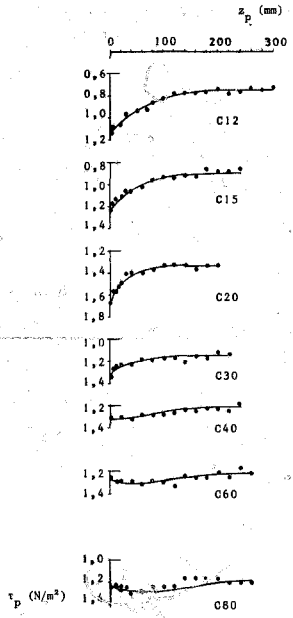


Fig. 4.10 (continued): Observed data superimposed on curves generated by shear stress profile model.

PART 2: DISCHARGE COMPUTATION AND RELATIVE APPARENT SHEAR STRESS PREDICTION

CHAPTER 5: DISCHARGE COMPUTATION

The need for accurate and practical methods for computing the discharge in a compound channel has already been emphasised. A survey of existing methods is presented here, outlining a history of the attempts that have been made to solve this problem. Using published flume data, five methods will be compared and assessed: two existing methods and three developed by the author.

5.1 SURVEY OF DISCHARGE COMPUTATION METHODS

In order to formulate an improved discharge computation method for compound channels, a comprehensive survey of all the existing methods was carried out. These methods are briefly described in order to paint a background to this problem. Particular attention will be paid to a number of the interface methods, as some of the ideas that they embrace will be further developed later in this chapter.

Prinos and Townsend (1984) observed that the methods of discharge computation fall roughly into three categories:

1. Treating the section as a single, composite channel with an averaged Manning's roughness coefficient n or an averaged hydraulic radius.
2. Methods based on correction factors.
3. Dividing the compound channel into sub-channels, calculating the discharge separately for each sub-section, and summing the discharges to obtain the total discharge for the compound section. The interfaces that separate the sub-sections may be vertical, horizontal or inclined. The hydraulic radius of each sub-section must account for the apparent shear stress on the interface. This is done by either evaluating the shear stress on the interface or by locating an interface where there is zero shear stress.

5.1.1 COMPOSITE CHANNEL APPROACH

Averaged hydraulic radius

Posey (1967) reported a method that uses diagonal interfaces to subdivide the compound section. The interfaces, shown in fig. 5.1, are such that they bisect the angles bcd and efg. An effective hydraulic radius is calculated for the entire section by weighting the subsections as follows:

$$R_{ave} = (A^2/abc + B^2/cdef + C^2/fgh)/(A + B + C) \qquad (5.1)$$

where A represents the area of section A, B the area of section B, etc. Note that the diagonal interfaces have been excluded from the wetted perimeters in this equation. This method is complicated to use because of the awkward geometry. Posey presented experimental data showing that this method produces poor results.

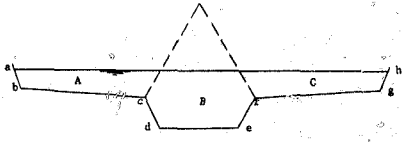


Fig. 5.1: Diagonal interfaces for calculating an effective hydraulic radius (Posey, 1967).

Averaged Manning's n

Yen and Overton (1973) evaluated three fairly well-established equations for calculating an equivalent Manning's n which can be used in applying Manning's equation to the composite section. The equations are:

$$n_e = \left(\Sigma \frac{P_i n_i^{3/2}}{P}\right)^{2/3} \qquad (5.2)$$

$$n_e = \left(\frac{\Sigma P_i n_i^{2}}{P^{1/2}}\right)^{1/2} \qquad (5.3)$$

$$n_e = \frac{PR^{2/3}}{\Sigma\left(\frac{P_i R_i^{2/3}}{n_i}\right)} \qquad (5.4)$$

where n_e = equivalent Manning's n for the composite section
n_i = Manning's n for the i'th subsection
P_i = wetted perimeter of the i'th subsection
R_i = hydraulic radius of the i'th subsection
P = wetted perimeter of the entire cross-section
R = hydraulic radius of the entire cross-section

The assumption made in developing equation 5.2 was that each sub-section has the same mean velocity, which is also equal to the mean velocity of the entire cross-section. This assumption is grossly in error, and the use of this equation produces poor results when applied to compound channels.

The assumption for equation 5.3 is that the total resistance is equal to the resistance summed over all the sub-sections. Yen and Overton reported that when applying this equation to compound channels, discharges were significantly over-estimated.

The assumption behind equation 5.4 was that the total discharge for the entire cross-section was equal to the sum of the discharges of the sub-sections. Yen and Overton did not evaluate this equation.

Having calculated an average n-value, the compound section is treated as a single composite section for discharge computation. Prinos and Townsend (1984) showed that this approach produces poor discharge estimates.

5.1.2 CORRECTION FACTORS

Methods based on corroction factors divide a channel into homogeneous sections, calculate the discharge separately for each section, and apply an empirical factor (k) to each section. If i refers to the i'th section then the total discharge is given by

$$Q = \Sigma k_i (1/n_i) A_i R_i^{2/3} S_i^{1/2} \qquad (5.5)$$

Le van Kiyen (1968) and Karasev (1969) presented correction factors for various hydraulic and geometric conditions. Prinos and Townsend (1984) found that these factors either over- or under-estimated the discharge.

5.1.3 INTERFACE APPROACH

Popular method

The most commonly used procedure is to divide the channel with vertical interfaces as shown in fig. 5.2. The vertical interfaces are included in the wetted perimeter of the main channel, because the shear force on these plains retards the flow in the main channel. They are excluded from the wetted perimeters of the flood plains because the shear stress on these plains does not retard the flood plain flow, but assists it. Because of its popularity this will be referred to as the "popular method".

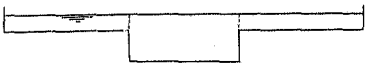


Fig. 5.2: Sub-division of channel using vertical interfaces.

Posey (1967) suggested that for d/h < 0,3 the interfaces should be included in the wetted perimeter of the main channel; for d/h > 0,3 they should be excluded; and they should be excluded from the flood plain wetted perimeter for all flow depths. This recommendation was based on flume studies.

Several researchers have tested the popular method on flume data and found that it significantly over-estimates the discharge at low flow depths (Sellin, 1964; Posey, 1967; Myers, 1978; Wormleaton, Allen and Hadjipanos, 1982; Prinos and Townsend, 1984). The reason for this is that including the vertical interfaces in the wetted perimeter of the main channel implicitly assumes that the average apparent shear stress on these interfaces is the same as the average shear stress on the main channel boundary. However, experiments have shown that the apparent shear stress can be considerably higher than the average shear stress on the boundary.

Wormleaton, Allen and Hadjipanos (1982) tested the popular method on laboratory data. Their results indicated that discharge will be over-estimated by up to 20% for d/D less than 0,26 if the main channel and flood plain are both smooth, and over-estimated by up to about 80% for d/D less than 0,43 if the flood plain is rough relative to the main channel. Similar trends were observed by Prinos and Townsend (1984). The rougher the flood plain is, the greater is the velocity difference between the main channel and flood plain; hence the turbulence at the interface is higher, resulting in a higher apparent shear stress on the interface, which the popular method does not cater for.

Despite the fact that the popular method has been shown conclusively to yield very poor estimates of discharge, it is still used extensively, probably because it is simple and easy to implement, and no satisfactory alternative has been proposed.

Shear force on interface

Wright and Carstens (1970) conducted laboratory experiments in which they measured apparent shear stress on the junction interface to be of the same order of magnitude as the boundary shear stress in the main channel.

Hence they proposed calculating the main channel average shear stress from γRS, in which the wetted perimeter includes the vertical junction planes. The shear force on the junction planes can then be calculated and applied as a propulsive force to the flood plain section. Essentially this is the same as the popular method, and the same criticisms apply. This approach falls down when the shear stress on the interface far exceeds that on the main channel boundary. When the author investigated main channel shear stresses using flume data published by Wormleaton, Allen and Hadjipanos (1982), it was found that the apparent shear stress τ_a reaches values up to five times γRS.

Inclined interface

A common approach to discharge analysis in compound channels is to use either vertical, diagonal or horizontal interfaces to separate the main channel and flood plain regions, and either include or exclude the interface planes in the wetted perimeters, according to the magnitude of the apparent shear stress on these interfaces. Yen and Overton (1973) proposed a new approach: the interface should have an angle of inclination to the horizontal of θ (fig. 5.3) such that there is zero longitudinal shear stress on the interface plane. The division line can therefore be excluded from the wetted perimeter.

The isovels are distorted in the region of the interface, and division lines can be drawn such that they intersect the isovels at right angles. Hence there are no velocity gradients normal to the division lines, and no momentum exchange occurs across them. They therefore form a more logical division between the main channel and flood plain flows than a vertical division line.

Yen and Overton found that the division lines are generally slightly curved but can usually be approximated by straight lines. They plotted θ as a function of the depth ratio for their flume data, and found that a smooth curve could be defined for each different geometry and boundary roughness.

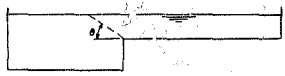


Fig. 5.3: Inclined division line used in Yen and Overton's approach (Yen and Overton, 1973).

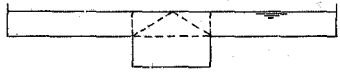


Fig. 5.4: Vertical, horizontal and inclined division lines evaluated by Wormleaton, Allen and Hadjipanos (1982).

Once θ has been established, it is a simple matter to apply Manning's equation to each sub-section, ignoring the division line from the wetted perimeters.

Yen and Overton maintained that Manning's n in each sub-section should be modified because it is influenced by channel geometry as well as boundary roughness, and they developed a modified version of Manning's equation to cater for this effect. However, the complexity of the equation renders it somewhat formidable.

Knight and Lai (1985) observed that the isovels at the interface clearly show that as the flow depth increases, the angle of inclination of the zero shear stress plane also increases. They observed a value for θ of about 50° for d/D = 0,41, and 5° for d/D = 0,13. Although these values would be different for different geometric and roughness conditions, they give an idea of the order of magnitude that can be expected. Knight and Lai concluded that the plane varies from an inclined one to a nearly horizontal one as flow depth decreases, which is the same as Yen and Overton's observations.

Although Yen and Overton's idea of an inclined interface is promising because of its *simplicity*, no one has developed it into a practically usable form by providing a generally applicable means of estimating θ.

λ-method

Wormleaton, Allen and Hadjipanos (1982) evaluated the use of vertical, horizontal and diagonal division lines (fig. 5.4) by applying them to flume data. They found that discharge is over-estimated by up to about 80% when using vertical interfaces, up to 60% when using diagonal interfaces, and 20% for a horizontal interface.

Wormleaton at al recommended using either diagonal or horizontal interfaces, because the apparent shear stresses are lower than on vertical interfaces. Using their own flume data they established a criterion to determine whether the interface should be included in the main channel wetted perimeter or ignored.

λ is defined as the ratio of the apparent shear stress on the diagonal or horizontal interface, to the average shear stress in the main channel,

$$\lambda = \tau_{ai}/\gamma RS \qquad (5.6)$$

where the wetted perimeter in R includes the interface. λ lies between 0 and 1,0. Their data indicate that if λ is less than 0,5 then the interface plane should be *excluded* from the wetted perimeter of the main channel, ie. it is assumed to offer no resistance to the flow; and for λ greater than 0,5 it should be *included* in the wetted perimeter, ie. assumed to offer the same resistance as the average for the rest of the main channel. The interface is always excluded from the flood plain wetted perimeter because it is assumed that wide flood plains will be considered, and therefore the propelling effect of the interface on the flood plain will be small. For convenience this will be referred to later as the λ-method.

Friction factor modification

Myers (1984) suggested that the traditional uniform flow formulae can be applied to compound channels without modification, and only the friction factor needs to be altered. He showed that friction factors are functions of channel geometry, the depth ratio and the Reynolds number, but he did not present a practical means of predicting the friction factor.

Model for natural channels

Pasche and Rouve (1985) investigated discharge computation for a section having a sloping main channel bank and a flood plain that is roughened with non-submerged vegetation (such as trees and bushes). They developed a complex set of equations, for which Pasche (1984) presented an algorithm for use on a personal computer. Their analysis was based on the assumption that the main channel - flood plain interface has the same effect as an imaginary solid vertical wall slightly offset into the flood plain.

None of the methods described in this section has been shown to produce truly reliable discharge predictions for all flow conditions.

5.2 DEVELOPMENT OF IMPROVED METHODS

The author's flume data were inadequate for use in developing a discharge computation model because the discharges could not be measured with sufficient accuracy using the available laboratory equipment, and also data with a range of bed roughnesses and geometries were required to formulate a generally applicable model. Accordingly the available published flume data were used: the data of Wormleaton, Allen and Hadjipanos (1982) comprising 40 data items, with four different flood plain roughnesses, one width of flood plain, and a variety of bed slopes; and the data of Knight and Demetriou (1983) comprising 18 items, using a smooth main channel and

TABLE 5.1: PERTINENT PARAMETERS IN PUBLISHED FLUME DATA

Parameters	Data of Wormleaton et al.	Data of Knight and Demetriou.
W_p/W_c	1,6	0,5; 1,0; 1,5
n_p/n_c	1; 1,27; 1,55; 1,91	1,0
d/D	0,11 - 0,43	0,11 - 0,51
S	0,00043; 0,00094; 0,00101; 0,0018; 0,00132	0,000966
τ_r	0,58 - 17,4	0,30 - 28,1
no. of items	40	18

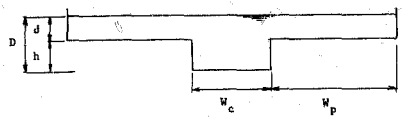


Fig. 5.5: Definition sketch for symbols used in chapters 5 and 6.

flood plain, one bed slope, and four different widths of flood plain. This makes a total of 58 data items. All the data are from symmetrical sections with a flood plain on either side. The ranges of salient parameters are given in table 5.1, and the data are listed in detail in Appendix D. Fig. 5.5 defines the parameters.

The following nomenclature for geometric parameters has been adopted for Part 2 of this report:

P_c = physical wetted perimeter of main channel
$= W_c + 2h$
P_p = physical wetted perimeter of flood plain
$= W_p + d$
P_c' = modified wetted perimeter of main channel
P_p' = modified wetted perimeter of flood plain
A_c = area of main channel
$= W_c D$
A_c' = modified area of main channel
A_p = area of flood plain
$= W_p d$
A_p' = modified area of flood plain

Two of the discharge computation methods discussed in 5.1 were selected for evaluation: the popular method, because it is commonly used, and the λ-method, because it is the most satisfactory method for practical application that has been proposed to date. These two methods were tested using 17 data items from the data of Wormleaton et al, and compared with methods developed by the author. A program was written for the HP85 micro computer to evaluate the five methods using rectangular flume data. The program, "QCOMP", is listed and described in Appendix C. One of the input parameters is τ_r which is required in some of the discharge computation methods, and was calculated from the values of apparent shear stress published with the flume data.

For each method the percent error was computed between the measured discharges and the predicted discharges, and the results presented in graphical form in fig. 5.6. The percent error is given as a function of

the depth ratio for a particular run of experiments, ie. for a particular bed slope and flood plain roughness. The general trend is that the error in computed discharges is greatest at low flow depths, which is when the turbulence intensity is at its highest. By comparing figs. 5.6(a) and (c) it can be seen that the rougher the flood plain is relative to the main channel, the more the discharge is over-estimated; and figs. 5.6(a) and (b) indicate that error increases with increasing bed slope.

The five methods are outlined below.

5.2.1 POPULAR METHOD

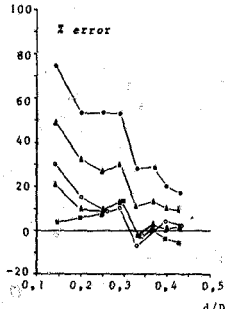
It can be seen in fig. 5.6 that at low flow depths the popular method grossly over-predicts the discharge, over-estimating by up to almost 90%. The reason for this is in the assumption made concerning the wetted perimeter, namely that the apparent shear stress on the interface is either zero or is the same as the average shear stress on the main channel boundary. For low flow depths the apparent shear stress has been shown to be many times this value.

The wetted perimeters of the main channel and flood plain may be defined as follows:

$$P_c' = P_c + 2kd \qquad (5.7)$$

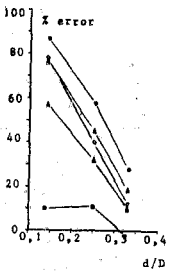
$$P_p' = P_p \qquad (5.8)$$

The popular method assumes that k = 1 for d/h < 0,3 (d/D < 0,23) and k = 0 for d/h > 0,3 (d/D > 0,23), which is a step function. In order to demonstrate the shortcomings of this assumption, the data of Wormleaton et al were used to generate true values of k. These are plotted in fig. 5.7, where it is evident that k should range from 0 to about 28, not from 0 to 1. A general trend is noticeable: the rougher the flood plain is relative to the main channel, the higher is the value of k, because the turbulence intensity is increased when the flood plain is roughened.



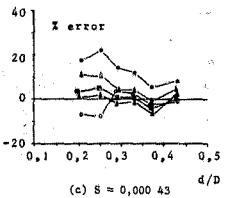
(a) S = 0,000 43

n_p/n_c = 1,9



(b) S = 0,000 94

n_p/n_c = 1,9



(c) S = 0,000 43

n_p/n_c = 1,3

- popular method
- k-method
- area method
- λ-method
- modified k-method

Fig. 5.6: Error in discharge computation, as tested on the data of Wormleaton, Allen and Hadjipanos (1982).

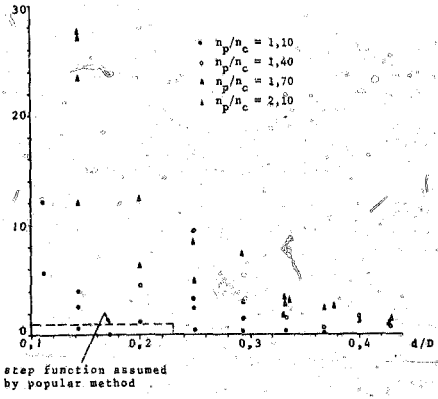


Fig. 5.7: Values of k derived from the data of Wormleaton, Allen and Hadjipanos (1982).

5.2.2 LAMBDA-METHOD

In his model describing the transverse deposition of sediment in compound channels, James (1985) used the λ-method for discharge calculation proposed by Wormleaton, Allen and Hadjipanos (1982). Wormleaton et al stated that there is no apparent advantage in using either the horizontal or diagonal interfaces. Since a horizontal interface creates an unrealistically small main channel section, James considered diagonal interfaces to be more appropriate. Accordingly diagonal interfaces are used here to evaluate the performance of the λ-method.

λ can be expressed as:

$$\lambda = \tau_{ai}/\tau_c \tag{5.9}$$

The average shear stress in the main channel (τ_c) is equal to the streamwise weight component of the water contained in the main channel section within the diagonal interfaces, divided by the total wetted perimeter of the main channel section:

$$\tau_c \approx \gamma AS/(P_c + 2l) \tag{5.10}$$

where A = area enclosed by the diagonal interfaces

l = length of one diagonal interface

The apparent shear stress on the diagonal interface (τ_{ai}) can be calculated from the following equation, which comes from equilibrium considerations:

$$\tau_{ai} = (\tau_r d - \tfrac{1}{4} W_c)\gamma dS/l \tag{5.11}$$

A routine was included in QCOMP to calculate values of λ using the measured values of τ_a published with the flume data.

Fig. 5.6 shows that, in comparison with the other methods, the λ-method yields fairly good estimates of discharge, except for the data set with a steep bed slope. In fig. 5.6(c) the discharge error takes a sudden jump from a negative to a positive value at d/D approximately equal to 0,25. This corresponds to the point where λ exceeds 0,5 and the interface is no longer included in the wetted perimeter of the main channel. Since the wetted perimeter represents the resistance to flow, this results in an increase in the predicted discharge. The popular method takes this jump at a depth ratio of 0,23, above which the vertical interface is excluded from the wetted perimeter. The λ-method is simply a refinement of the popular method: diagonal interfaces are used instead of vertical, because the apparent shear stress is lower on a diagonal interface than a vertical one; and the inclusion of the interface in the main channel wetted perimeter is based on a better criterion than the depth ratio. Since the depth ratio is not the sole indicator of turbulent intensity, it is simplistic to attempt to use it to determine the value of k, as is demonstrated in fig. 5.7.

The λ-method, although seen in fig. 5.6 to give reasonable estimates of discharge, is by no means ideal for practical applications. James found

that the discharges predicted by this method are not always accurate because "the apparent shear stress criterion is rather vague and requires further experimental investigation" (James, 1984: p76). He also found that the use of this method can lead to the main channel velocities being calculated smaller then the flood plain velocities. Although this method has serious shortcomings, a survey of the literature indicates that it is the most satisfactory method that has been proposed to date. It is therefore necessary either to improve on this method or to develop a better method.

5.2.3 AREA METHOD

The author investigated three approaches to the problem of discharge computation. The first one modifies the areas of the main channel and flood plain, hence the name "area method."

This method is based on Yen and Overton's proposition of an interface inclined into the main channel at an angle that is determined by the level of turbulence such that there is zero shear stress on the interface (Yen and Overton, 1973). Referring to fig. 5.8, the area correction ΔA may be derived theoretically as follows.

Consider the equilibrium of forces in the flood plain region, when a vertical interface divides the main channel from the flood plain:

$$SF_p - \tau_a d = \gamma A_p S$$

where SF_p is the shear force on the physical wetted perimeter of the flood plain, P_p. Consider equilibrium when an inclined interface is used, such that there is zero shear force on the interface:

$$SF_p = \gamma(A_p + \Delta A)S$$

Combining these two equations yields

$$\gamma(A_p + \Delta A)S - \tau_a d = \gamma A_p S$$

Simplifying:

$$\Delta A \approx \tau_r d^2 \qquad (5.12)$$

This could be further reduced to solve for θ:

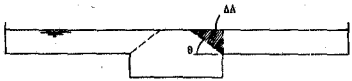


Fig. 5.8: Area adjustment.

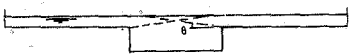


Fig. 5.9: Intersecting diagonals at low flow depths.

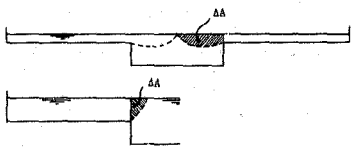


Fig. 5.10: Probable shapes of zero shear stress interfaces.

$$\cot\theta = 2\tau_r \qquad (5.13)$$

Having defined θ, Yen and Overton divide the compound channel into main channel and flood plain regions by means of the inclined interfaces, and exclude the interfaces from the wetted perimeters. However, when the author applied this to the flume data, it was found that for low flow depths the two diagonals intersect, as shown in fig. 5.9.

To avoid this problem ΔA can be used directly. This also has the advantage that no knowledge is required of the shape of the interface, and it is not necessary to assume that the interface is a straight line. The main channel and flood plain are simply separated using a zero shear

stress interface of unknown shape (something like those sketched in fig. 5.10) which is excluded from the wetted perimeter.

An area adjustment is made as follows:

$$A_c' = W_c D - 2\Delta A$$
$$= A_c - 2\Delta A \qquad (5.14)$$

$$A_p' = W_p d + \Delta A$$
$$= A_p + \Delta A \qquad (5.15)$$

For an asymmetrical channel having only one flood plain, the modified area of the main channel would be

$$A_c' = A_c - \Delta A. \qquad (5.16)$$

When the area adjustment has been made the discharge can be calculated by applying Manning's equation to each sub-section, using the modified areas and the physical wetted perimeters.

The author used the flume data to generate values of ΔA, using the measured values of τ_r. It was found that for very low flow depths ΔA would protrude slightly below bank full level, ie. ΔA was greater than $\frac{1}{2}W_c d$. However, ΔA always remained a very small fraction of A_c, and so this is not significant.

Fig. 5.6 shows that the area method performs very favourably compared with the other methods. Sometimes it over-estimates the discharge, which could be attributed to Yen and Overton's belief that the friction factor needs to be modified as a result of the turbulence phenomenon. Good results could be obtained from the area method if correction factors were developed for Manning's n. Alternatively the solution could be simplified by lumping together the two effects of adjusted area and modified friction factor, and using ΔA to account for both effects. An empirical correction to the theoretical equation (5.12) for ΔA would be required, so that ΔA fully accounts for the turbulence phenomenon.

The writer investigated the possibility of developing such a correction using the flume data. Values of ΔA were generated that exactly predicted the measured discharges, and were plotted as functions of parameters such as v_c/v_p, τ_r and $\tau_r d^2$. (v_c and v_p are the average velocities in the main

channel and flood plain regions respectively.) There was too much scatter for any good relationships to be defined, and additional parameters may be required in order to compress this scatter.

5.2.4 K-METHOD

As has already been pointed out, the wetted perimeter in a resistance equation is the means of accounting for the shear stress on the boundary. The larger the wetted perimeter, the greater is the resistance to flow, and the lower is the discharge. In the main channel of a compound section the wetted perimeter has to account for two effects if a traditional resistance equation is being used: a high apparent shear stress on the interface, and a reduction in the shear stress on the physical boundary of the main channel. The wetted perimeter could be modified as follows to account for this, assuming vertical interfaces dividing the main channel and flood plain regions:

$$P_c' = P_c + 2k_c d. \qquad (5.17)$$

k_c will cater both for the increase in resistance caused by the apparent shear stress on the interface, and for the reduction in average channel boundary shear. k_c will always be positive because the increase in interfacial shear stress is always greater than the decrease in boundary shear stress. The reason for this is that the shear force on the interface is equal to the reduction in shear force on the main channel boundary, but the shear force on the interface acts on a far smaller area than the shear force on the boundary, and so the shear stress on the interface is far higher than the decrease in shear stress on the boundary.

The apparent shear stress on the interface has a propelling effect on the flood plain flow. The shear stresses on the bed of the flood plain are increased near the junction because of the increased velocities. The net effect is a reduction in the resistance to the flood plain flow. The propelling effect of the interface and the distortion of the shear

stresses on the bed of the flood plain can be lumped into a single flood plain factor k_p that will decrease the wetted perimeter as follows:

$$P_p' = P_p - k_p d \tag{5.18}$$

A theoretical derivation of equations for calculating k_c and k_p follows.

Consider equilibrium of forces in the main channel:

$$2\tau_a d + \tau_c P_c = \gamma A_c S$$

where τ_c is the average shear stress on the physical wetted perimeter, P_c.

Define k_c such that

$$\tau_c(P_c + 2k_c d) = \gamma A_c S.$$

Combining these two equations gives:

$$\frac{1}{k_c} = \frac{1}{\tau_r}\frac{A_c}{P_c}\frac{1}{d} \sim 2\frac{d}{P_c} \tag{5.19}$$

Similarly considering equilibrium of the flood plain:

$$\tau_a d + \gamma A_p S = \tau_p P_p$$
$$\tau_p(P_p - k_p d) \simeq \gamma A_p S$$

Combining gives:

$$\frac{1}{k_p} = \frac{1}{\tau_r}\frac{A_p}{P_p}\frac{1}{d} + \frac{d}{P_p} \tag{5.20}$$

QCOMP uses equations 5.19 and 5.20 to calculate values of k_c and k_p, and then uses Manning's equation to compute the discharge. The results of applying the flume data to the k-method are shown in fig. 5.6, where it can be seen that this method performs significantly better than the popular method, but it still badly over-estimates discharges at low flow depths. As with the area method, equations 5.19 and 5.20 need an empirical correction in order to predict discharges accurately. The reason for the disappointing performance of this method is probably because because Manning's n needs to be modified to account for the fact that the resistance offered by the shear stress on the vertical interfaces is not the same as that posed by the bed roughness on the physical boundary.

The flume data used in this analysis do not include separate discharges for the main channel and flood plain regions, and therefore it was not possible to generate actual values of k_c and k_p for comparison with those predicted by equations 5.19 and 5.20 with a view to finding empirical modifications.

Two other avenues for modifying equations 5.19 and 5.20 were pursued. The first involved finding a factor k for each data item such that if k_c and k_p were replaced with $k.k_c$ and $(1/k).k_p$, the discharge would be calculated correctly. Attempts to correlate k with parameters such as τ_r and $\tau_r S$ were unsuccessful. The second approach used k_p as calculated by equation 5.20, but modified k_c to $k.k_c$. Attempts were made to correlate this with τ, Δv and $\Delta v/v_c$, where v_c is the average main channel velocity calculated using the k-method, and Δv is the difference between the average main channel and flood plain velocities calculated using the k-method. This was unsuccessful, either because no correlation was found, or because of too much scatter to define a meaningful relationship.

In order to investigate this further, flume data would be required from which the actual values of k_c and k_p could be calculated.

5.2.5 MODIFIED K-METHOD

The k-method can be simplified by defining the wetted perimeter as follows, assuming vertical interfaces:

$$P_c' = P_c + 2kd \qquad (5.21)$$

$$P_p' = P_p \qquad (5.22)$$

Equation 5.22 implies that the interface is always omitted from the whetted perimeter of the flood plain, which is a good assumption provided the flood plain is wide, because the propelling effect of the main channel flow will then be small (James, 1984: p74). A relationship for k must be sought, using a suitable parameter as the independent variable representing the turbulence intensity at the interface.

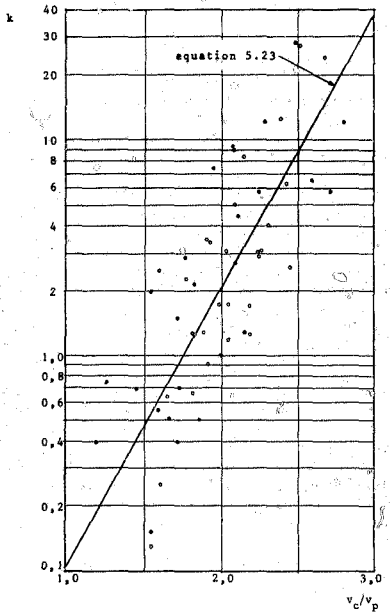


Fig. 5.11: Relationship for the k-factor in the modified k-method.

- ○ data of Wormleaton, Allen and Hadjipanos (1982)
- • data of Knight and Demetriou (1983)

The λ-method is similar to this approach, since it assumes a wide flood plain and hence omits the interface from the wetted perimeter, adopting a step function for k. k is assigned a value of 1,0 or 0, depending on the value of λ, which is the ratio of apparent shear stress on the diagonal interface to the average shear stress on the entire main channel wetted perimeter.

The author used the flume data to generate values of k (some of which are presented in fig. 5.7 as a function of d/D, demonstrating the inadequacy of the depth ratio to account for the turbulence intensity). The k-factors were plotted versus $\tau_a/\gamma RS$, a parameter similar to λ. Here τ_a is the apparent shear stress on the vertical interface; γRS is the average shear stress on the main channel wetted perimeter; and R is the hydraulic radius of the main channel, including the vertical interfaces in the wetted perimeter. It was found that although there was a trend, there was far too much scatter to define a meaningful relationship.

Another parameter that can be used to represent the turbulent intensity is the velocity difference between the main channel and flood plain sections. It has been used as one of the independent variables in empirical equations that predict the apparent shear stress on the vertical interfaces, which will be dealt with in the following chapter. Fig. 5.11 shows k as a function of v_c/v_p, which is the average velocity in the main channel divided by the average velocity in the flood plain region. These velocities were calculated using the values of k generated from the flume data. Although there is some scatter in fig. 5.11, it is not excessive, and a linear function can be defined on a semi-log basis:

$$\log k = 1.274\ (v_c/v_p) - 2.235 \qquad (5.23)$$

The line was fitted by least squares regression, with a correlation coefficient of 0,766. It is valid for v_c/v_p from 1 to 3.

The discharge in a symmetrical compound section can be calculated using Manning's equation:

$$Q = Q_c + 2Q_p$$
$$= (A_c/n_c)R_c^{2/3}S^{1/2} + 2(A_p/n_p)R_p^{2/3}S^{1/2} \quad (5.24)$$

where $R_c = A_c/(P_c + 2kd)$

$R_p = A_p/P_p$

Since k is a function of v_c/v_p, an iterative solution is required. A value for v_c/v_p is assumed, k calculated using equation 5.23, v_c/v_p calculated from

$$v_c/v_p = (n_p/n_c)R_c^{2/3}R_p^{-2/3}, \quad (5.25)$$

k is then re-calculated using the value of v_c/v_p, and so on until k converges. When this method was used to predict the discharges for the flume data using QCOMP, it was found that convergence was very slow, and often the computations would become unstable and diverge. This problem was solved by incorporating a simple accelerator in the convergence procedure to prevent instability. If i represents the i'th iteration, the procedure that QCOMP uses can be represented as in fig.5.12. This was found to converge in every case.

Fig. 5.6 shows the performance of the modified k-method when used to predict discharges for the data of Wormleaton et al. The maximum error in discharge computation is 12% which is acceptable considering inaccuracies in estimating parameters such as the bed roughness of a real channel. The modified k-method performs significantly and consistently better than the other methods shown in fig. 5.6, except for fig. 5.6(c) where the area method shows marginally better discharge estimates. However, both are within 5% of measured discharges, which can be considered to be the range of possible error in the measurement of the flume discharges.

In view of the good performance of the modified k-method as well as its simplicity, it can be considered to be a viable discharge computation method for application to real channels. If separate k-values for the main channel and flood plain regions could be calculated from flume data and defined separately as functions of v_c/v_p, the scatter in fig. 5.11

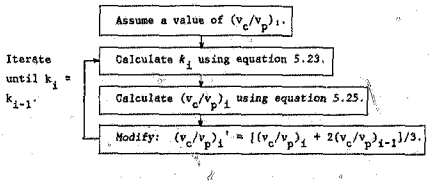


Fig. 5.12: Iterative procedure used in QCOMP for calculating k.

could probably be considerably reduced. Assuming that $k_p = 0$ means that k_c has to account for flood plain effects as well as main channel effects.

It must be borne in mind that this method cannot be applied to narrow flood plains. According to the data used to develop this method, a flood plain is sufficiently wide for the method to be applied if $W_p/W_c \geq 1,0$, ie. the width of the flood plain is at least equal to the width of the main channel.

Until this method is refined or a better alternative proposed, it can be used for practical situations with confidence in its reliability. It is definitely a great improvement of the λ-method which is the only reasonably good method presented in the literature.

5.2.6 ASSESSMENT OF METHODS

From the preceding discussion and studying fig. 5.6, the following conclusions can be drawn:

1. The popular method grossly over-estimates discharges at low flow depths, and cannot be seriously considered for discharge computation in compound channels.

2. The k-method and area method are potentially good and conceptually sound, and further research should be directed towards developing empirical modifications.
3. If the relative apparent shear stress τ_r can be predicted or calculated, the *area method can* be used in its present form as an improvement on the popular method and the λ-method.
4. The λ-method estimates discharges with fairly reasonable reliability, but is rather crude and needs refinement.
5. The modified k-method has been shown to produce the best results of all. It should be further refined, and should be tested on a wider range of compound channel data. In the interim it can be used with a good measure of confidence in its reliability, as indicated by the good discharge predictions shown in fig. 5.6.

CHAPTER 6: RELATIVE APPARENT SHEAR STRESS PREDICTION

The relative apparent shear stress, τ_r, was defined in 4.2 as $\tau_A/\tau_{p=}$ or $\tau_a/\gamma dS$. τ_r must be known in order to use the shear stress profile model presented in Part 1 . It is also required for some of the discharge prediction methods presented in the previous chapter: the area method, k-method and λ-method. It is therefore necessary to find a means of predicting τ_r for any given compound channel.

A few researchers have proposed equations to predict this parameter.

6.1 PREVIOUS RESEARCH

Rajaratnam and Ahmadi

Rajaratnam and Ahmadi (1981) proposed the following equation for τ_r, already dealt with in this report:

$$\tau_r = 0{,}15\ (D/d - 1)^2 \qquad (6.1)$$

This equation is too simplistic to be of much practical use, because it assumes that the turbulence intensity is a function of D/d only. Furthermore it was derived from smooth flume data and cannot accommodate roughened flood plains.

Bairol and Ervine

Bairol and Ervine (1984) conducted a flume study on geometric factors using a smooth section, and they proposed an equation for the relative apparent shear stress in terms of D/d, W_c/h and W_p/h. Since the roughness of the flood plain has a strong influence on the apparent shear stress, this equation is only applicable to smooth sections. They also presented

a relationship in the form of a family of curves, expressing the apparent shear stress as a function of geometric factors and the velocity difference between the main channel and the flood plain.

Wormleaton, Allen and Hadjipanos

Wormleaton et al (1982) presented an equation for the apparent shear stress that is a statistical fit to data. Various geometries and roughnesses were used which makes the equation fairly comprehensive:

$$\tau_a = 13{,}84\ (\Delta v)^{0{,}882}(D/h)^{-3{,}123}(W_p/W_c)^{-0{,}727} \qquad (6.2)$$

where Δv = difference in average velocity between main channel and flood plain (m/s), calculated using Manning's equation.

τ_a is in N/m²

For the purpose of this study equation 6.2 can be expressed as follows, by dividing by ρdS and rewriting the depth ratio term:

$$\tau_x = (0{,}001412/dS)(\Delta v)^{0{,}882}(1 - d/D)^{3{,}123}(W_p/W_c)^{-0{,}727} \qquad (6.3)$$

Both symmetrical and asymmetrical channel data were used to formulate this equation. Wormleaton et al stated that independent checks seem to indicate that this equation is reliable over a range of roughnesses and geometries, although they admitted that more data is needed for a full analysis of the problem.

Prinos and Townsend

Prinos and Townsend (1984) carried out a statistical regression analysis on observed data, and obtained the following equation:

$$\tau_a = 0{,}874\ (d/D)^{-1{,}129}(W_p/W_c)^{-0{,}514}(\Delta v)^{0{,}92} \qquad (6.4)$$

where τ_a is in N/m². Dividing by ρdS, this equation can be re-written as:

$$\tau_r = (1/11213dS)(d/D)^{-1,129}(W_p/W_c)^{-0,514}(\Delta v)^{0,92} \qquad (6.5)$$

Prinos and Townsend found this equation to give good results over a wide range of flow conditions. They used data with various geometries and roughnesses, some symmetrical and some asymmetrical, with both rectangular and trapezoidal main channel sections.

They did not indicate how Δv is to be obtained; nor did they define W_c, although it appears to be the bottom width of the main channel (fig. 6.1). If this is so then the term (W_p/W_c) in equation 6.5 is meant to account both for the effect of the relative widths of the main channel and flood plain, as well as for the steepness of the main channel bank.

Knight and Hamed

Knight and Hamed (1984) conducted extensive flume studies and presented relationships for the shear force on the flood plain boundary, main channel boundary and vertical interface, as functions of d/D, n_p/n_c and geometry. These equations can be re-arranged to give a complex equation for τ_r. A comprehensive range of flood plain roughnesses and widths have been considered. However, the major shortcoming of this relationship is that it is independent of the bed slope, which the flume data of Wormleaton et al show to be of importance.

6.2 ASSESSMENT OF EQUATIONS

Before developing a new equation it is important to consider existing equations so as to ascertain what form of equation has been shown to give good results, and whether it is necessary to develop a new equation or not. The equations for the relative apparent shear stress described above have been developed on larger data sets than that available to the author; therefore it would be advantageous if one or more of them could be shown to be reliable and practically applicable.

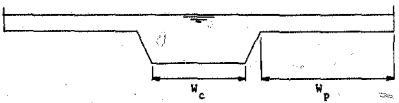


Fig. 6.1: Definition sketch for the equation of Prinos and Townsend (1984), equation 6.3.

Rajaratnam and Ahmadi's equation 6.1 is far too simplistic to be considered. The equations of Bairol and Ervine (1984) are of little practical use because roughened flood plains cannot be catered for, and in the field, the flood plain is often rougher than the main channel bed, greatly increasing the velocity difference and hence the turbulence intensity at the interface. Knight and Hamed's relationship does not incorporate the bed slope, which is an important parameter.

The equations of Wormleaton et al (6.3) and Prinos and Townsend (6.5) both satisfy the following criteria:

- They seem to include all the important parameters.
- They are simple and therefore should be easy to apply.
- They have been developed from fairly comprehensive data sets, incorporating roughened flood plains and both symmetrical and asymmetrical sections.

In addition, the equation of Prinos and Townsend (6.5) can account for a main channel that has a sloping bank.

In these equations, W_p/W_c accounts for geometry; d/D caters for the strong correlation between τ_r and the flow depth; Δv is a general indicator of turbulence intensity, and includes the effects of relative flood plain and main channel roughnesses, and the hydraulic radii of the main channel and flood plain sections; both equations give τ_r as proportional to 1/d, which will be shown to be true later in this chapter; and the bed slope is found in the denominator of these equations, as well as being implicit in the Δv term.

From these considerations the Wormleaton equation (6.3) and the Prinos equation (6.5) appear to be promising as potential equations for practical application. In order to assess their performance they were tested on the flume data of Wormleaton et al (1982) and Knight and Demetriou (1983), described in the previous chapter in section 5.2. It must be noted that the Wormleaton data set formed part of the data from which the Wormleaton equation was derived.

The main problem is in defining Δv. Prinos and Townsend did not specify how Δv is to be calculated. Wormleaton et al specified using Manning's equation, but made no indication as to what assumptions should be made concerning the wetted perimeters of the main channel and flood plains for obtaining the hydraulic radii. Before either of these equations can be used in practice, this issue must be clarified. Accordingly the author tried various methods for calculating Δv, the results of which are shown in figures 6.2 to 6.6, where the experimentally measured values of τ_r are plotted on the horizontal axis, and the vertical axis represents the values of τ_r predicted using either the Wormleaton or the Prinos equation. The computer program "TPRED" was developed for carrying out these computations and is listed and detailed in Appendix 3.

Fig. 6.2 shows the performance of the Wormleaton equation when the popular method for discharge computation is used to calculate the values of Δv. It is evident that this does not produce acceptable results, τ_r always being over-estimated. Since τ_r is proportional to (Δv) raised to the power of some constant, over-estimation of τ_r corresponds to values of Δv that are too high, ie. unrealistically high channel velocities or low flood plain velocities. The popular method uses a main channel wetted perimeter that is too small, and therefore the flow resistance in the main channel is too low. This results in main channel velocities that are too high (and hence discharge over-estimation). The Prinos equation was found to behave very similarly when used in conjunction with the popular method.

Fig. 6.3 shows the Wormleaton equation using the k-method to evaluate Δv. Since Δv is a function of τ_r, an iterative solution procedure has to be adopted. In TPRED a value of τ_r is assumed, k_c and k_p calculated,

Δv calculated, and then the Wormleaton equation is used to calculate τ_r. This is repeated until τ_r converges. It was found that τ_r converged slowly, oscillating between two values, and gradually centring in on a steady value. Sometimes it would diverge until computation was terminated by τ_r becoming large enough to generate a negative Δv. This problem was solved by using a simple accelerator in which the τ_r calculated in the i'th iteration ($\tau_{r(i)}$) is averaged with that calculated in the previous iteration ($\tau_{r(i-1)}$), and the average weighted in favour of $\tau_{r(i-1)}$ to prevent divergence or instability. This is shown in the flow chart in fig. 6.7, and was found to converge very rapidly in about four iterations. The flume data of Wormleaton et al shows very little scatter in fig. 6.3; that of Knight and Demetriou shows significant over-estimation of τ_r for narrow flood plains, and good results for wider plains. This is probably because the term in W_p/W_c does not adequately account for a narrow flood plain, and therefore the Wormleaton equation should only be used in conjunction with the k-method if $W_p/W_c \geq 1,0$.

The Prinos equation was also evaluated in conjunction with the k-method, and fig. 6.4 shows results that are almost as good as the Wormleaton equation, with the same observations about the flood plain being applicable.

Finally the Wormleaton and Prinos equations were used in conjunction with the modified k-method (figs. 6.5 and 6.6). Since this method is implicit in Δv, iterative solution was used to find Δv, as shown in fig. 5.12. This value was then used in the Wormleaton or Prinos equation to calculate Δv. In figs. 6.5 and 6.6 it is evident that this approach is particularly sensitive to narrow flood plains; W_p/W_c must be at least equal to 1,5 for good estimates of τ_r. This is to be expected because of the assumption implicit in the modified k-method, namely that $k_p = 0$, which is only true for wide flood plains, as discussed in the previous chapter.

Apart from the data for narrow flood plains, figs. 6.5 and 6.6 indicate good, reliable performance of these equations. The Prinos equation tends to under-estimate for τ_r between about 1 and 10, but not by a significant amount. Both equations over-estimate for very small values of τ_r (between

about 0,6 and 1,0), but the same trend is noticeable in all the graphs 6.2 to 6.6.

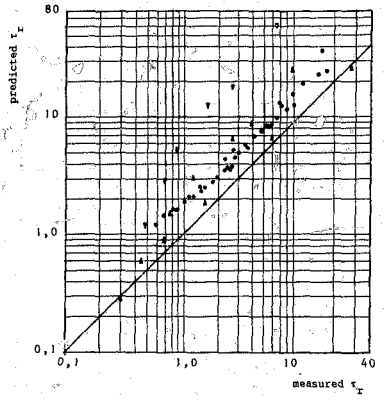
It can be concluded that either the k- or the modified k-method can be used to calculate Δv for use in the Wormleaton and the Prinos equations, with good results, as long as the flood plains are not narrow. For the k-method, W_p/W_c must not be less than 1,0; and for the modified k-method, not less than 1,5.

Future research could be directed towards developing an equation of the following form:

$$\tau_r = k_1 (W_p/d)^{k_2} (1 - v_c/v_p)^{k_3} (1 - d/D)^{k_4} (R_c/R_p)^{k_5} \qquad (6.6)$$

These parameters are suggested for the following reasons:

- W_p/d . In the next section it will be shown that τ_r is proportional to W_p/d.
- S. The bed slope is an important parameter as is shown by the data of Wormleaton et al.
- $(1 - v_c/v_p)$ would be an improvement on Δv because it is dimensionless. When $v_c = v_p$ the equation would yield $\tau_r = 0$.
- $(1 - d/D)$ ensures that τ_r approaches zero as d/D approaches 1,0.
- R_c/R_p accounts for geometry better than W_c/W_p, because the depths of the channel and plain sections are incorporated in the hydraulic radii, and therefore the ratio of hydraulic radii includes the effects of W_c/W_p and W_c/h. Any shape of main channel could be catered for, not only rectangular sections.



- Wormleaton, Allen and Hadjipanos (1982) $W_p/W_p \approx 1,6$
- Knight and Demetriou (1983): $W_p/W_c = 1,5$
- Knight and Demetriou (1983): $W_p/W_c = 1,0$
- Knight and Demetriou (1983): $W_p/W_c = 0,5$

Fig. 6.2: Assessment of the Wormleaton equation in conjunction with the popular method.

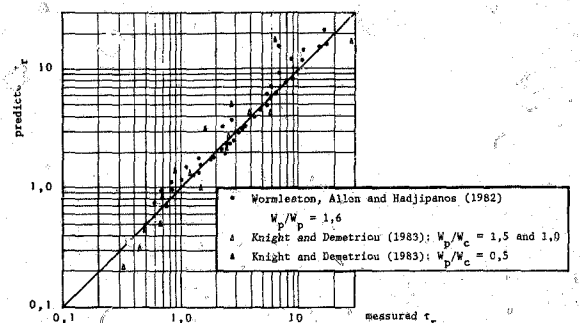


Fig. 6.3: Assessment of the Wormleston equation in conjunction with the k-method.

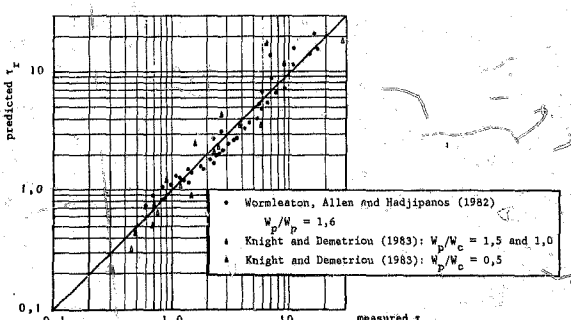


Fig. 6.4: Assessment of the Prinos equation in conjunction with the k-method.

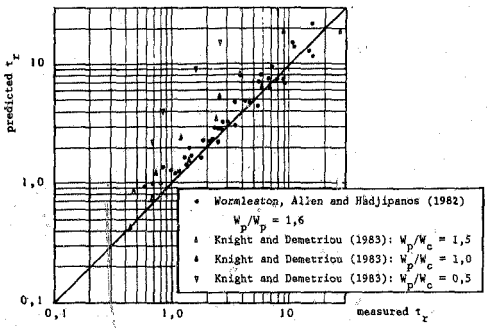


Fig. 6.5: Assessment of the Wormleaton equation in conjunction with the modified k-method.

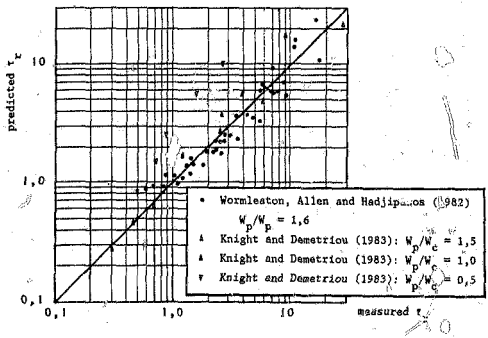


Fig. 6.6: Assessment of the Prinos equation in conjunction with the modified k-method.

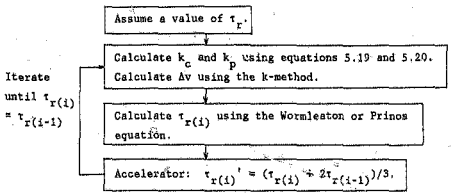


Fig. 6.7: Iterative procedure used in TPRED for calculating τ_r.

6.3 DEVELOPMENT OF A NEW EQUATION

The author used the available flume data to develop a new equation for predicting the relative apparent shear stress, with the following three objectives:

1. To produce an equation that is semi-empirical, ie. has a partly theoretical derivation, and not merely a statistical regression in which no understanding is required of the form of the equation.
2. To provide an equation whose parameters will apply to channels of any shape, and not just rectangular channels. This means using wetted *perimeters and* hydraulic radii instead of widths and heights.
3. In order to be universally applicable this equation should cater for both symmetrical and asymmetrical sections.

In order to satisfy the first objective, the following theoretical derivation was developed.

Consider a symmetrical compound channel, ie. one having two flood plains (fig. 6.8). The equations of equilibrium for the main channel and flood plain sections are:

$$SF_p = \gamma A_p S + \tau_a d$$
$$SF_c + 2\tau_a d = \gamma A_c S$$

where SF_p = shear force on P_p, the physical wetted perimeter of the flood plain.

SF_c = shear force on P_c, the physical wetted perimeter of the main channel.

Combining these two equations yields:

$$\frac{\tau_a}{\gamma d S} = \frac{SF_p A_c - SF_c A_p}{d^2 (SF_c + 2SF_p)} \qquad (6.7)$$

Now $SF_c = \bar{\tau}_c P_c$ where $\bar{\tau}_c$ is the average shear stress acting on the physical wetted perimeter of the main channel, P_c. Similarly $SF_p = \bar{\tau}_p P_p$.

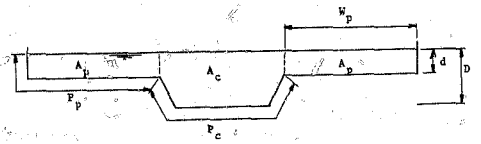
Substituting into equation 6.7 and rearranging gives:

$$\tau_r = \frac{W_p}{d}\left[\frac{(\bar{\tau}_p/\bar{\tau}_c)(R_c/R_p) - 1}{2(\bar{\tau}_p/\bar{\tau}_c)(P_p/P_c) + 1}\right] \qquad (6.8)$$

where $R_c = A_c/P_c$
$R_p = A_p/P_p$

Equation 6.8 can be considered to be a general equation describing the relative apparent shear stress in a symmetrical compound channel. For an asymmetrical channel, ie. only one flood plain, the 2 drops out of the denominator. Note that τ_r is proportional to W_p/d, which has been alluded to earlier in this chapter. The problem now is to find an expression for

$\bar{\tau}_p/\bar{\tau}_c$, as $\bar{\tau}_p$ and $\bar{\tau}_c$ are not the same as when there is no turbulent interaction.



1: Geometrical parameters for equations 6.8 and 6.12.

The s... proposed by previous researchers, outlined earlier ... his chapter, fall roughly into two categories:

1. Equations in which τ_r is a function of Δv and a few other parameters. The Wormleaton equation and Prinos equation both fall into this category, as well as the graphical relationship presented by Bairol and Ervine (1984).
2. Equations in which τ_r is a function of geometric and section properties such as d/D, n_p/n_c, W_p/W_c and W_c/h. These include the equations of Bairol and Ervine (1984) and Knight and Hamed (1984).

The first category could be called the *velocity approach*, and relies on the fact that the turbulent interaction depends to a large extent on the velocity difference between the main channel and flood plain. The second category could be termed the *geometric approach*; it simply identifies all the important parameters and fits an equation to the data.

The velocity approach could be used for defining $\bar{\tau}_p/\bar{\tau}_c$. In the derivation of uniform flow formulae for open channels, it is assumed that the average shear stress on the channel boundary is proportional to the square of the average velocity. For a compound channel where the turbulent interaction influences the velocities and boundary shears, it can be assumed that the

shear stresses are proportional to the velocity raised to some constant, ie.

$$\bar{\tau}_p = k_1 v_p^{k_2} \tag{6.9}$$

$$\bar{\tau}_c = k_2 v_c^{k_2} \tag{6.10}$$

Hence $\bar{\tau}_p/\bar{\tau}_c$ in equation 6.8 can be expressed as:

$$\bar{\tau}_p/\bar{\tau}_c = k v_p^{k_2}/v_c^{k_2}. \tag{6.11}$$

In simple channels, k is a function of boundary roughness and hydraulic radius. For a compound channel it is probably a function of these two parameters, and possibly also of some parameters such as d/D which account for the turbulence phenomenon. In the present study this has not been followed up because of lack of data giving v_c and v_p. Future research could be directed towards this.

The approach that was adopted here is similar to the geometric approach mentioned above. The important parameters on which $\bar{\tau}_p/\bar{\tau}_c$ depends were identified, and a regression analysis carried out to find empirical constants. In choosing the important parameters, a study of the literature was made to ascertain what other researchers have used or recommended. The parameters on which $\bar{\tau}_p/\bar{\tau}_c$ depends must be the same as those on which the turbulence intensity depends, because the shear stresses are distorted as a direct result of the turbulence.

Initially when research started being focused on compound channels in the 1960s, the depth ratio was the only parameter incorporated in experimental analyses. Even to the present day it has been considered to be one of the main variables, since for any one geometry and roughness of compound channel, the turbulence intensity increases as the flow depth decreases.

Gradually other parameters have been recognised as being important. Prinos and Townsend (1984) and Prinos, Townsend and Tavoularis (1985) found that not only the depth ratio is important, but also the roughness of the flood plain; by measuring turbulent intensities, it was found that turbulence is greater when the flood plain is roughened. Wormleaton,

Allen and Hadjipanos (1982) and Knight and Demetriou (1983) incorporated the ratio of the flood plain width to the main channel width (W_p/W_c) in their relationships for τ_a. Myers (1984) carried out a dimensional analysis on compound channels, and identified R_p/R_c, the ratio of hydraulic radii, as one of the important parameters. This incorporates both lateral dimensions as well as shape effects of the main channel and flood plain. Pasche and Rouvé (1985) observed that the slope of the main channel bank influences the turbulence phenomenon.

In a number of analyses, Knight and his co-workers used four independent variables (referring to fig. 6.9):

$\alpha = B/b$

$\beta = d/D$

$\gamma = n_p/n_c$

$\delta = b/h$

(Knight and Demetriou, 1983; Knight, Demetriou and Hamed, 1983; Knight and Hamed, 1984; Knight, Demetriou and Hamed, 1984.) γ accounts for the relative roughness of the main channel and flood plain. β is the simple depth ratio. α and δ indicate that the widths and proportions of the main channel and flood plains are important.

Although Knight's relationships do not take the bed slope into account, an examination of the flume data of Wormleaton et al shows that it has a strong influence on the turbulence phenomenon, and should not be ignored.

The author identified four effects that need to be considered, and selected the following parameters as independent variables:

1. *The depth effect.* The variable d/D accounts for the flow depth.

2. *The roughness effect.* The rougher the flood plain is relative to the main channel, the greater is the velocity difference, and hence the shear stresses on the interface are higher. The parameter n_p/n_c represents this.

3. *The slope effect.* The influence of the bed slope S on the turbulence intensity has been neglected by most researchers, except for where it is implicit in a Δv term.

4. *Geometric effects.* The shapes, widths and proportions of the main channel and flood plain are important because they define the physical boundaries to the turbulent interaction zone. For example, the narrower a flood plain is, the more influence the far bank has on the turbulence at the junction of the main channel and flood plain. Two parameters have been chosen to represent the geometric effects: R_c/D and W_p/d. R_c/D is the hydraulic radius of the main channel relative to the flow depth in the main channel, and approaches unity for a very wide channel. The advantage of using the hydraulic radius is that a channel with a sloping bank can be catered for. W_p/d represents the width that is available for the turbulent interaction zone on the flood plain.

A regression analysis was carried out using all the flume data of Wormleaton et al and Knight and Demetriou. A software package (mentioned in 4.3) for the HP9816 micro computer was used, facilitating non-linear multiple regression and user-specification of the form of regression equation. The analysis yielded the following equation:

$$\tau_p/\tau_c = (0{,}00586 - 1{,}460\ S)(d/D)^{1{,}43}(n_p/n_c)^{0{,}318}(R_c/D)^{-9{,}04}(W_p/d)^{0{,}581} \qquad (6.12)$$

Fig. 6.10 shows the data used in the regression analysis. Apart from a bit of scatter at low τ_r, the correlation is good; the remaining scatter can be considered to be within the range of experimental accuracy of the flume data. The over-estimation of τ_r for τ_r between about 0,6 and 1,0 follows the same pattern as in figs. 6.3 to 6.6, and therefore it may be caused by systematic experimental error in the flume data, and not a shortcoming in the equation.

Equation 6.12 can be used with equation 6.8 to predict the relative apparent shear stress in a symmetrical compound channel. Where there is only one flood plain, equation 6.12 must be assumed to apply for the asymmetrical case, and the 2 omitted from the denominator of equation 6.8.

Equations 6.8 and 6.12 may appear to be somewhat complicated, but this is necessary in order to account adequately for the turbulence phenomenon, which is a complex process.

Unfortunately only data for symmetrical channels with rectangular cross sections were available for this analysis. It remains to be seen, in the light of future research, if equation 6.12 applies to asymmetrical channels with only one flood plain, and if the parameter R_c/D adequately accounts for the effect of slope of the main channel bank in trapezoidal sections.

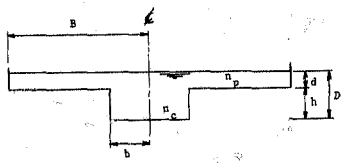


Fig. 6.9: Symbols used by Knight and co-workers.

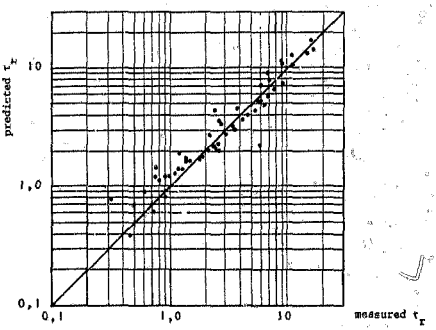


Fig. 6.10: Assessing equations 6.8 and 6.12, using the flume data of Wormleaton, Allen and Hadjipanos (1982) and Knight and Demetriou (1983).

CONCLUSIONS

From the analyses and discussions in this report one can gain a qualitative appreciation of the effects of various parameters on the turbulence phenomenon. These can be summarised as follows:

- There is an inverse relationship between turbulence intensity and flow depth; the turbulence intensity increases with decreasing depth ratio.

- The rougher the flood plain is relative to the main channel, the greater is the turbulence intensity.

- A sloping main channel bank generally reduces the turbulence intensity, the probable explanation being that a sloping bank is not as abrupt a transition from the deep main channel to the shallow flood plain as a vertical bank is. Different behaviour is evident for a steep bank at very low flow depths: the turbulence intensity is increased, which indicates a more efficient transfer of momentum to the flood plain under these conditions.

- Bed slope has an effect on the turbulence intensity, which most researchers have neglected.

- Geometric effects are rather difficult to evaluate. If the flood plain is narrow relative to the main channel, then the turbulence will be influenced by the flood plain width. For the conditions investigated in the present study, namely d/D not greater than about 0,5, it appears that if W_p/W_c is greater than 1,0 to 1,5 then the flood plain can be treated as hydraulically "wide" and it can be safely assumed that the width of the flood plain does not influence the turbulence. It is not certain from this study how the shape and proportions of the main channel influence the turbulence intensity, or the implications of a symmetrical versus asymmetrical section.

A model for predicting shear stresses on a flood plain has been developed using the relative apparent shear stress τ_r as the independant parameter. This model demonstrates the convenience of using a single independent variable to represent the turbulence intensity instead of the traditional

approach of using various geometric and flow parameters in any model dependent on the turbulence intensity. Using τ_z has been shown in this study to account successfully for the main channel bank slope and the depth ratio in the shear stress profile model. Since τ_z has been used as the independent variable, the model may be applied to any roughness and geometry. However, the fact that the model was developed using a smooth compound section of one particular geometry means that the extent to which τ_z caters for roughness and geometric effects remains to be seen in the light of future research. The model displays a good fit to the data from which it was derived, which means that it can be used confidently over a range of flow depths and bank slopes. The broader application of the model to different geometries and boundary roughnesses has to be assumed until more data become available with which to verify it.

From the measured flume data it has been shown that the shear stress profile on a flood plain is not altered by more than about 15% by introducing a sloping main channel bank, which is not of major significance. For some flow depths it is not altered at all. This applies to main channel and flood plain beds of the same roughness, which are the conditions for which the bank slope is most significant. It could be concluded that under these conditions the steepness of the main channel bank influences the flood plain shear stresses noticeably but not appreciably. For flood plains that are rough relative to the main channel the effect of bank slope will be masked by the roughness effects, and will have a considerably smaller effect on the shear stresses. Investigations in channels with rough flood plains would be beneficial but beyond the scope of the present study.

The evaluation of discharge computation methods using published flume data confirmed that the popular method grossly over-estimates discharges at low flow depths because of the assumption made concerning the wetted perimeter. Although this method is simple and easy to apply, it should not be used at all because it is unreliable. The λ-method proposed by Wormleaton, Allen and Hadjipanos (1982) is the most satisfactory method presented in the literature. It yields reasonably good discharge estimates under most conditions, but would need to be refined to be fully

reliable. The area method performs slightly better than the λ-method. Empirical adjustments need to be made to account for boundary roughness effects. The k-method, using vertical interfaces, incorporates theoretical equations for modifying the main channel and flood plain wetted perimeters. It yields disappointing results, badly over-estimating discharges at low flow depths, and needs empirical corrections. The k-method and area method both have sound theoretical bases and are potentially good methods. Further research could be directed towards modifying them for practical use. The area method can be used in its present form as an improvement on the λ-method. The modified k-method, applicable to sections with wide flood plains, expresses an empirical correction to the main channel wetted perimeter in terms of the velocity ratio v_c/v_p. It yields consistently good discharge estimates, better than the other four methods. It could be improved by modifying the flood plain wetted perimeter, and should be tested on a wider range of geometric and flow conditions, especially on sections with a sloping main channel bank. Nevertheless it can be considered to be fairly comprehensive since the data used in its development include a variety of bed roughnesses and flood plain widths. It appears to be the most satisfactory method that has been proposed to date, and its use is therefore recommended. Iterative solution is required as described in chapter 5.

For discharge computation the following three approaches are suggested:

1. The area method in conjunction with equations 6.8 and 6.12 for computing τ_r.
2. The λ-method with τ_r calculated either by equations 6.8 and 6.12, the Wormleaton equation (6.3) or the Prinos equation (6.5). If the Wormleaton or Prinos equations are used then iterative solution is necessary.
3. The modified k-method. This requires no knowledge of τ_r, but the equations must be solved iteratively for the velocity ratio.

Of these three, the modified k-method has been shown to produce the best results.

The prediction of the relative apparent shear stress τ_r is necessary for the shear stress profile model and for three of the discharge computation methods discussed in chapter 5. One of the following approaches may be adopted:

1. The author's equations 6.8 and 6.12.
2. The Wormleaton or Prinos equation, with Av calculated iteratively using either the k-method or the modified k-method.

The author's equations have a number of advantages over the Wormleaton equation and the Prinos equation: the former do not require iterative solution; they have the sound basis of a semi-theoretical derivation, ie. they are semi-empirical as opposed to entirely empirical; the author's equations can cater for any shape of main channel because the hydraulic radius is used; and they can be applied when the flood plain is narrow. The Wormleaton equation and the Prinos equation have the advantages of being simpler, and of being developed from wider data sets than the author's equation 6.12. However, all these equations for relative apparent shear stress need to be tested on larger data sets in order to establish universal validity.

Limits of applicability must be taken into account when applying the results of this study:

- Relative apparent shear stress in the shear stress profile model: $\tau_r = 0{,}02 - 6{,}0$. The model cannot be used when $\tau_r > 6$, and further experiments with a roughened flood plain would be needed if the model was to be extended to higher values of τ_r. For $\tau_r < 0{,}02$ the distortion of the shear stress profile is small; τ_{pm} is less than 10% greater than τ_{pw}. Therefore as a first approximation the distortion of the shear stress profile could be neglected and τ_p assumed to be equal to τ_{pw} right up to the junction with the main channel.

- Velocity ratio in the k-method for discharge computation: $v_c/v_p = 1{,}0 - 3{,}0$. For $v_c/v_p < 1{,}0$ it can be assumed that $k = 0$, because the turbulence intensity is very low. In the unlikely event of v_c/v_p

being greater than 3,0 the k-value corresponding to $v_c/v_p = 3,0$ should be used as an approximation.

- Depth ratio in Part 1: d/D = 0,1 - 0,43. The shear stress profile model can be applied to values of d/D greater than 0,43 as this will be accommodated in the variable τ_r.

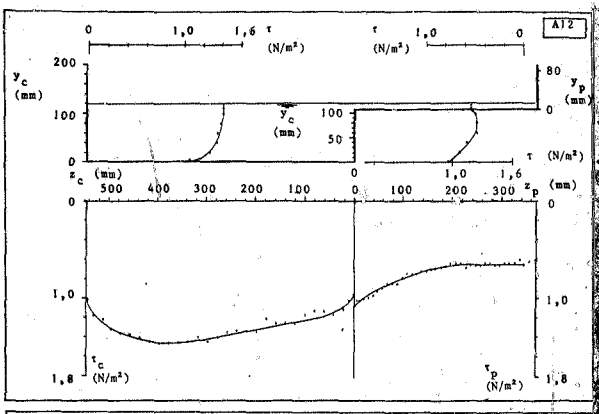
- Depth ratio in Part 2: d/D = 0,1 to 0,51. For d/D greater than about 0,5 it can be assumed that the apparent shear stress is zero, since the turbulence intensity is very low for higher flow depths and reaches zero for d/D somewhere between 0,4 and 1,0 (Bairol and Ervine, 1984).

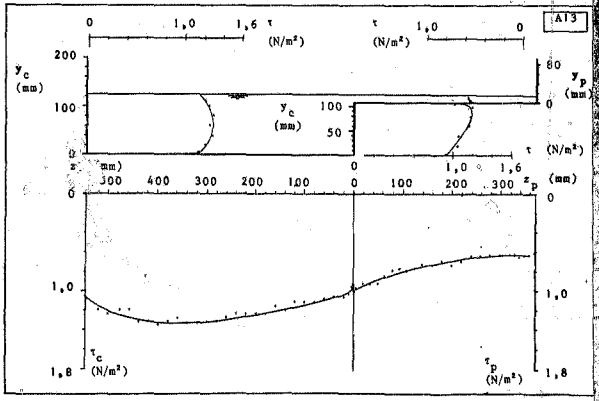
- *Slope of main* channel bank: $\alpha = 30°$, $60°$ and $90°$. The shear stress profile model should not be applied when α is less than $30°$, which was the lowest bank slope used in the author's experiments.

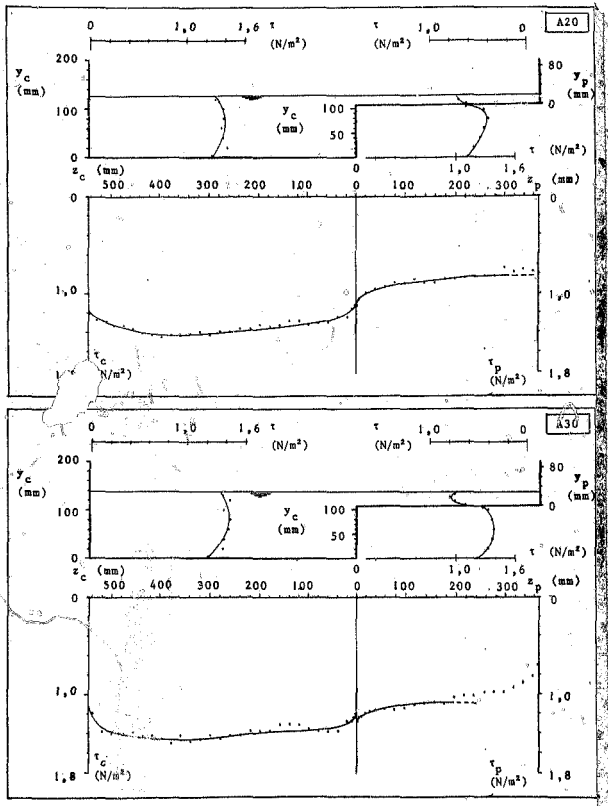
The subject of compound channel analysis is far from being thoroughly understood by experts in the field. The present study is another step towards clarifying the uncertain issues and providing practical methods for shear stress and discharge computations in compound channel analysis.

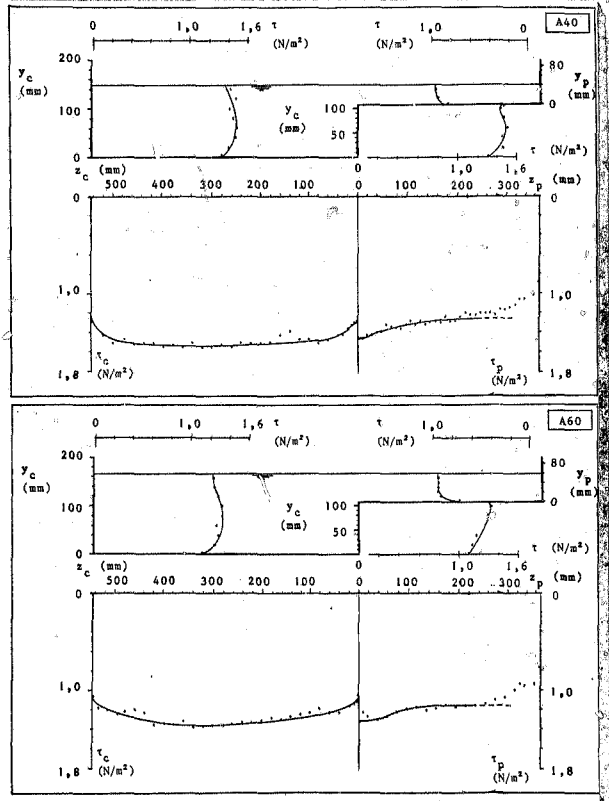
APPENDICES

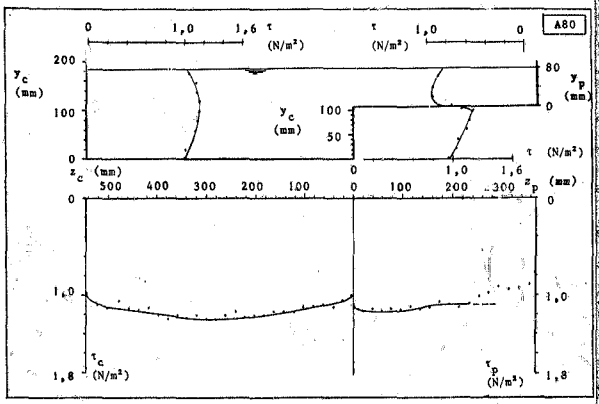
APPENDIX A: OBSERVED SHEAR STRESS PROFILES

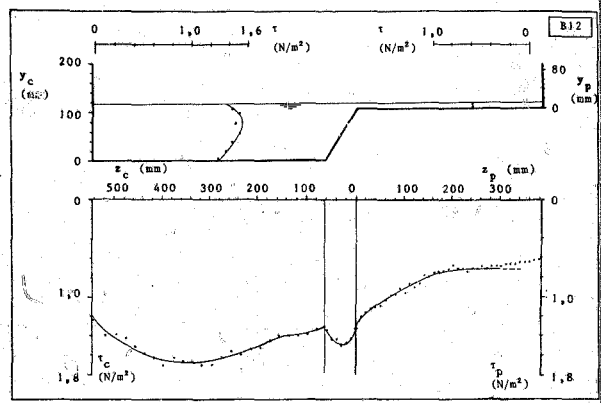

A12
0
1,0
1,6 τ
(N/m²)
τ
(N/m²)
1,0
0
200
100
0
y_c
(mm)
80
y_p
(mm)
0
100
50
y_c
(mm)
τ
(N/m²)
z_c (mm)
500 400 300 200 100 0
0 100 200 300 z_p (mm)
0
1,0
1,8
τ_c (N/m²)
τ_p (N/m²)

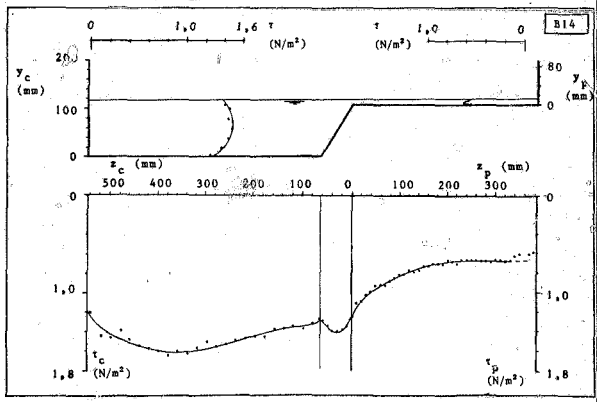

A13
0
1,0
1,6 τ
(N/m²)
τ
(N/m²)
1,0
0
200
100
0
y_c
(mm)
80
y_p
(mm)
0
100
50
y_c
(mm)
τ
(N/m²)
z_c (mm)
300 400 300 200 100 0
0 100 200 300 z_p (mm)
0
1,0
1,8
τ_c (N/m²)
τ_p (N/m²)

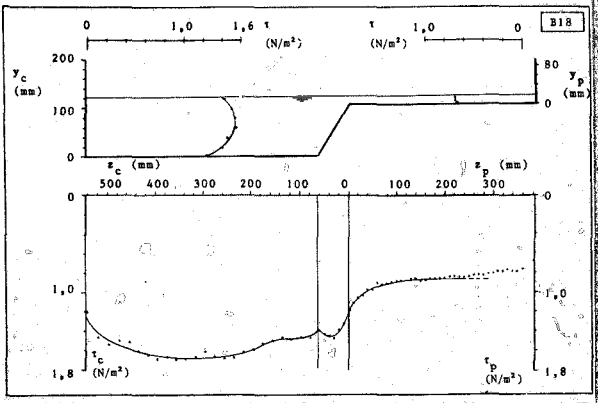

A20
A30
τ (N/m²)
y_c (mm)
y_p (mm)
z_c (mm)
z_p (mm)
τ_c (N/m²)
τ_p (N/m²)

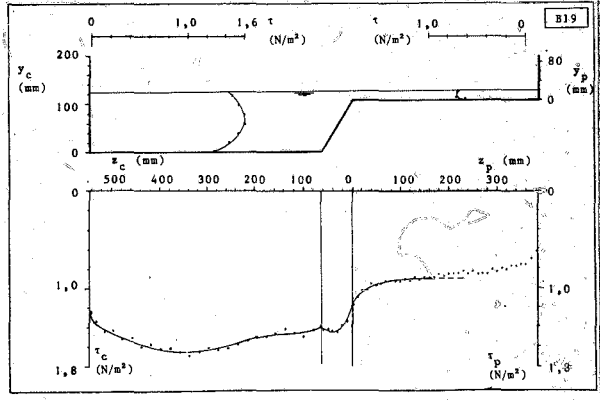

A40
A60
τ (N/m²)
y_c (mm)
y_p (mm)
z_c (mm)
z_p (mm)
τ_c (N/m²)
τ_p (N/m²)

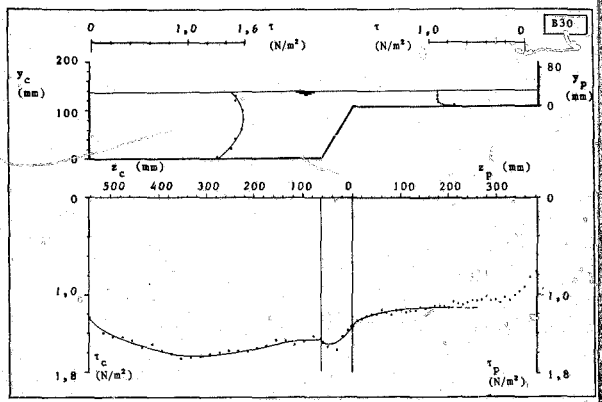

A80
0
1,0
1,6
τ
(N/m²)
200
100
0
y_c
(mm)
80
y_p
(mm)
z_c
500
400
300
200
100
z_p
1,0
1,8
τ_c
τ_p

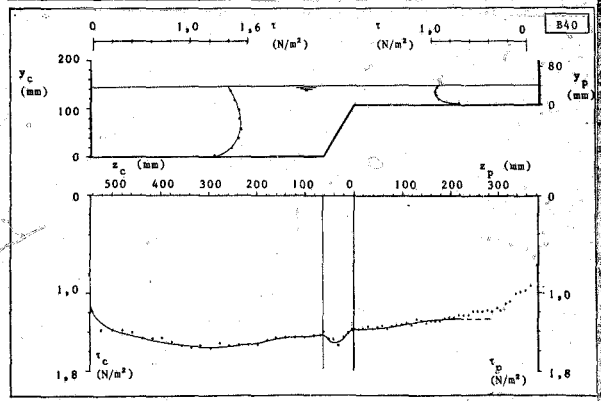

B12
0
1,0
1,6 τ
(N/m²)
τ
(N/m²)
1,0
0
200
100
0
y_c
(mm)
80
0
y_p
(mm)
z_c (mm)
z_p (mm)
500 400 300 200 100 0 100 200 300
0
1,0
1,8
τ_c (N/m²)
τ_p (N/m²)

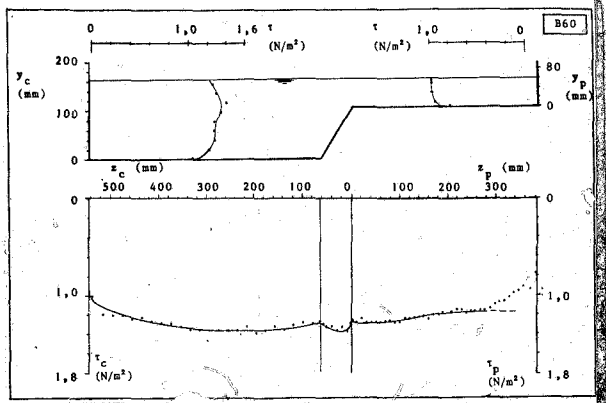

B14
0
1,0
1,6 τ
(N/m²)
τ
(N/m²)
1,0
0
200
100
0
y_c
(mm)
80
0
y_p
(mm)
z_c (mm)
z_p (mm)
500 400 300 200 100 0 100 200 300
0
1,0
1,8
τ_c (N/m²)
τ_p (N/m²)

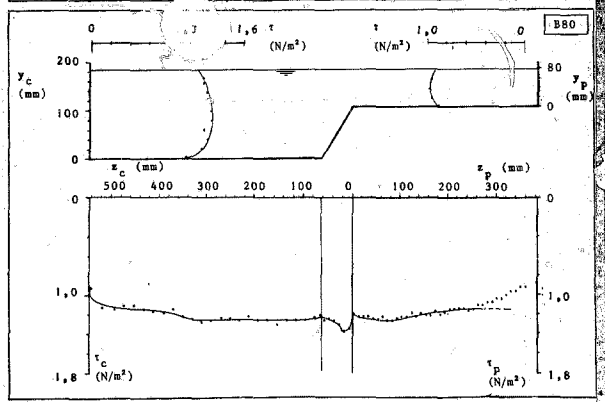

B18
0 1,0 1,6 τ (N/m²)
τ 1,0 0 (N/m²)
200
100
0
y_c (mm)
80
0
y_p (mm)
z_c (mm)
500 400 300 200 100 0
z_p (mm)
0 100 200 300
1,0
1,8
τ_c (N/m²)
τ_p (N/m²)

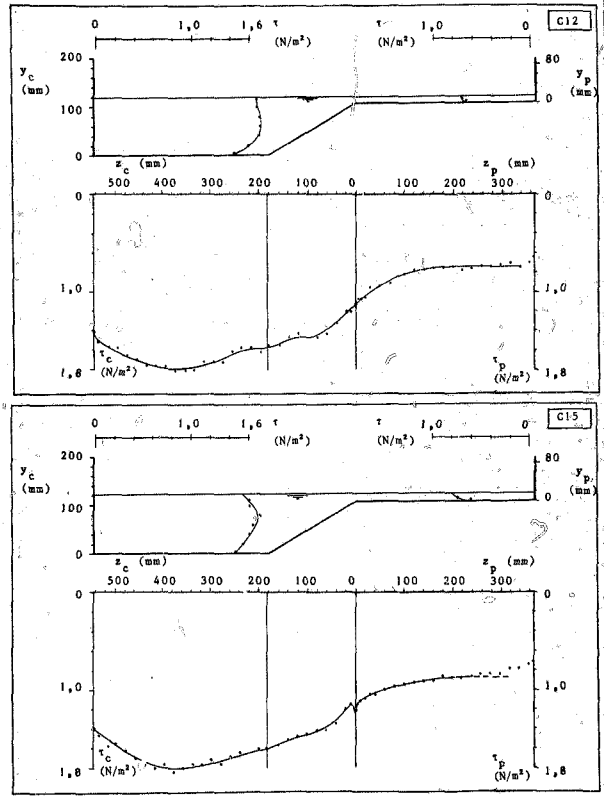

B19
0 1,0 1,6 τ (N/m²)
τ 1,0 0 (N/m²)
200
100
0
y_c (mm)
80
0
y_p (mm)
z_c (mm)
500 400 300 200 100 0
z_p (mm)
0 100 200 300
1,0
1,8
τ_c (N/m²)
τ_p (N/m²)


B30
0
1,0
1,6 τ
(N/m²)
τ
1,0
0
200
100
0
y_c
(mm)
80
0
y_p
(mm)
z_c (mm)
500 400 300 200 100 0
z_p (mm)
100 200 300
1,0
1,8
τ_c (N/m²)
τ_p (N/m²)

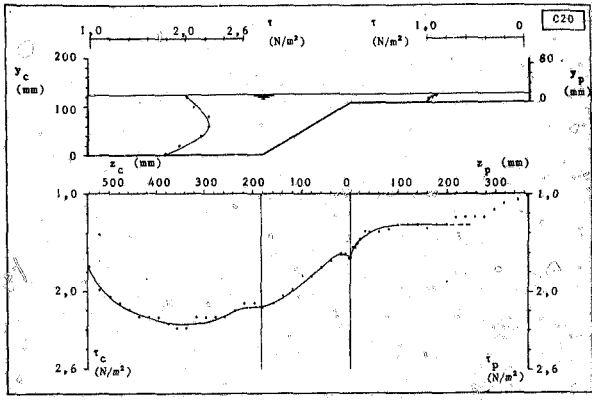

B40
0
1,0
1,6 τ
(N/m²)
τ
1,0
0
200
100
0
y_c
(mm)
80
0
y_p
(mm)
z_c (mm)
500 400 300 200 100 0
z_p (mm)
100 200 300
1,0
1,8
τ_c (N/m²)
τ_p (N/m²)

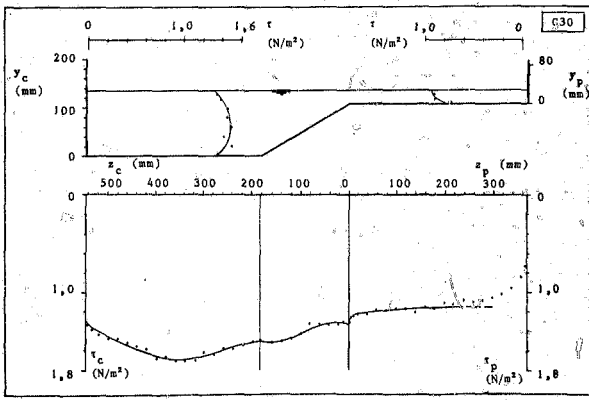

B60
0
1,0
1,6 τ
(N/m²)
τ
(N/m²)
1,0
0
200
100
0
y_c
(mm)
80
0
y_p
(mm)
z_c (mm)
500 400 300 200 100 0
z_p (mm)
100 200 300
0
1,0
1,8
τ_c
(N/m²)
τ_p
(N/m²)

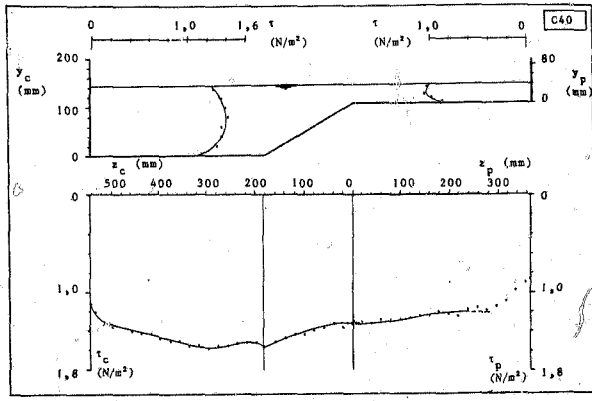

B80
0
1,6 τ
(N/m²)
τ
(N/m²)
1,0
0
200
100
0
y_c
(mm)
80
0
y_p
(mm)
z_c (mm)
500 400 300 200 100 0
z_p (mm)
100 200 300
0
1,0
1,8
τ_c
(N/m²)
τ_p
(N/m²)

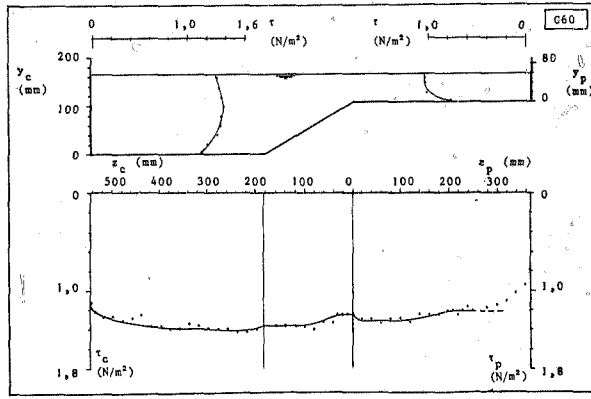


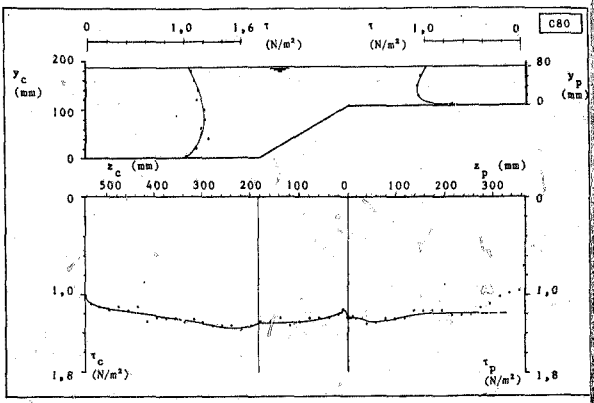
Appendix A: Observed shear stress profiles


C20
τ (N/m²)
τ (N/m²)
y_c (mm)
y_p (mm)
z_c (mm)
z_p (mm)
τ_c (N/m²)
τ_p (N/m²)


C30
τ (N/m²)
τ (N/m²)
y_c (mm)
y_p (mm)
z_c (mm)
z_p (mm)
τ_c (N/m²)
τ_p (N/m²)


C40
0
1,0
1,6 τ
(N/m²)
τ
1,0
0
(N/m²)
200
100
0
y_c (mm)
80
0
y_p (mm)
z_c (mm)
z_p (mm)
500 400 300 200 100 0 100 200 300
0
1,0
1,8
τ_c (N/m²)
τ_p (N/m²)


C60
0
1,0
1,6 τ
(N/m²)
τ
1,0
0
(N/m²)
200
100
0
y_c (mm)
80
0
y_p (mm)
z_c (mm)
z_p (mm)
500 400 300 200 100 0 100 200 300
0
1,0
1,8
τ_c (N/m²)
τ_p (N/m²)


C80
0
1,0
1,6 τ
(N/m²)
τ
(N/m²)
1,0
0
200
100
0
y_c
(mm)
80
0
y_p
(mm)
z_c (mm)
z_p (mm)
500 400 300 200 100 0 100 200 300
0
1,0
1,8
τ_c
(N/m²)
τ_p
(N/m²)

APPENDIX B: RAJARATNAM AND AHMADI'S RELATIONSHIP FOR APPARENT SHEAR STRESS

Rajaratnam and Ahmadi (1981) proposed a relationship for $\tau_a/\tau_{p\infty}$ as a function of the inverse depth ratio D/d. Their derivation is given below, followed by a critical appraisal of the relationship.

B1 Simplified derivation

If τ is the turbulent mean shear stress in any vertical plane in the mixing region on the flood plain, located at a distance z_p from the interface, then the shear force on this plane is:

$$\tau d = \int_{z_p}^{l_p} (\tau_p - \tau_{p\infty}) dz_p \qquad (B1)$$

Now introduce a parameter η such that $\eta = z_p/b_p$, and b_p is defined such that $b_p = z_p$ when $(\tau_p - \tau_{p\infty})/(\tau_{pj} - \tau_{p\infty}) = 0{,}50$. From their experiments Rajaratnam and Ahmadi found that $l_p \approx 2{,}5\ b_p$. This is very approximate and is simply the average of all the values of l_p that were measured. The above expression (B1) becomes:

$$\tau d = (\tau_{pj} - \tau_{p\infty}) b_p \int_{\eta}^{2{,}5} f(\eta) d\eta$$

$$= (\tau_{pj} - \tau_{p\infty}) b_p F(\eta)$$

For τ_a, the apparent shear stress at the interface, $z_p = 0$ and $F(\eta) = 1$. Therefore

$$\tau_a d = (\tau_{pj} - \tau_{p\infty}) b_p \qquad (B2)$$

Two empirical relationships developed by Rajaratnam and Ahmadi are now used:

$$b_p/d = 0{,}64\ (D/d - 1) \qquad (B3)$$

$$\tau_{pj}/\tau_{p\infty} - 1 = 0{,}24\ (D/d - 1) \qquad (B4)$$

Equations B3 and B4 are substituted into equation B2 to give:

$$\begin{aligned}\tau_a/\tau_{p\infty} &= (0{,}64)(0{,}24)(D/d - 1)^2 \\ &= 0{,}154(D/d - 1)^2 \\ &\approx 0{,}15(D/d - 1)^2 \end{aligned} \qquad (B5)$$

This relationship is plotted in fig. B1.

B2 Shortcomings of this derivation

Several shortcomings can be identified:

1. The relationship for τ_{pj} (equation B4) is assumed to be linear, whereas plotting the author's data in the same form indicates that the relationship should be non-linear.
2. Equation B3 for b_p is a very poor fit to the observed data, as can be seen in fig. B2. The fit is so bad that the use of this equation can hardly be justified.
3. It is assumed that l_p is equal to a constant multiplied by b_p, and there is no evidence to substantiate this assumption of linearity.

Equation B5 gives the apparent shear stress τ_a equal to zero when D/d equals 1,0. However, Bairol and Ervine (1984) maintained that this is not always true, but τ_a is zero for D/d somewhere between 1,0 and 2,5.

These considerations make the validity of equation B5 questionable.

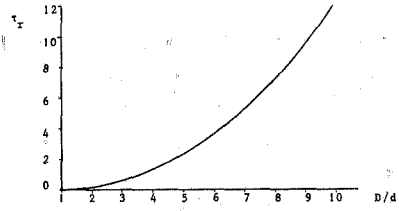


Fig. B1: Curve for equation B5.

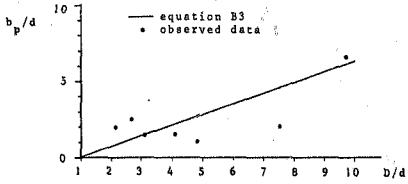


Fig. B2: Relationship for b_p, equation B3.
The observed data from which this was derived is shown on the graph.

APPENDIX C: COMPUTER PROGRAMS

Computer programming was not one of the objectives of this research project, but merely a tool to facilitate efficient data manipulation. For this reason programs were written for the *HP85 micro computer*, which is simple to learn how to use, and utilises fairly versatile BASIC programming language.

C1 PROGRAMS FOR DATA MANIPULATION

C1.1 Recording data

Name: "READ"

Purpose

To read in an observed shear stress profile and store it as a two-dimensional matrix on tape. One dimension of the matrix consists of z_p-values, and the other dimension is the corresponding shear stress readings.

Variables (Refer to fig. C1.)

A(100,2)	name of matrix
A$	name of data file
A(I,1)	lateral distance across flood plain (z_p^i)
A(I,2)	shear stress at a position defined by z_p (τ_p^i)
I	counter
N	number of shear stress readings

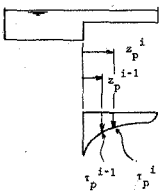


Fig. C1: Definition sketch.

Listing.

```
 10 ! "READ"
 12 CLEAR
 20 DISP "READING IN SHEAR STRES
    S DATA"
 21 DISP "AND STORING IT ON TAPE
    "
 30 OPTION BASE 1
 40 DIM A(100,2),A$[6]
 50 DISP "FILE NAME"
 51 INPUT A$
 60 DISP "NUMBER OF ELEMENTS"
 70 INPUT N
 80 DISP "ENTER Z, SHEAR STRESS"
 90 FOR I=1 TO N
100 INPUT A(I,1),A(I,2)
110 NEXT I
120 CREATE A$,1,(1+2*N)*8
130 ASSIGN# 1 TO A$
140 PRINT# 1 ; N
150 FOR I=1 TO N
160 PRINT# 1 ; A(I,1),A(I,2)
170 NEXT I
180 ASSIGN# 1 TO *
190 DISP "DATA HAS BEEN STORED."
200 DISP "PROGRAM FINISHED."
210 END
```

C1.2 Integration of a shear stress profile

Name: "INT" (INTegrate)

Purpose

To integrate a shear stress profile on the flood plain in order to calculate the apparent shear force on the bed of the flood plain.

Variables

A(100,2)	name of matrix
A$	name of data file
A(I,1)	lateral distance across flood plain (z_p^i)
A(I,2)	shear stress at a position defined by z_p (τ_p^i)
A(I-1,1)	z_p^{i-1}
A(I-1,2)	τ_p^{i-1}
I	counter
N	number of shear stress readings
S	shear force
T	$\frac{1}{2}(\tau_p^i - \tau_p^{i-1})$
Z	$\Delta z = z_p^i - z_p^{i-1}$

```
 10 ! "INT"
 20 CLEAR
 30 DISP "INTEGRATING SHEAR STRE
    SS"
 40 DISP "PROFILE."
 50 OPTION BASE 1
 60 DIM A(100,2),A$[6]
 70 DISP "DATA FILE NAME"
 80 INPUT A$
 90 ASSIGN# 1 TO A$
100 READ# 1 ; N
110 FOR I=1 TO N
120 READ# 1 ; A(I,1),A(I,2)
130 NEXT I
140 ! PERFORM INTEGRATION
150 S=0
160 FOR I=2 TO N
170 Z=A(I,1)-A(I-1,1)
180 T=(A(I,2)+A(I-1,2))/2
190 S=S+Z*T
200 NEXT I
205 S=S/1000
210 DISP "THE SHEAR FORCE IS",S,
    " N/m."
230 DISP "END"
240 END
```

C1.3 Calculation of apparent shear stress

Name: "APP" (APParent shear stress)

Purpose

To calculate the apparent shear stress on the interface between the main channel and flood plain, by integrating the distorted portion of the shear stress profile:

$$\tau_a d = \int_{z_p=0}^{z_p=1} (\tau_p - \tau_{p\infty}) dz_p$$

Variables

A(100,2)	name of matrix
A$	name of data file
A(I,1)	lateral distance across flood plain ($z_p{}^i$)
A(I,2)	shear stress at a position defined by z_p ($\tau_p{}^i$)
A(I-1,1)	$z_p{}^{i-1}$
A(I-1,2)	$\tau_p{}^{i-1}$
I	counter
N	number of shear stress readings
P	plateau shear stress ($\tau_{p\infty}$)
S	apparent shear force ($\tau_a d$)
T	$\frac{1}{2}(\tau_p{}^i - \tau_p{}^{i-1}) - \tau_{p\infty}$
Z	$\Delta z = z_p{}^i - z_p{}^{i-1}$

```
 10 ! "APP"
 20 CLEAR
 30 DISP "FINDING APPARENT SHEAR
    FORCE."
 50 OPTION BASE 1
 60 DIM A(100,2),A$[63]
 70 DISP "DATA FILE NAME"
 80 INPUT A$
 82 DISP "PLATEAU SHEAR STRESS"
 83 INPUT P
 90 ASSIGN# 1 TO A$
100 READ# 1; N
110 FOR I=1 TO N
120 READ# 1 ; A(I,1),A(I,2)
130 NEXT I
140 ! PERFORM INTEGRATION
150 S=0
160 FOR I=2 TO N
170 Z=A(I,1)-A(I-1,1)
180 T=(A(I,2)+A(I-1,2))/2-P
190 S=S+Z*T
200 NEXT I
205 S=S/1000
210 DISP "THE APPARENT SHEAR FOR
    CE",S,"N/m."
230 DISP "END"
240 END
```

C1.4 Dimensionless shear stress parameter

Name: "DIM" (DIMensionless shear stress parameter)

Purpose

This program computes a value of the dimensionless shear stress parameter used by Rajaratnam and Ahmadi (1981), for each value of τ_p in a flood plain shear stress profile.

Variables

A(100,2)	name of matrix
A$	name of data file
A(I,1)	lateral distance across flood plain (z_p^i)
A(I,2)	shear stress at a position defined by z_p (τ_p^i)
I	counter
P	dimensionless shear stress parameter: $(\tau p. - \tau_{p\infty})/(\tau pm. - \tau_{p\infty})$
P1	τ_{pm}
P2	$\tau_{p\infty}$

Listing

```
 10 ! "DIM"
 20 CLEAR
 30 DISP "CALCULATION OF SHEAR"
 31 DISP "STRESS PARAMETER."
 32 ! READ IN AND DISPLAY DATA F
    ILE.
 40 OPTION BASE 1
 50 DIM A(100,2),A$[6]
 60 DISP "FILE REQUIRED"
 70 INPUT A$
 80 ASSIGN# 1 TO A$
 90 READ# 1 ; N
100 FOR I=1 TO N
110 READ# 1 ; A(I,1),A(I,2)
120 NEXT I
130 DISP "NUMBER OF ELEMENTS IS"
    ;N
140 DISP "Z (mm), SHEAR STRESS (
    Pa)."
150 FOR I=1 TO N
160 DISP A(I,1),A(I,2)
170 NEXT I
180 ASSIGN# 1 TO *
190 DISP "Press CONTINUE when re
    ady."
200 PAUSE
210 ! INPUT PARAMETERS
220 CLEAR
230 DISP "MAX. SHEAR STRESS"
240 INPUT P1
250 DISP "PLATEAU SHEAR STESS"
260 INPUT P2
270 ! CALCULATE DIMENSIONLESS SH
    EAR STRESS.
280 DISP "DIMENSIONLESS SHEAR ST
    RESS"
290 DISP "PARAMETERS:"
300 DISP " "
310 FOR I=1 TO N
320 P=(A(I,2)-P2)/(P1-P2)
330 DISP A(I,1),P
340 NEXT I
350 DISP "END"
360 END
```

C1.5 Normalising a shear stress profile

Name: "NORM" (NORMalise)

Purpose

To normalise a shear stress profile with respect to some important parameter; eg. express all the shear stresses on the flood plain as τ_p/τ_{pj}, *ie. normalise* with respect to τ_{pj}.

Variables

A(100,2)	name of matrix
A$	name of data file
A(I,1)	lateral distance across flood plain (z_p^i)
	or across the *main channel* (z_c^i)
A(I,2)	shear stress at a position defined by z_p (τ_p^i)
	or by z_c (τ_c^i)
I	counter
P	*normalised* flood plain shear stress (τ_p^i/P1) or
	main channel shear stress (τ_c^i/P1)
P1	value with respect to which the profile is normalised

Listing

```
 10 ! "NORM"
 20 CLEAR
 30 DISP "NORMALISATION OF SHEAR
    "
 31 DISP "STRESS PROFILE."
 32 ! READ IN AND DISPLAY DATA F
    ILE."
 40 OPTION BASE 1
 50 DIM A(100,2),A$[60]
 60 DISP "FILE REQUIRED"
 70 INPUT A$
 80 ASSIGN# 1 TO A$
 90 READ# 1 ; N
100 FOR I=1 TO N
110 READ# 1 ; A(I,1),A(I,2)
120 NEXT I
130 DISP "NUMBER OF ELEMENTS IS"
    ,N
140 DISP "Z (mm), SHEAR STRESS (
    Pa)."
150 FOR I=1 TO N
160 DISP A(I,1),A(I,2)
170 NEXT I
180 ASSIGN# 1 TO *
190 DISP "Press CONTINUE when re
    ady."
200 PAUSE
210 ! INPUT PARAMETERS
220 CLEAR
230 DISP "INPUT the value by whi
    ch the"
240 DISP "shear stresses are to
    be"
250 DISP "normalised."
260 INPUT P1
270 CLEAR
280 PRINT "NORMALISED SHEAR STRE
    SSES:"
290 PRINT " "
300 PRINT " "
310 FOR I=1 TO N
320 P=A(I,2)/P1
330 PRINT USING 331 ; A(I,1),P
331 IMAGE DDD,3X,DD.DD
340 NEXT I
350 DISP "END"
351 BEEP
360 END
```

C2 SHEAR STRESS PROFILE MODEL

Name: "SSP" (Shear Stress Profile)

Purpose

This program was written to generate the family of curves for τ_p/τ_{p_m} shown in fig. 4.7, and to generate curves for fig. 4.9 where observed profiles are compared with predicted profiles.

Operation

The program takes a value of the relative apparent shear stress τ_r and generates a profile of τ_p, the flood plain shear stresses.

Variables

A,B,C,D,K	constants in the exponential equations, eqns. 4.9 - 4.11.
L	length of interaction zone in flood plain region (l_p)
T	relative apparent shear stress (τ_a/τ_{p_m})
T1	plateau shear stress on flood plain (τ_{p_m})
T2	peak shear stress ratio (τ_{pm}/τ_{p_m})
T3	dimensionless local shear stress (τ_p/τ_{p_m})
T4	local shear stress on flood plain (τ_p)
X	dimensionless lateral distance across flood plain (z_p/l_p)
Z	lateral distance across flood plain (z_p)

Listing

```
 10 ! "SSP"
 11 CLEAR
 20 DISP "HOLDEN'S MODEL FOR THE
    SHEAR"
 30 DISP "STRESS PROFILE ON A FL
    OOD"
 40 DISP "PLAIN."
 50 ! DATA INPUT
 60 DISP "RELATIVE APPARENT SHEA
    R STRESS"
 70 INPUT T
 80 DISP "PLATEAU SHEAR STRESS:"
 90 INPUT T1
 95 DISP "LENGTH OF INTERACTION
    ZONE"
 96 INPUT L
100 PRINT "RELATIVE APPARENT SHE
    AR STRESS:",T
110 PRINT "PLATEAU SHEAR STRESS"
    ,T1
120 ! CALCULATIONS
130 T2=.0116*(LGT(T)+2)^4.09+1.0
    9
135 CLEAR
140 DISP "RATIO OF PEAK TO PLATE
    AU IS:",T2
150 DISP "DO YOU WANT TO CHANGE
    THIS?"
160 DISP "Y/N"
170 INPUT A$
180 IF A$="Y" THEN DISP "NEW VAL
    UE"
190 IF A$="Y" THEN INPUT T2
200 PRINT "RATIO OF PEAK TO PLAT
    EAU IS:",T2
210 ! SHAPE PARAMETERS
220 IF T>=.25 THEN 290
230 IF T<=.1 THEN 340
240 B=.56*LGT(T)+4.32
250 K=-4.1*LGT(T)-1.46
260 A=1
270 C=0
271 D=0
280 GOTO 400
290 A=1
300 B=4.05-.253*T
310 C=0
311 D=0
320 K=1
330 GOTO 400
340 B=.56*LGT(T)+4.32
350 C=-.912*(LGT(T)+1)
360 D=36.7*LGT(T)+67.9
370 K=-4.1*LGT(T)-1.46
380 IF T>.07 THEN A=1.013*LGT(.1
    01/T)^.00194
390 IF T<=.07 THEN A=1.006+4.435
    *EXP(-11.34*(T-.02)^.156)
400 ! CALCULATE T3 AND T4.
410 PRINT " "
420 PRINT "SHEAR STRESS PROFILE.
    "
430 PRINT "z/l; ratio of shear s
    tress"
440 PRINT "to Plateau shear stre
    ss;"
445 PRINT "distance z;"
450 PRINT "absolute shear stress
    "
460 PRINT " "
470 X=0
480 FOR I=1 TO 21
490 T3=1+(T2-1)*(A*EXP(-B*X^K)-C
    *EXP(-D*X))
500 T4=T3*T1
503 Z=X*L
510 PRINT USING 520 ; X,T3,Z,T4
520 IMAGE D.DD,3X,D.DD,5X,3D.D,3
    X,DD.DDD
530 X=X+.05
540 NEXT I
550 DISP "FINISHED"
560 BEEP
570 END
```

Sample output

A typical output is shown below, in which the first column is z_p/l_p, the second is τ_p/τ_{pp}, the third is z_p (in mm), and the fourth is τ_p (in N/m^2).

```
RELATIVE APPARENT SHEAR STRESS:
  .13
PLATEAU SHEAR STRESS  1.21
RATIO OF PEAK TO PLATEAU IS:
 1.099

SHEAR STRESS PROFILE.
z/l; ratio of shear stress
to plateau shear stress;
distance z;
absolute shear stress

0.00    1.10        0.0     1.330
 .05    1.10       10.0     1.329
 .10    1.10       20.0     1.327
 .15    1.09       30.0     1.323
 .20    1.09       40.0     1.317
 .25    1.08       50.0     1.309
 .30    1.07       60.0     1.301
 .35    1.07       70.0     1.291
 .40    1.06       80.0     1.281
 .45    1.05       90.0     1.271
 .50    1.04      100.0     1.261
 .55    1.03      110.0     1.252
 .60    1.03      120.0     1.244
 .65    1.02      130.0     1.237
 .70    1.02      140.0     1.231
 .75    1.01      150.0     1.225
 .80    1.01      160.0     1.221
 .85    1.01      170.0     1.218
 .90    1.00      180.0     1.216
 .95    1.00      190.0     1.214
1.00    1.00      200.0     1.213
```

C3 DISCHARGE COMPUTATION

Name: "QCOMP" (Q (discharge) COMPutation)

Purpose

This program evaluates five discharge computation methods:

1. popular method
2. k-method
3. modified k-method
4. area method
5. λ-method

QCOMP is designed for use with flume data. For each method the discharge *in a symmetrical*, rectangular compound channel is computed and compared with the known discharge for that section.

Application

QCOMP was used with the flume data of Wormleaton, Allen and Hadjipanos (1982) to evaluate the performance of the above discharge computation methods, and the results presented in fig. 5.6.

Operation

Subroutines were used fairly extensively in order to create as structured a program as possible within the limits of the HP85 BASIC.

Each discharge computation method involves *modifying* either the wetted perimeters or the areas of the main channel and flood plain regions, or both. Unmodified parameters are initially calculated as follows:

$$A_c = W_c D$$
$$A_p = W_p d$$
$$P_c = W_c + 2h$$

$$P_p = W_p + d$$

Each discharge computation method is dealt with by a separate subroutine which either adopts or adjusts these parameters, and then passes them on to the discharge subroutine, which calculates the discharge in each sub-section and then sums the discharges to get the discharge for the composite section.

The value of τ_r required in the input data is that which was measured in the flume experiments, and it is used to calculate k_c and k_p in the k-method, ΔA in the area method and λ in the λ-method.

The structure of QCOMP is as follows:

Read in data.
Compute general geometric properties.
MENU: Select desired discharge computation method:

(1) popular method
(2) k-method
(3) modified k-method
(4) area method
(5) λ-method

(1) POPULAR METHOD

Assign values to areas and wetted perimeters.
Go to discharge subroutine.
Return to menu.

(2) K-METHOD

Calculate k_c and k_p.
Modify wetted perimeters and assign areas.
Go to discharge subroutine.
Return to menu.

(3) MODIFIED K-METHOD

Calculate k iteratively , using the discharge subroutine to generate v_c/v_p.

Return to menu.

(4) AREA METHOD

Calculate ΔA and modify A_c and A_p.
Assign values to wetted perimeters.
Go to discharge subroutine.
Return to menu.

(5) λ-*METHOD*

Calculate and display λ.
Calculate areas and wetted perimeters.
Go to discharge subroutine.
Return to menu.

Discharge subroutine:

Calculate discharges of main channel and flood plain portions.
Calculate and display total discharge.
Calculate and display the percent error in discharge.

Variables

A	area adjustment for the area method (ΔA)
A1	area of main channel ($A_c = W_c D$)
A2	area of flood plain ($A_p = W_p d$)
A3	area assigned to the main channel for use in the discharge subroutine
A4	area assigned to the flood plain for use in the discharge subroutine
D1	flow depth in main channel (D)
D2	flow depth on flood plain (d)
H	height of step (h)
K	k-value for the modified k-method, i'th iteration
K1	k-value for main channel (k_c)
K2	k-value for flood plain (k_p)
K4	k- value for the modified k-method, (i-1)'th iteration
K5	absolute value of (K - K4)
L	length of diagonal interface in the λ-method (l)

N1	Manning's n for the main channel (n_c)
N2	Manning's n for the flood plain (n_p)
P1	physical wetted perimeter of main channel (P_c)
P2	physical wetted perimeter of flood plain (P_p)
P3	wetted perimeter assignad to main channel for use in the discharge subroutine
P4	wetted perimeter assigned to the flood plain for use in the discharge subroutine
Q	*total discharge in compound channel*
Q1	discharge of main channel portion
Q2	discharge of both flood plains
Q5	measured section discharge
R	lambda (λ)
T	relative apparent shear stress (τ_r)
T4	apparent shear stress on diagonal interface (τ_{ai})
T5	average shear stress on wetted perimeter of main channel
V	velocity ratio for the i'th iteration $(v_c/v_p)_i$
V1	average velocity in flood plain region (v_p)
V2	average velocity in main channel region (v_c)
V3	velocity ratio for the (i-1)'th iteration $(v_c/v_p)_{i-1}$
W1	width of main channel (W_c)
W2	width of flood plain (W_p)

Listing

```
10 ! "QCOMP"
20 CLEAR
30 DISP "DISCHARGE COMPUTATION
   METHODS"
40 DISP " "
50 !
60 ! DATA
70 ! Nc,h,Wp
80 DATA 152,76,228
90 ! Np,Nc
100 DATA .01, .009
110 ! SLOPE S
120 DATA .000966
130 READ W1,H,W2,N2,N1,S
140 DISP "FP FLOW DEPTH d (mm)"
150 INPUT D2
160 DISP "RELATIVE APPARENT SHEA
    R STRESS"
170 INPUT T
180 DISP "DISCHARGE (l/s)"
190 INPUT Q5
200 Q5=Q5/1000
210 W1=W1/1000
220 W2=W2/1000
230 H=H/1000
240 D2=D2/1000
250 CLEAR
260 D1=D2+H
270 A1=W1*D1
280 A2=W2*D2
290 P1=W1+2*H
300 P2=W2+D2
310 CLEAR
320 DISP USING 330
330 IMAGE 2/,29("*"),2/
340 DISP "Select an option:"
350 DISP "  Popular method (P)"
360 DISP "  K-method (K)"
370 DISP "  Modified k-method (M
    )"
380 DISP "  Area method (A)"
390 DISP "  Lambda method (L)"
400 INPUT B$
410 DISP USING 330
420 IF B$="P" THEN GOSUB 490
430 IF B$="K" THEN GOSUB 620
440 IF B$="A" THEN GOSUB 790
450 IF B$="L" THEN GOSUB 1040
460 IF B$="M" THEN GOSUB 1240
470 GOTO 310
480 !
490 ! Popular method.
500 B=D2/H
510 IF B>.3 THEN P3=P1
520 IF B<.3 THEN P3=P1+2*D2
530 P4=P2
540 A3=A1
550 A4=A2
560 CLEAR
570 DISP "POPULAR METHOD."
580 DISP " "
590 GOSUB 910
600 RETURN
610 !
620 ! K-method
630 K1=1/(A1/T/D2/P1-2*D2/P1)
640 K2=1/(A2/D2/T/P2+D2/P2)
650 P3=P1+2*K1*D2
660 P4=P2-K2*D2
670 A3=A1
680 A4=A2
690 CLEAR
700 DISP "K-METHOD."
710 DISP " "
720 DISP USING 740 ; "Kc:",K1
730 DISP USING 740 ; "Kp:",K2
740 IMAGE K,2X,DD,DD
750 DISP " "
760 GOSUB 910
770 RETURN
780 !
790 ! Area method.
800 A=T*D2^2
810 A3=A1-2*A
820 A4=A2+A
830 P3=P1
840 P4=P2
850 CLEAR
860 DISP "AREA METHOD."
870 DISP " "
880 GOSUB 910
890 RETURN
900 !
910 ! Discharge computation.
920 Q1=A3/N1*(A3/P3)^(2/3)*S^.5
930 Q2=2*(A4/N2)*(A4/P4)^(2/3)*S
    ^.5
940 Q=(Q1+Q2)*1000
950 DISP USING 980 ; Q
960 E=Q/Q5/10-100
970 DISP USING 990 ; E
980 IMAGE "Discharge (l/s):",2X,
    3D.D
990 IMAGE "% error:",2X,DDD.D,2/
1000 IF B$="M" THEN RETURN
1010 DISP "Press CONTINUE to con
     tinue."
1020 PAUSE
1030 RETURN
1040 !
1050 ! Lambda method.
1060 CLEAR
1070 DISP "LAMBDA METHOD."
1080 DISP " "
1090 L=SQR(D2^2+(W1/2)^2)
1100 A3=A1-D2*W1/2
1110 A4=A2+D2*W1/4
1120 T4=9800*D2*S*(T*D2-W1/4)/L
1130 T5=9000*A3*S/(P1+2*L)
1140 R=T4/T5
```

```
1150 IF R<=.5 THEN P3=P1
1160 IF R>.5 THEN P3=P1+2*L
1170 P4=P2
1180 DISP USING 1190 ; "Lambda:"
     ;R
1190 IMAGE K,2X,DD.DDD
1200 DISP " "
1210 GOSUB 910
1220 RETURN
1230 !
1240 ! Modified k-method.
1250 K=1
1260 V3=2
1270 CLEAR
1280 DISP "MODIFIED K-METHOD."
1290 DISP " "
1300 P3=P1+2*K*D2
1310 P4=P2
1320 A3=A1
1330 A4=A2
1340 DISP USING 1350 ; "K-value"
     ;K
1350 IMAGE K,2X,DD.DD
1360 GOSUB 910
1370 K4=K
1380 V1=Q1/A1
1390 V2=Q2/A2^2
1400 V=V1/V2
1410 V=(V+2*V3)/3
1420 V3=V
1430 K=1.274*V-2.235
1440 K=10^K
1450 K5=ABS(K-K4)
1460 IF K5>.005 THEN GOTO 1300
1470 DISP "Press CONTINUE to ret
     urn to"
1480 DISP "  the main menu."
1490 PAUSE
1500 RETURN
```

Sample output

```
 ISCHARGE COMPUTATION METHODS

F FLOW DEPTH d (mm)
?
19.6
RELATIVE APPARENT SHEAR STRESS
?
5.948
DISCHARGE (l/s)
?
7.50

********************************

Select an option:
  Popular method (P)
  K-method (K)
  Modified k-method (M)
  Area method (A)
  Lambda method (L)
?
P

********************************

POPULAR METHOD.

Discharge (l/s):     8.0
% error:             6.8

Press CONTINUE to continue.

********************************

Select an option:
  Popular method (P)
  K-method (K)
  Modified k-method (M)
  Area method (A)
  Lambda method (L)
?
K

********************************

K-METHOD.

Kc:   3.56
Kp:   4.27

Discharge (l/s):     7.7
% error:             2.1

Press CONTINUE to continue.

********************************

Select an option:
  Popular method (P)
  K-method (K)
  Modified k-method (M)
  Area method (A)
  Lambda method (L)
?
M

********************************

MODIFIED K-METHOD.

K-value    1.00
Discharge (l/s):     8.0
% error:             6.8

K-value    1.98
Discharge (l/s):     7.6
% error:             1.2

K-value    1.69
Discharge (l/s):     7.7
% error:             2.7

K-value    1.58
Discharge (l/s):     7.8
% error:             3.3

K-value    1.53
Discharge (l/s):     7.8
% error:             3.6

K-value    1.51
Discharge (l/s):     7.8
% error:             3.7

K-value    1.50
Discharge (l/s):     7.8
% error:             3.8

Press CONTINUE to return to
  the main menu.

********************************

Select an option:
  Popular method (P)
  K-method (K)
  Modified k-method (M)
  Area method (A)
  Lambda method (L)
?
```

```
*******************************

AREA METHOD.

Discharge (l/s):     7.3
% error:    -2.3

Press CONTINUE to continue.

*******************************

Select an option:
  Popular method (P)
  K-method (K)
  Modified k-method (M)
  Area method (A)
  Lambda method (L)
?
L

*******************************

LAMBDA METHOD.

Lambda:     .694

Discharge (l/s):     6.7
% error:    -11.3

Press CONTINUE to continue.

*******************************

Select an option:
  Popular method (P)
  K-method (K)
  Modified k-method (M)
  Area method (A)
  Lambda method (L)
?
```

C4 RELATIVE APPARENT SHEAR STRESS PREDICTION

Name "TPRED" (T (τ_r) PREDiction)

Purpose

The purpose of TPRED is to evaluate the Wormleaton equation and the Prinos equation for predicting the relative apparent shear stress in a compound channel (equations 6.3 and 6.5) using flume data from a symmetrical, rectangular section. To calculate values of Δv these equations are used in conjunction with the following discharge computation methods:

popular method
k-method
modified k-method
area method

Application

This program was used to prepare figs. 6.2 to 6.6.

Operation

The structure of TPRED is similar to that of QCOMP. The input value of τ_r is used as an initial estimate in those methods which require iterative calculation of τ_r. The structure of TPRED is outlined below.

Read in data.
Compute general geometric parameters.
MAIN MENU: Select desired discharge computation method for use in conjunction with the equations for τ_r.
(1) popular method
(2) k-method
(3) modified k-method
(4) *area method*

(1) POPULAR METHOD

Use the discharge routine to calculate Δv, and τ_r

Return to main menu.

(2) K-METHOD

SUB MENU: Select the Wormleaton or the Prinos equation.

Using the discharge subroutine, calculate k_c and k_p iteratively.

Display the value of τ_r at each iteration.

SUB-MENU: (1) Try the other equation (return to first sub-menu).

(2) Return to main menu.

(3) MODIFIED K-METHOD

Using the discharge subroutine to generate values of v_c and v_p, *calculate k iterstively.*

Using the final value of k, calculate τ_r for the Wormleaton equation and the Prinos equation.

Return to main menu.

(4) AREA METHOD

SUB-MENU: Select the Wormleaton or the Prinos equation.

Using the discharge subroutine, calculate ΔA iteratively.

Display the value of τ_r at each iteration.

SUB-MENU: (1) Try the other equation (return to first sub-menu).

(2) Return to main menu.

Discharge subroutine:

Computes discharges and velocities of the main channel and flood plain regions.

Calculates τ_r using the Wormleaton equation and the Prinos equation.

Variables

A	area adjustment for the area method (ΔA)
A1	area of main channel ($A_c = W_c D$)
A2	area of flood plain ($A_p = W_p d$)

A3	area assigned to the main channel for use in the discharge subroutine
A4	area assigned to the flood plain for use in the discharge subroutine
D1	flow depth in main channel (D)
D2	flow depth on flood plain (d)
H	height of step (h)
K	k-value for the modified k-method, i'th iteration
K1	k-value for main channel (k_c)
K2	k-value for flood plain (k_p)
K4	k- value for the modified k-method, (i-1)'th iteration
K5	absolute value of (K - K4)
L	length of diagonal interface in the k-method (l)
N1	*Manning's n* for the main channel (n_c)
N2	Manning's n for the flood plain (n_p)
P1	physical wetted perimeter of main channel (P_c)
P2	physical wetted perimeter of flood plain (P_p)
P3	wetted perimeter assigned to main channel for use in the discharge subroutine
P4	wetted perimeter assigned to the flood plain for use in the discharge subroutine
Q	total discharge in compound channel
Q1	discharge of main channel portion
Q2	discharge of both flood plains
R	lambda (λ)
T	current value of τ_r in the i'th iteration ($\tau_{r(i)}$)
T1	τ_r computed with the Wormleaton equation
T2	τ_r computed with the Prinos equation
T3	τ_r in the (i-1)'th iteration ($\tau_{r(i-1)}$)
T4	the absolute value of ($\tau_{r(i)} - \tau_{r(i-1)}$)
T5	*average shear stress* on wetted perimeter of main channel
V	either the velocity ratio $(v_c/v_p)_i$ or the difference between the main channel and flood plain velocities $(\Delta v)_i$ in the i'th iteration
V1	average velocity in flood plain region (v_p)
V2	average velocity in *main channel region* (v_c)
V3	either the velocity ratio $(v_c/v_p)_{i-1}$ or the

velocity difference $(\Delta v)_{i-1}$ in the (i-1)'th iteration

W1 width of main channel (W_c)

W2 width of flood plain (W_p)

Listing

```
10 ! "TPRED"
20 CLEAR
30 DISP "ASESSING WORMLEATON AN
   D PINOS"
40 DISP "EQUATIONS."
50 DISP " "
60 !
70 ! DATA
80 ! Wc,h,Wp
90 DATA 152,76,228
100 ! Np,Nc
110 DATA .01, .009
120 ! SLOPE S
130 DATA .000966
140 READ W1,H,W2,N2,N1,S
150 DISP "FP FLOW DEPTH d (mm)"
160 INPUT D2
170 DISP "INITIAL ESTIMATE OF RE
   LATIVE"
180 DISP " APPARENT SHEAR STRESS
   (T)"
190 INPUT T
200 W1=W1/1000
210 W2=W2/1000
220 H=H/1000
230 D2=D2/1000
240 D1=D2+H
250 A1=W1*D1
260 A2=W2*D2
270 P1=W1+2*H
280 P2=W2+D2
290 CLEAR
300 DISP USING 310
310 IMAGE "/,29(""*""),2/
320 DISP "Select an option:"
330 DISP "  Popular method (P)"
340 DISP "  K-method (K)"
350 DISP "  Modified k-method (M
   )"
360 DISP "  Area method (A)"
370 INPUT B$
380 DISP USING 310
390 IF B$="P" THEN GOSUB 450
400 IF B$="K" THEN GOSUB 600
410 IF B$="M" THEN GOSUB 1470
420 IF B$="A" THEN GOSUB 880
430 GOTO 290
440 !
450 ! Popular method.
460 CLEAR
470 B=D2/H
480 IF B> 3 THEN P3=P1
490 IF B<3 THEN P3=P1+2*D2
500 P4=P2
510 A3=A1
520 A4=A2
530 CLEAR
540 DISP "POPULAR METHOD."
550 DISP " "
560 GOSUB 1180
570 GOSUB 1360
580 RETURN
590 !
600 ! K-method
610 CLEAR
620 DISP "Do you want Wormleaton
   or"
630 DISP "Prinos? (W/P)"
640 INPUT C$
650 CLEAR
660 DISP "K-METHOD."
670 IF C$="W" THEN DISP "Wormlea
   ton's prediction of T:"
680 IF C$="P" THEN DISP "Prinos'
   prediction of T:"
690 K1=1/(R1^(2/3))^2*2*D2/P1)
700 K2=1/(R2^(2/3))^2*D2/P2)
710 P3=P1+2*K1*D2
720 P4=P2-K2*D2
730 A3=A1
740 A4=A2
750 GOSUB 1180
760 GOSUB 1300
770 T4=ABS(T-T3)
780 IF T4> .005 THEN GOTO 690
790 DISP " "
800 DISP "SELECT:"
810 DISP "  Try the other equati
   on? (1)"
820 DISP "  Return to main menu?
   (2)"
830 INPUT F
840 IF F=1 THEN GOTO 610
850 IF F=2 THEN RETURN
860 RETURN
870 !
880 ! Area method.
890 CLEAR
900 DISP "Do you want Wormleaton
   or"
910 DISP "Prinos? (W/P)"
920 INPUT C$
930 CLEAR
940 DISP "AREA METHOD."
950 IF C$="W" THEN DISP "Wormlea
   ton's prediction of T:"
960 IF C$="P" THEN DISP "Prinos'
   prediction of T:"
970 A3=T*D2^2
980 A3=A1-2*A
990 A4=A2+A
1000 P3=P1
1010 P4=P2
1020 CLEAR
1030 GOSUB 1180
1040 GOSUB 1300
1070 T4=ABS(T-T3)
1080 IF T4> .005 THEN GOTO 690
1090 DISP " "
1100 DISP "SELECT:"
```

```
1110 DISP "  Try the other equa
     tion? (1)"
1120 DISP "  Return to main menu
     ? (2)"
1130 INPUT F
1140 IF F=1 THEN GOTO 890
1150 IF F=2 THEN RETURN
1160 RETURN
1170 !
1180 ! Discharge computation.
1190 Q1=A3/N1*(A3/P3)^(2/3)*S^.5
1200 Q2=2*(A4/N2)*(A4/P4)^(2/3)*
     S^.5
1210 B=(Q1+Q2)*1000
1220 V1=Q1/A1
1230 V2=Q2/A2
1240 IF B$="M" THEN RETURN
1250 V=V1-V2
1260 T3=T
1270 T1=.001412/D2/S*V^.862*(1-D
     2/D1)^3.123*(W1/W2)^.727
1280 T2=1/(112134*D2*S)*V^.92*(D1
     /D2)^1.129*(W1/W2)^.514
1290 RETURN
1300 IF C$="N" THEN T=T1
1310 IF C$="P" THEN T=T2
1320 DISP USING 1330 ; T
1330 IMAGE 2X,DD.DD
1340 T=(T+2*T3)/3
1350 RETURN
1360 DISP USING 1420 ; T1
1370 DISP USING 1430 ; T2
1380 DISP " "
1390 DISP "Press CONTINUE to ret
     urn to"
1400 DISP "the main menu."
1410 PAUSE
1420 IMAGE "Wormleston's predict
     ion of T=",2X,DD.DD
1430 IMAGE "Prinos' prediction o
     f T=",1X,DD.DD
1440 RETURN
1450 !
1460 ! Modified k-method
1470 K=1
1480 V3=2
1490 CLEAR
1500 DISP "MODIFIED K-METHOD."
1510 DISP " "
1520 P3=P1+2*K*D2
1530 P4=P2
1540 A3=A1
1550 A4=A2
1560 GOSUB 1180
1570 DISP USING 1580 ; "K=",K,"V
     c/Vp=",V1/V2
1580 IMAGE 2(3X,K,1X,DD.DD)
1590 V=V1/V2
1600 V=(V+2*V3)/3
1610 V3=V
1620 K=K
1630 K=1.274*V-2.235
1640 K=10^K
1650 K5=ABS(K-K4)
1660 IF K5>.001 THEN GOTO 1520
1670 DISP " "
1680 GOSUB 1250
1690 GOSUB 1360
1700 RETURN
1710 END
```

Sample output

Note that in the example below, using the area method induced an error message, because a negative Δv was generated in the first iteration.

```
ASSESSING WORMLEATON AND PINOS
EQUATIONS

FP FLOW DEPTH d (mm)
?
20
INITIAL ESTIMATE OF RELATIVE
 APPARENT SHEAR STRESS (T)
?
6

*******************************

Select an option:
  Popular method (P)
  K-method (K)
  Modified k-method (M)
  Area method (A)
?
P

*******************************

POPULAR METHOD.

Wormleaton's prediction of T:
    6.44
Prinos' prediction of T:  5.09

Press CONTINUE to return to
 the main menu.

*******************************

Select an option:
  Popular method (P)
  K-method (K)
  Modified k-method (M)
  Area method (A)
?
K

*******************************

Do you want Wormleaton or
Prinos? (W/P)
?
W
K-METHOD.
Wormleaton's prediction of T:
    2.28
    3.43
    3.83
    3.97
    4.00
    4.05
    4.05

SELECT:
  Try the other equation? (1)
  Return to main menu? (2)

Do you want Wormleaton or
Prinos? (W/P)
?
P
K-METHOD.
Prinos' prediction of T:
    3.14
    3.36
    3.45
    3.49
    3.51
    3.51

SELECT:
  Try the other equation? (1)
  Return to main menu? (2)
?
2

*******************************

Select an option:
  Popular method (P)
  K-Method (K)
  Modified k-method (M)
  Area method (A)

*******************************
```

```
MODIFIED K-METHOD.

    K:  1.00    Vc/Vp:  1.94
    K:  1.94    Vc/Vp:  1.81
    K:  1.64    Vc/Vp:  1.85
    K:  1.53    Vc/Vp:  1.86
    K:  1.48    Vc/Vp:  1.87
    K:  1.45    Vc/Vp:  1.87
    K:  1.44    Vc/Vp:  1.88
    K:  1.44    Vc/Vp:  1.88
    K:  1.44    Vc/Vp:  1.88
    K:  1.44    Vc/Vp:  1.88

Wormleaton's prediction of T:
  6.06
Prinos' prediction of T:  4.78

Press CONTINUE to return to
the main menu.

******************************

Select an option:
  Popular method (P)
  K-method (K)
  Modified k-method (M)
  Area method (A)
?
A

******************************

Do you want Wormleaton or
Prinos? (W/P)
?
W
AREA METHOD.
Wormleaton's prediction of T:
Error 9 on line 1270 : NEG^NON-I
NT
```

APPENDIX D: PUBLISHED FLUME DATA

This data was used in chapters 5 and 6 to test and develop equations for discharge computation and relative apparent shear stress prediction. It consists of 40 data items published by Wormleaton, Allen and Hadjipanos (1982) and 18 published by Knight and Demetriou (1983). The data was collected in symmetrical, rectangular flumes.

D1 Data of Wormleaton, Allen and Hadjipanos (1982)

desig-nation	d (mm)	D (mm)	d/D		S	discharge (l/s)	τ_a (N/m^2)	τ_r
A1	15	135	0,111	0,011	0,000 43	13,4	1,031	16,310
A2	20	140	0,143	0,011	0,000 43	16,0	0,929	11,020
A3	30	150	0,200	0,011	0,000 43	20,5	0,750	5,933
A4	40	160	0,250	0,011	0,000 43	26,0	0,597	3,542
A5	50	170	0,294	0,011	0,000 43	31,0	0,499	2,368
A6	60	180	0,333	0,011	0,000 43	37,0	0,365	1,444
A7	70	190	0,368	0,011	0,000 43	43,5	0,252	0,854
A8	15	135	0,111	0,011	0,000 94	17,2	1,540	11,150
A9	20	140	0,143	0,011	0,000 94	25,7	1,304	7,078
A10	25	145	0,172	0,011	0,000 94	29,2	1,279	5,554
A11	40	160	0,250	0,011	0,001 01	35,2	0,990	2,501
A12	20	140	0,143	0,011	0,001 80	31,0	2,085	5,921
B1	31	151	0,205	0,014	0,000 43	17,0	0,864	6,614
B2	40	160	0,250	0,014	0,000 43	20,5	0,720	4,271
B3	50	170	0,294	0,014	0,000 43	26,0	0,597	2,833
B4	60	180	0,333	0,014	0,000 43	31,0	0,480	1,898
B5	70	190	0,368	0,014	0,000 43	38,0	0,385	1,305
B6	90	210	0,429	0,014	0,000 43	48,0	0,218	0,375

desig-nation	d (mm)	D (mm)	d/D	n_p	S	discharge (l/s)	τ_s (N/m^2)	τ_r
C1	20	140	0,143	0,017	0,000 43	11,5	1,269	15,060
C2	30	150	0,200	0,017	0,000 43	15,0	0,978	7,736
C3	40	160	0,250	0,017	0,000 43	18,0	0,786	4,663
C4	50	170	0,294	0,017	0,000 43	22,5	0,656	3,113
C5	60	180	0,333	0,017	0,000 43	28,0	0,560	2,215
C6	70	190	0,368	0,017	0,000 43	30,5	0,442	1,498
C7	80	200	0,400	0,017	0,000 43	37,0	0,344	1,020
C8	90	210	0,429	0,017	0,000 43	43,0	0,256	0,675
D1	20	140	0,143	0,021	0,000 43	9,0	1,467	17,410
D2	30	150	0,200	0,021	0,000 43	12,0	1,163	9,199
D3	40	160	0,250	0,021	0,000 43	15,0	0,925	5,488
D4	50	170	0,294	0,021	0,000 43	17,5	0,761	3,612
D5	60	180	0,333	0,021	0,000 43	24,0	0,648	2,563
D6	70	190	0,368	0,021	0,000 43	27,5	0,529	1,793
D7	80	200	0,400	0,021	0,000 43	33,0	0,400	1,187
D8	90	210	0,429	0,021	0,000 43	38,0	0,311	0,820
D9	20	140	0,143	0,021	0,000 94	12,5	1,613	8,755
D10	40	160	0,250	0,021	0,000 94	21,3	1,011	2,744
D11	60	180	0,333	0,021	0,000 94	35,5	0,758	1,371
D12	20	140	0,143	0,021	0,001 32	15,0	1,788	6,911
D13	40	160	0,250	0,021	0,001 32	25,5	1,173	2,267
D14	60	180	0,333	0,021	0,001 32	42,0	0,843	1,086

Parameters common to all experiments:

W_c = 290 mm

W_p = 460 mm

h = 120 mm

n_c = 0,010

D2 Data of Knight and Demetriou (1983)

desig-nation	d (mm)	D (mm)	d/D	W_p (mm)	discharge (l/s)	τ_a (N/m^2)	τ_r
1	9,2	85,2	0,108	76	5,20	0,562	6,450
2	18,5	94,5	0,196	76	6,40	0,467	2,666
3	24,3	100,3	0,242	76	7,30	0,376	1,633
4	37,5	113,5	0,330	76	9,45	0,312	0,880
5	49,8	125,8	0,396	76	11,70	0,330	0,700
6	73,8	149,8	0,493	76	17,10	0,340	0,487
7	11,5	87,5	0,131	152	5,00	0,982	9,017
8	20,1	96,1	0,209	152	6,70	0,741	3,895
9	24,9	100,9	0,247	152	8,05	0,610	2,586
10	36,1	112,1	0,322	152	11,15	0,404	1,181
11	49,0	125,0	0,392	152	15,15	0,347	0,748
12	73,2	149,2	0,491	152	23,40	0,314	0,454
13	9,0	85,0	0,106	228	4,90	2,394	28,10
14	19,6	95,6	0,205	228	7,50	1,104	5,948
15	26,1	102,1	0,256	228	9,10	0,618	2,500
16	36,2	114,2	0,335	228	13,50	0,527	1,457
17	51,4	127,4	0,403	228	18,00	0,332	0,682
18	77,8	153,8	0,506	228	29,40	0,223	0,302

Parameters common to all experiments:

W_c = 152 mm
h = 76 mm
n_p = 0,010
n_c = 0,009
S = 0,010 966

REFERENCES

Bairol J I and Ervine D A (1984): Resistance to flow in channels with overbank flood plain flow. Proceedings of the first international conference on hydraulic design in water resources engineering: channels and channel control structures, University of Southampton, April 1984, pp 4-137 - 4-150.

Barishnikov and Ivanov (1971): Role of flood plain in flood discharge of a river channel. Proceedings, 14'th international conference of the International Association for Hydraulic Research, Paris, France, 1971.

Ghosh S N and Jena S B (1971): Boundary shear distribution in open compound channel. Proceedings, Institution of Civil Engineers, London, vol. 49, August 1971, pp 417 - 430.

Graf W H (1971): Hydraulics of sediment transport. Publisher McGraw-Hill, 1971.

Hwang L and Laursen E M (1963): Shear measurement technique for rough surfaces. Proceedings, ASCE, Journal of Hydraulics Division, vol. 89, HY2, March 1963, pp 19 - 38.

James C S (1984): Numerical modelling of gold transport and deposition. Doctoral thesis, Civil Engineering Department, University of the Witwatersrand, Johannesburg, 1984.

James C S (1985): Sediment transfer to overbank sections. Journal of Hydraulic Research, vol. 23, no. 5, 1985.

Karasov J F (1969): Influence of the banks and flood plain on channel conveyance. Soviet Hydrology: selected paper 1969, no.5.

Knight D W and Demetriou J D (1983): Flood plain and main channel flow interaction. Proceedings, ASCE, Journal of Hydraulics Division, vol. 109, HY8, August 1983, pp 1073 - 1092.

Knight D W, Demetriou J D and Hamed M E (1983): Hydraulic analysis of channels with flood plains. Paper from International conference on hy-

draulic aspects of floods and flood control, London, 13 - 15 September 1983, editors Stephens and Stapleton, pp 129 - 144.

Knight D W, Demetriou J D and Hamed M E (1984): Stage-discharge relationships for compound channels. Proceedings of the first International conference on hydraulic design in water resources engineering: channels and channel control structures, University of Southampton, April 1984, pp 4.21 - 4.36.

Knight D W and Hamed M E (1984): Boundary shear in symmetrical compound channels. Proceedings, ASCE, Journal of Hydraulics Division, vol. 110, HY 10, October 1984, pp 1412 - 1430.

Knight D W and Lai C J (1985): Turbulent flow in compound channels and ducts. International symposium on refined flow modelling and turbulence measurements, USA, September 1985.

Knight D W and Patel H S (1985): Boundary shear in smooth rectangular ducts. Journal of Hydraulic Engineering, New York, vol. 111, no. 1, 1985, pp 29 - 47.

Le van Kiyen (1968): Hydraulic computation of flood plain channels. Selected papers 1968, no. 4.

Myers R C (1978): Momentum transfer in a compound channel. Journal of Hydraulic Research, Delft, vol. 16, 1978, pp 139 - 150.

Myers R C (1984): Frictional resistance in channels with flood plains. Proceedings of the first international conference on hydraulic design in water resources engineering: channels and channel control structures, University of Southampton, April 1984, pp 4.73 - 4.88.

Myers R C and Elsawy E M (1975): Boundary shear in channel with flood plain. Proceedings, ASCE, Journal of Hydraulics Division, vol. 101, HY7, July 1975, pp 933 - 946.

Pasche R (1984): Turbulenzmechanismen in naturnahen fliesgewassern und die moglichkeiten ihrer mathematischen erfassung. Nittoilungen, Institut fur wasserbau und wasserwirtschaft, T H Aschen, Heft 52, 1984.

Pasche E and Rouve G (1985): Overbank flow with vegetatively roughened flood plains. Proceedings, ASCE, Journal of Hydraulic Division, vol. 111, HY9, September 1985, pp 1262 - 1278.

Patel V C (1965): Calibration of the Preston tube and limitations on its use in pressure gradients. Journal of Fluid Mechanics, vol. 23, 1965, pp 185 - 208.

Posey C J (1967): Computation of discharge including overbank flow. Civil Engineering, ASCE, April 1967, pp 62 - 63.

Preston J H (1954): The determination of turbulent skin friction by means of pitot tubes. Journal of Royal Aeronautical Society, vol. 58, 1954, pp 109 - 121.

Prinos P and Townsend R D (1984): Comparison of methods for predicting discharge in compound open channels. Advances in water resources, Southampton UK, vol. 7, no. 4, 1984, pp 180 -187.

Prinos P, Townsend R and Tavoularis S (1985): Structure of turbulence in compound channel flows. Proceedings, ASCE, Journal of Hydraulics Division, vol. 111, HY9, September 1985, pp 1246 - 1261.

Radojkovic (1976): Mathematical modelling of rivers with flood plains. Rivers '76, vol. 1, pp 56 - 64.

Rajaratnam N and Ahmadi R M (1979): Interaction between main channel and flood plain flows. Proceedings, ASCE, Journal of Hydraulics Division, vol. 105, HY5, May 1979, pp 573 - 588.

Rajaratnam N and Ahmadi R (1981): Hydraulics of channels with flood plains. Journal of Hydraulic Research, vol. 19, no. 1, 1981, pp 43 - 60.

Sellin R H (1964): A laboratory investigation into the interaction between the flow in the channel of a river and that over its flood plain. La Houille Blanche, Grenoble, France, no. 7, 1964, pp 793 - 802.

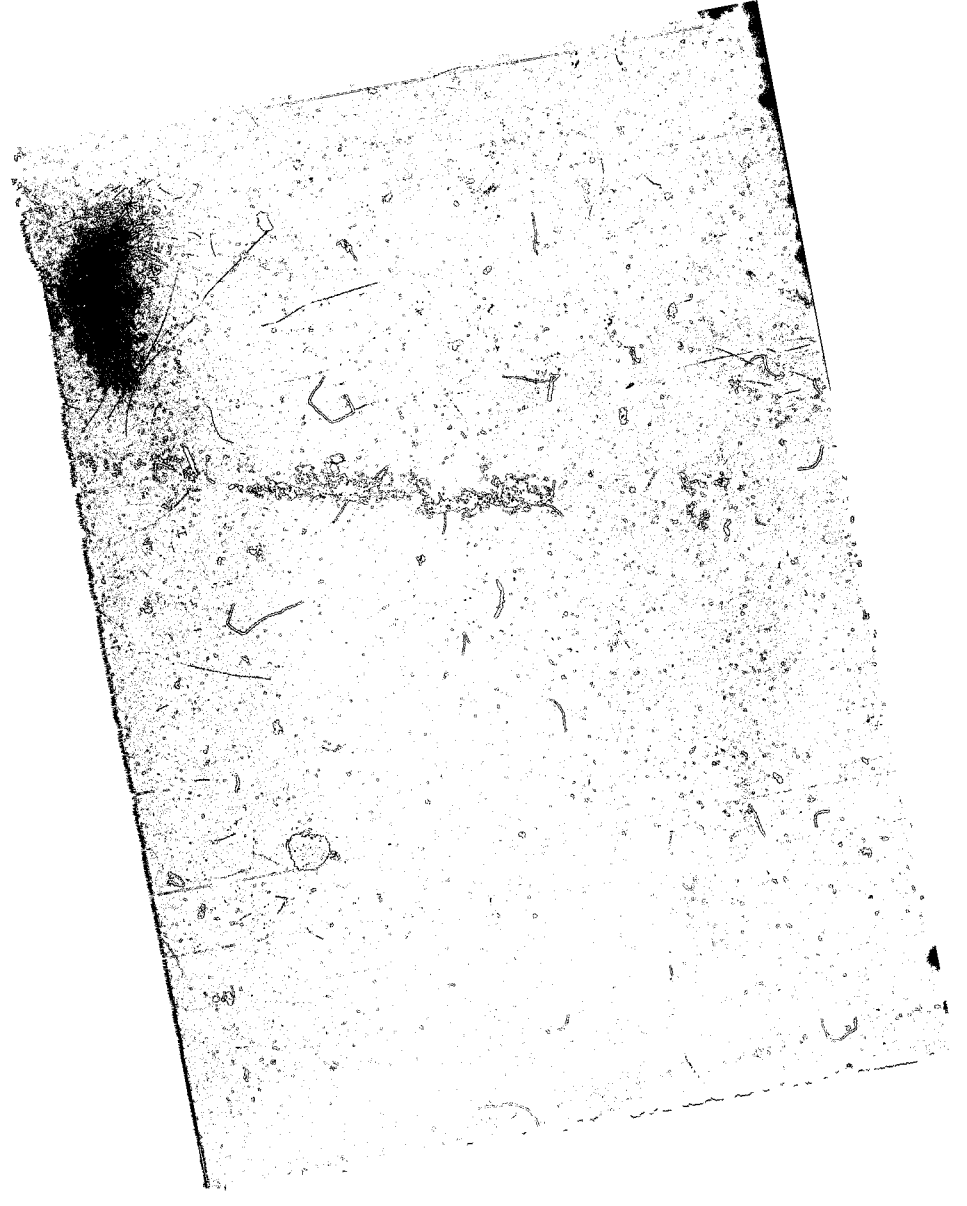
Wormleaton P R, Allen J and Hadjipanos P (1982): Discharge assessment in compound channel flow. Proceedings, ASCE, Journal of Hydraulics Division, vol. 108, HY9, September 1982, pp 975 - 994.

Wright R R and Carstens M R (1970): Linear momentum flux to overbank sections. Proceedings, ASCE, Journal of Hydraulics Division, September 1970, pp 1781 - 1793.

Yen C and Overton D E (1973): Shape effects on resistance in flood plain channels. Proceedings, ASCE, Journal of Hydraulics Division, vol. 99, HY1, January 1973, pp 219 - 238.

Zheleznyakov G V (1965): Relative deficit of mean velocity of unstable river flow, kinematic effect in river beds with flood plains. Proceedings of the 11'th international conference of the international association for hydraulic research, Leningrad, USSR, 1965.

Zheleznyakov G V (1971): Interaction of channel and flood plain streams. IAHR congress, Paris, vol. 5, 1971, pp 145 - 148.



Author Holden Andrew
Name of thesis Shear Stresses And Discharges In Compound Channels. 1986

PUBLISHER:
University of the Witwatersrand, Johannesburg
©2013

LEGAL NOTICES:

Copyright Notice: All materials on the University of the Witwatersrand, Johannesburg Library website are protected by South African copyright law and may not be distributed, transmitted, displayed, or otherwise published in any format, without the prior written permission of the copyright owner.

Disclaimer and Terms of Use: Provided that you maintain all copyright and other notices contained therein, you may download material (one machine readable copy and one print copy per page) for your personal and/or educational non-commercial use only.

The University of the Witwatersrand, Johannesburg, is not responsible for any errors or omissions and excludes any and all liability for any errors in or omissions from the information on the Library website.